RR-PRODIGAL - A Model for Estimating the Probabilities of Defects in Reactor Pressure Vessel Welds

Prepared by
O. J. V. Chapman/RRA
F. A. Simonen/PNNL

Pacific Northwest National Laboratory

Rolls-Royce and Associates

$O/_1$

$DF\phi2$

AVAILABILITY NOTICE

Availability of Reference Materials Cited in NRC Publications

NRC publications in the NUREG series, NRC regulations, and *Title 10, Energy,* of the *Code of Federal Regulations,* may be purchased from one of the following sources:

1. The Superintendent of Documents
   U.S. Government Printing Office
   P.O. Box 37082
   Washington, DC 20402–9328
   <http://www.access.gpo.gov/su_docs>
   202–512–1800

2. The National Technical Information Service
   Springfield, VA 22161–0002
   <http://www.ntis.gov/ordernow>
   703–487–4650

The NUREG series comprises (1) technical and administrative reports, including those prepared for international agreements, (2) brochures, (3) proceedings of conferences and workshops, (4) adjudications and other issuances of the Commission and Atomic Safety and Licensing Boards, and (5) books.

A single copy of each NRC draft report is available free, to the extent of supply, upon written request as follows:

Address: Office of the Chief Information Officer
            Reproduction and Distribution
             Services Section
            U.S. Nuclear Regulatory Commission
            Washington, DC 20555–0001
E–mail: <GRW1@NRC.GOV>
Facsimile: 301–415–2289

A portion of NRC regulatory and technical information is available at NRC's World Wide Web site:

    <http://www.nrc.gov>

All NRC documents released to the public are available for inspection or copying for a fee, in paper, microfiche, or, in some cases, diskette, from the Public Document Room (PDR):

NRC Public Document Room
2121 L Street, N.W., Lower Level
Washington, DC 20555–0001
<http://www.nrc.gov/NRC/PDR/pdr1.htm>
1–800–397–4209 or locally 202–634–3273

Microfiche of most NRC documents made publicly available since January 1981 may be found in the Local Public Document Rooms (LPDRs) located in the vicinity of nuclear power plants. The locations of the LPDRs may be obtained from the PDR (see previous paragraph) or through:

    <http://www.nrc.gov/NRC/NUREGS/
    SR1350/V9/lpdr/ntml>

Publicly released documents include, to name a few, NUREG-series reports; *Federal Register* notices; applicant, licensee, and vendor documents and correspondence; NRC correspondence and internal memoranda; bulletins and information notices; inspection and investigation reports; licensee event reports; and Commission papers and their attachments.

Documents available from public and special technical libraries include all open literature items, such as books, journal articles, and transactions, *Federal Register* notices, Federal and State legislation, and congressional reports. Such documents as theses, dissertations, foreign reports and translations, and non-NRC conference proceedings may be purchased from their sponsoring organization.

Copies of industry codes and standards used in a substantive manner in the NRC regulatory process are maintained at the NRC Library, Two White Flint North, 11545 Rockville Pike, Rockville, MD 20852–2738. These standards are available in the library for reference use by the public. Codes and standards are usually copyrighted and may be purchased from the originating organization or, if they are American National Standards, from—

American National Standards Institute
11 West 42nd Street
New York, NY 10036–8002
<http://www.ansi.org>
212–642–4900

RR-PRODIGAL - A Model for Estimating the Probabilities of Defects in Reactor Pressure Vessel Welds

Prepared by
O. J. V. Chapman/RRA
F. A. Simonen/PNNL

Pacific Northwest National Laboratory
Operated by Battelle Memorial Institute

Pacific Northwest National Laboratory
Richland, WA 99352

Subcontractor:
Rolls-Royce and Associates
Derby, DE2 8BJ
United Kingdom

S. N. Malik, NRC Project Manager

Abstract

In evaluating the probability of failure of a weld, one of the most difficult problems is determining a defect distribution and density. Several attempts have been made to estimate these parameters for specific cases using the technical opinions of welding engineers with significant experience in weld fabrication processes for reactor pressure vessels (U.S. designs). Some data exists for specific applications which can also help in assessing these parameters. However, the approach used here is somewhat different. Both the technical expertise of welding process engineers and mathematical modeling are used, not to attempt to describe the defect distribution and density directly, but to build a model that will simulate the weld manufacture and the errors that lead to different types of defects. In this way, the model attempts to build up, rather than measure, a defect distribution and density for a given type or family of welds. What follows is a brief description of this modeling, which is then used to predict the measured databases that now exist for welds ranging from one to eight inches thick.

The initial modeling carried out by Rolls-Royce Associates (RRA) was for pipe welds and vessel welds less than about four inches in thickness. Later, this was expanded in a collaborative program with Battelle Pacific Northwest National Laboratory (PNNL) for vessels with weld thicknesses of eight inches, as would be encountered in commercial nuclear power plants. The model-building procedure described above was therefore repeated to obtain a second set of parameters suitable for these welds.

A further collaborative program was undertaken with PNNL in 1996 to model cladding welds and their interactions with the main vessel welds. Adjustments to the methodology for the main vessel welds were also discussed. Again, the model-building procedure was repeated to obtain new and revised parameters suitable for all the welds.

The chapters and appendixes of this report describe the flaw simulation methodology, provide guidance for the use of the computer code RR-PRODIGAL which implements the methodology, and describe example calculations using RR-PRODIGAL.

Contents

Contents

Figures

Executive Summary

The U.S. Nuclear Regulatory Commission (NRC) has supported research at Pacific Northwest National Laboratory (PNNL) to establish a better basis for estimating the distributions of flaws in RPV welds. The present report describes work on a modeling approach to predict flaw distributions based on knowledge of the vessel dimensions, welding practices, and inspection procedures. This project was a collaborative program between PNNL and Rolls-Royce and Associates (RRA).

In evaluating the probability of failure of a weld, one of the most difficult problems is determining a defect distribution and density. Several attempts have been made to estimate these parameters for specific cases using expert elicitation. Some data exist for specific applications which can also help in assessing these parameters. However, the approach used in the present work is somewhat different. Both expert elicitation and mathematical modeling are used, not to attempt to describe the defect distribution and density directly, but to build a model that will simulate the weld manufacture and the errors that lead to different types of defects. In this way, the model attempts to build up, rather than measure, a defect distribution and density for a given type or family of welds. The present report provides a description of this modeling, along with its application to predict flaw distributions for comparison with existing measurement databases for welds ranging from one to eight inches thick.

The initial modeling carried out by RRA was for pipe welds and vessel welds of less than about four inches in thickness. The original RRA model was developed to predict the frequency at which flaws occur during multi-pass welding, to simulate the depths and other important characteristic of these flaws, and to simulate the effects of radiographic and surface examinations on the resulting flaw distributions. The original work was expanded, as described in the present report, in a collaborative program with PNNL to address vessels with weld thicknesses of eight inches or more, as would be encountered in commercial nuclear power plants.

The model-building procedure was repeated in the current work to obtain a revised set of parameters suitable for thick section vessel welds. This collaborative program by PNNL and RRA was undertaken in 1996 to model cladding welds and their interactions with the main vessel welds. Adjustments were also made to the methodology for the main vessel welds.

The collaborative effort by PNNL and RRA had several objectives:

- Review the original RRA model and establish its potential for estimating the number and sizes of flaws in the welds of the reactor pressure vessels used in the US at commercial nuclear power plants,

- Revise and enhance the RRA methodology to permit more accurate simulations of weld flaws, with particular attention to flaws associated with vessel cladding,

- Document details of the flaw estimation methodology and issue a report describing the methodology and associated computer code,

- Provide a UNIX-based computer code (RR-PRODIGAL) for use by NRC staff (and others) to calculate flaw distributions which can be used as inputs to probabilistic fracture mechanics calculations,

- Compare the predicted flaw densities and size distributions from RR-PRODIGAL with experimental data from examinations of reactor vessels, both to validate the predictions of the code and to establish the ability of RR-PRODIGAL to address the effects of vessel-to-vessel differences on flaw distributions, and

- Simulate the flaws in some representative reactor pressure vessels and provide the resulting detailed descriptions of flaw densities, flaw depths, flaw lengths, and flaw locations within the vessel wall to Oak Ridge National Laboratory for use in calculations of vessel failure probabilities.

Two meetings were held as part of the research project, which enabled RRA and PNNL personnel to engage in discussions with groups of experts in the areas of vessel welding and inspection practices. These discussions confirmed the basic soundness of the original RRA methodology, and provided insights which improved the quality of the assumptions and inputs to the model.

The final version of the RR-PRODIGAL code was applied to predict the flaws in the Pressure Vessel Research User Facility (PVRUF) vessel. These predicted distributions were compared with the distribution of flaws found by PNNL from detailed examinations of the vessel welds. Good agreement was observed between the predicted and measured flaw distributions for a range of flaw depths extending out to the maximum measured flaw depth of 17 mm. It was concluded that the RR-PRODIGAL code provides an acceptable mechanistic model to estimate the occurrence rates for flaw sizes larger than those in the database obtained from the PVRUF vessel examinations.

This report describes the flaw simulation methodology, provides guidance in use of the RR-PRODIGAL computer code, and describes example calculations using RR-PRODIGAL.

Acknowledgments

Acronyms

ASME	American Society of Mechanical Engineers
BNFL	British Nuclear Fuels Limited
CLD	Crack-Like Defects
DHC	Delayed Hydrogen Cracking
EBW	Electron Beam Welding
EPRI	Electric Power Research Institute
FCAW	Flux-Cored Arc Welding
GMAW	Gas Metal Arc Weld
GTAW	Gas Tungsten Arc Weld
H&H	Halmshaw and Hunt
HAZ	Heat Affected Zone
LW	Laser Welding
MIG	Metal Inert Gas Welding
MMA	Manual Metal Arc
MMAW	Manual Metal Arc Weld
MT	Magnetic Particle Testing
NE	Nuclear Electric
NRC	U.S. Nuclear Regulatory Commission
ORNL	Oak Ridge National Laboratory
PDF	Probability Density Function
PDR	Public Document Room
PNNL	Pacific Northwest National Laboratory
PT	Penetrant Testing
PVRUF	Pressure Vessel Research User Facility
PWHT	Post-Weld Heat Treatment
RPV	Reactor Pressure Vessel
RRA	Rolls-Royce and Associates
SAFT-UT	Synthetic Aperture Focusing Technique Ultrasonic Testing
SAW	Submerged Arc Welding
SMAW	Shielded Metal Arc Weld
SRC	Stress Relief Cracks

Acronyms

STAW	Gas Tungsten Arc Weld
TIG	Tungsten Inert Gas
UK	United Kingdom
US	United States
USA	United States of America

1.0 Introduction

The estimated numbers and sizes of flaws in reactor pressure vessel (RPV) welds are important inputs to probabilistic fracture mechanics calculations for predicting failure probabilities for reactor pressure vessels. But unfortunately, they are also the inputs which are believed to have the greatest levels of uncertainty. To reduce the level of uncertainty, the U.S. Nuclear Regulatory Commission (NRC) has supported research at Pacific Northwest National Laboratory (PNNL) to establish a better basis for estimating the distributions of flaws in RPV welds. One project has involved the detailed examination of vessels which were fabricated for nuclear plants that were later cancelled. These examinations have used both ultrasonic methods and destructive examination to confirm the presence and the sizes of defects.

The present report describes work on another project, which has developed a modeling approach to predict flaw distributions based on knowledge of the vessel dimensions, welding practices, and inspection procedures. This project was a collaborative program between PNNL and Rolls-Royce and Associates (RRA). The work was built on prior work by RRA which modeled welds for piping and for vessels of less than about four inches in thickness. The original RRA model was developed to predict the frequency at which flaws occur during multi-pass welding, the depths and other important characteristic of these flaws, and the effects of radiographic and surface examinations on the resulting flaw distributions. The original work was then expanded in the collaborative program, as described in the present report, to address vessels with wall thicknesses of eight inches or more, as would be encountered in commercial nuclear power plants.

The modeling approach used both expert elicitation and mathematical modeling to build a computer code that simulates the weld manufacture and the errors that lead to different types of defects. In this way, the model attempts to predict a defect distribution and density for a given type or family of welds. The present report provides a description of this modeling, along with its application to predict flaw distributions for comparison with existing measurement databases for welds ranging from one to eight inches thick.

The collaborative effort by PNNL and RRA had several objectives:

- Review the original RRA model and establish its potential for estimating the number and sizes of flaws in the welds of the reactor pressure vessels used in the US at commercial nuclear power plants,

- Revise and enhance the RRA methodology to permit more accurate simulations of weld flaws, with particular attention to flaws associated with vessel cladding,

- Document details of the flaw estimation methodology and issue a report describing the methodology and associated computer code,

- Provide a UNIX-based computer code (RR-PRODIGAL) for use by NRC staff (and others) to calculate flaw distributions which can be used as inputs to probabilistic fracture mechanics calculations,

- Compare the predicted flaw densities and size distributions from RR-PRODIGAL with experimental data from examinations of reactor vessels, both to validate the predictions of the code, and to establish the ability of RR-PRODIGAL to address the effects of vessel-to-vessel differences on flaw distributions, and

- Simulate the flaws in some representative reactor pressure vessels and provide the resulting detailed descriptions of flaw densities, flaw depths, flaw lengths, and flaw locations within the vessel wall to Oak Ridge National Laboratory for use in calculations of vessel failure probabilities.

This report describes the flaw simulation methodology, provides guidance in use of the RR-PRODIGAL computer code and describes example calculations using RR-PRODIGAL. The main body of the report was prepared by RRA to describe the overall approach used to simulate defects in welds. Chapter 2.0 defines the problem, reviews some early approaches to it, and describes the most recent efforts to extend the approach to vessels

fabricated in the USA. Chapter 3.0 describes the RR-PRODIGAL model and its major features. Chapter 4.0 details how the model was used in Monte Carlo simulations. Chapter 5.0 discusses several prior comparisons of model predictions with measured flaw data. These results show that the original RRA model was somewhat conservative because it tended to predict more flaws of a given size than were observed in actual welds. Chapter 6.0 summarizes the conclusions based upon this work, and Chapter 7.0 provides further references.

Appendixes A and B were prepared by RRA to provide further details and background information on the RR-PRODIGAL model. Appendix A documents the numerical parameters used within RR-PRODIGAL to estimate flaw occurrence rates and to characterize flaw dimensions and orientations. Appendix B describes welding practices used to fabricate vessels and piping systems, and documents the rationale used by welding experts to quantify the numerical parameters discussed in Appendix A.

Appendix C provides information on and results of example calculations with the model used within RR-PRODIGAL to predict the effectiveness of radiographic inspections.

Results of calculations with the revised version of the RR-PRODIGAL code are presented in Appendix D. These results show relatively close agreement between predicted and measured flaw distributions, due in large measure to a more refined approach to account for the flaws associated with slag inclusions. Appendix E provides output files from example calculations described in Appendix D.

The final two Appendices (F and G) provide guidance to users of the RR-PRODIGAL code. Appendix G gives instructions for installing the code on a UNIX-based SUN workstation. The code uses interactive screen-based menus to generate input for calculations and has extensive internal documentation in the form of help menus. Therefore, the code requires a minimum of user documentation. Appendix F was prepared on the basis of PNNL experience in using RR-PRODIGAL to cover some issues not otherwise addressed. The descriptions of example calculations in Appendix D also provide guidance and insights to assist in developing mathematical models of weld and in interpreting the results of calculations.

2.0 Background on RR-PRODIGAL

Estimation of defect distribution and densities in pressure vessel welds has proven to be extremely difficult. Several attempts have been made to assess these parameters for specific cases using teams of experts, probably the best known being the Marshall Committee (Marshall 1982). The problem with such an approach is that it requires a significant effort from a variety of experts for every weld being considered.

The Marshall Committee, which could call upon the services of many eminent experts representing the various relevant disciplines, considered a weld in a reactor pressure vessel approximately eight inches thick.

At Rolls-Royce and Associates (RRA), early attempts to transfer this distribution to a wide range of different welds highlighted a whole new set of problems that required almost as much effort and expertise as the original problem. A program of work was therefore started in the mid-eighties to create a form of an expert system model that would generate a defect distribution and density for multi-pass welds.

To create this model, two expert panels were assembled, one consisting of professional welding metallurgists, the other of practical welding engineers. The experience of the personnel of these two panels covered over a decade's development of weld procedures and personnel qualification for nuclear standard welding, together with production experience with early nuclear plants. The two teams were kept separate in order to establish a degree of independence, although clearly the experience of the two teams derives from a common development/production program. At the end of the exercise, the resulting model predictions of weld repairs were compared with the production experience. While this data was somewhat limited in its detail, it did provide a further independent qualifier. This initial work was restricted to welds of up to approximately four inches in thickness.

In 1994, a contract was formalized with Battelle Pacific Northwest National Laboratory (PNNL) to update this simulation program with regard to thicker section welds, up to eight and even ten inches thickness, that would be typical of commercial nuclear pressure vessels in the USA. A group of experts met in Washington in December 1994 (Simonen 1994) to go through the ranking and scorings that were currently contained within the simulation, and to see how applicable these were to the thicker section welds.

The various experts agreed with the general construction of the model and were in reasonable agreement about the scoring for probability of defect occurrence used for the thinner section welds. They did feel, however, that some of the scoring needed modification for the thicker vessels. The group restricted itself to considering only those materials and weld procedures applicable to reactor pressure vessels (RPV) as built for the US nuclear industry.

A second meeting of the experts (Simonen 1996) took place in 1996 at which they discussed cladding welds, and modifications to the main vessel weld logic agreed to at the previous meeting. The cladding weld logic and main vessel weld logic were considered to be very similar.

What follows is a description of how RRA constructed the original simulation, together with the work to validate this first program against two independent sources of data. The modified program, changed to be more representative of the thicker section welds for US RPVs, is currently being used to predict the outcome of a destructive examination of the RPV manufactured for the Midland Power Station and the Pressure Vessel Research User Facility (PVRUF). This work has been carried out independently by PNNL and will be reported separately. For completeness, some preliminary comparisons are included here against the Midland RPV, and for the PVRUF vessel in Appendix D. Installation guidance for the program is given in Appendix G. All tables shown in this report are for the thicker section RPV welds.

3.0 Building the Model

The model consists of several elements which begin with a procedure for estimating the frequencies at which defects occur during welding. This is followed by the assignment of the sizes and other characteristics for the defects. The final step is to estimate the effects of inspections on the population of defects.

3.1 Defect Density

The first step in building the RRA model was to invite the welding metallurgist to list the types of defects that occur in welded structures of interest to the nuclear industry. This list was then discussed with the stress engineers to establish which of these defects had the potential to develop into a growing crack. For example, it was concluded that single pores, or even small clusters of pores, were unlikely to pose any problem as initial defects. However, non-symmetrical pores, which are termed pores with tails or pipes, were felt to be potential crack initiators within the weld.

The resulting sets of defects were then referred to as 'crack-like defects' (CLDs). These are detailed in Appendix B. The welding metallurgists were then asked to list all the commonly used welding processes and to rank the CLDs from 1 to 10, from lowest expected frequency to highest expected frequency, against these processes. It soon became clear that other factors as well as the welding processes had to be considered in order to obtain a ranking. As the ranking developed, the question of exactly what was being ranked was discussed, and the conclusion was that this ranking, in some way, reflects the metallurgists' judgment as to the likelihood of a given defect type occurring under a particular combination of conditions. There was then a discussion as to whether or not different scorings under the different conditions for a given type of defect should be added or multiplied. It was decided that the individual scorings reflected independent probabilities of producing the defect, and hence multiplication was the more appropriate operation. It was at this time that zero was added to the ranking range. The results are given in Tables A.1 and A.2 of Appendix A.

Given that it had already been agreed that the scoring represents a likelihood of defect occurrence, the next step was to convert this likelihood to an actual rate of defect generation.

To do this, the practical experience accumulated over many years of weld manufacture and repair was applied. However, this experience had to be modified because it was agreed for this exercise that the relationship between the scoring and the defect occurrence was proportional to the total length of the weld beads that made up the weld, and not simply the length of finished weld. It was also agreed that weld stops and starts would have a significant effect on the introduction of defects, so this was added as an extra source for the center line type of defect. The different experts then focused on those areas with which they had the most personal experience and progressed from scoring to determining the actual rates of occurrence for these cases. The relative rankings of the finished estimates were then assessed for possible reconsideration. This concluded with an agreed value to convert the scoring to a rate of defect occurrence.

All parameters for thick vessels and cladding are shown in Appendix A.

3.2 Initial Defect Size

The first expert elicitation on defect sizing quickly concluded that, while the expertise available could attempt to describe some form of end defect size distribution, its real expertise lay in assessing, for each given defect type, the size of a single defect of that type at initiation. Each type of defect was then considered in turn, and it was concluded that for the defect types associated with multi-pass welds, the bead size could act as a normalizing factor at defect initiation.

The outcome of these discussions was a statistical distribution, in the form of a Weibull distribution. While these distributions are normalized to the bead size, they are not restricted to it; that is to say, they are not truncated at the

bead depth. It was felt that some defects could grow through the bead in which they initiated down into the material below, for example, shrinkage cracks.

After the discussion of defect size in terms of its through-wall dimension, the question of its length along the weld was addressed. It was decided to relate this to the final defect depth in terms of an aspect ratio and to describe this again in terms of a Weibull distribution.

It was felt at that time that a description of its through-wall and length dimensions was sufficient for each type of defect and indeed, from a fracture mechanics view-point, it certainly is. However, in parallel with this work, the question of the weld build inspection was being pursued. This is discussed in the next section, but the feedback from these expert elicitations was that the defect angle and the separation between the surfaces or gap of the defect were important parameters; so the group of experts was reconvened and these two extra dimensions were added to the defect description.

The final outcome of this part of the work was a set of Weibull distributions for each CLD that described its through-wall depth, length, average separation between the faces, and its angle. However, these distributions apply only at initiation and the question was then asked about the probability of these defects, once initiated, to propagate on through the weld as it was being constructed. In this way, a relatively small defect, initiated early in the welding process, could grow into a very large defect before the weld was completed. Thus, an attribute called 'forward propagation' was added to the defect descrip-tion. An alternative title for this attribute could be 'error reoccurrence'! Whichever term is your preference, the object of the attribute is as follows: given that an error has occurred, what is the probability that this existing error will cause the same error to occur again, just above the already existing error, or that some form of propaga-tion of the error will occur? This attribute is assigned as a conditional probability. The ability of the welder to observe and correct the error was also considered for each type of propagating defect. All of these values for thick section welds are tabulated in Appendix A.

3.3 Effect of Weld Build Inspection

In order to measure the effect of inspection, it is neces-sary to derive an efficiency curve for the various inspec-tion techniques. For the welds in question, the techniques used at build were radiography and various surface techniques.

For these techniques, it was decided to continue with the same logic adopted for the defects themselves, i.e., a combination of theoretical models and engineering judg-ment would be built into the simulation. The following is a brief description of how the two techniques were handled.

3.4 Radiography

Each defect, except a pore with a tail, is treated as a slot with a given depth at some angle and with a mean separa-tion between the faces. The radiographic setup, (i.e., double wall single image using an isotope, etc.) is then input so that the relative position and angle to the source and film are known for all the simulated defects. Radio-graphic theory is then applied to evaluate the density change produced by the defect. The probability of detect-ing the defect is then evaluated using experimentally determined inspection capabilities.

For the pores with tails, it was felt that the probability of finding an isolated pore with radiography is very good; the real question is the ability of the inspector to distin-guish between a benign single pore and a pore with a tail. In the end, this inspection efficiency had to be purely judgmental.

The radiographic modeling is described in Appendix C.

3.5 Surface Inspections

For surface inspections, the expert judgments were against the ability to detect a given width and length. Within the weld build simulation, only surface-breaking defects are considered, together with their widths and lengths, to determine the probability of detection. It was

considered that detecting a defect with a surface-breaking width of 0.07 mm or greater is a near certainty. However, if the surface-breaking defect width is less than 0.01 mm, this probability of detection is set to zero. The surface finish is included within the judgment-based inspection efficiencies.

3.6 Post Weld Heat Treatment

Stress relief cracking from post weld heat treatment is covered separately (see Appendix B), but it was decided that this treatment could independently affect any delayed hydrogen cracking that may occur. This effect is input as a distributed extension to any delayed hydrogen cracking that is simulated at build (see Figure A.15 of Appendix A).

3.7 Post Weld Machining

Post weld machining is considered in order to account for any defects that might be buried at build, but exposed to any surface inspection after machining. It is interesting to reflect on how this affects the probability of having a surface-breaking defect in a weld that is subject to a dye-penetrant inspection both before and after the capping weld is dressed off. The exposure of subsurface defects results in a net increase in the number of surface-breaking defects. However, this effect is more than offset by the enhanced ability of dye-penetrant exams to detect defects for a machined surface as opposed to a rough as-welded surface.

4.0 The Simulation

The simulation program pulls together all the expert knowledge and builds, within the pseudo-world of the computer, a large number of identical welds. This is done using a Monte-Carlo simulation. The object of the simulations is to reproduce, albeit in a simple form, the way in which defects initiate and interact. With several thousand such simulations, it is possible to realize the very rare event of a large defect. At the same time, the simulation will reproduce the more common occurrences of the small defects that we would expect to observe from the small sample of true welds that are available for close inspection.

The simulation represents the weld buildup as a single set of building blocks, as shown in Figure 1.

A - Heat Affected Zone (HAZ) Crack
B - Centreline Crack
C - Pore with Tail
D - Lack of Inter-Run Fusion
E - Lack of Sidewall Fusion
F - Inter-Run Slag
G - Sidewall Slag
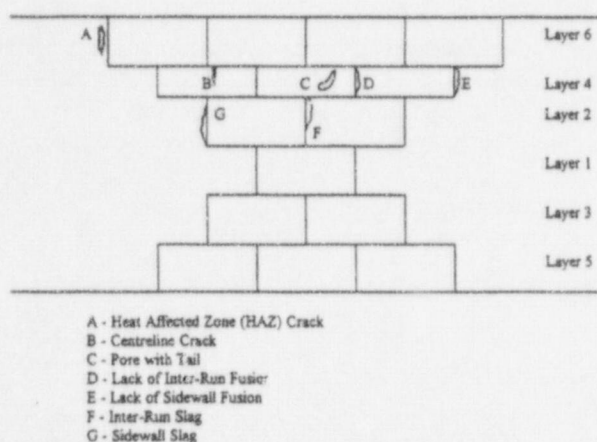
Figure 1. Schematic Representation of Weld Buildup and the Position of Different Types of Crack-Like Defects

After a defect initiates, its depth and dimensions are randomly chosen using information from Table A.3 in Appendix A. The next consideration is whether the defect type can propagate forward. Should propagation occur, the defect is taken on into the next layer available for further propagation. As soon as it fails to propagate into the next layer of weld beads, it is assumed to be left behind by the welding process and its initial depth is adjusted, depending on the number of propagations that have occurred. After the defect depth is simulated, its length is randomly chosen from the appropriate distribution.

Cladding defects behave in much the same manner as the parent weld defects, except that certain types of defects which are close to the weld/clad interface can snap through into the main weld from the cladding or into the interface from the main vessel weld.

The defect width and angle are not simulated; these are used only in the radiographic and dye-penetrant inspection simulations.

This simulation procedure gives the depth and length of a single defect at initiation. If a second defect initiates within the vicinity of this first defect, the probability of the two defects interacting must be considered.

In order to assess whether interaction takes place, each defect is considered to have an influence zone around it. If two influence zones overlap, the defects join to form a single CLD with dimensions that encompass the two original defects. Note that the defect density is then adjusted for the two CLDs becoming one.

The size of the influence zone is set using a simple linear elastic fracture mechanics criterion, as follows:

$$\text{Plastic Zone } R = \frac{1}{2\pi}\left[\frac{K}{\sigma_y}\right]^2$$

where

$K = F\sigma\sqrt{\pi a}$
$F = $ Constant
$\sigma_y = $ Yield Stress
$\sigma = $ Membrane Stress
$a = $ Defect Size.

Now let $\sigma = A\sigma_y$, where A is some constant; then

$$R = \frac{1}{2} a(FA)^2$$

Values for F range from 1 to 1.2. If we associate A with say, a hydro test, a value of 0.7 to 0.8 would be realistic. Combining these gives an $(FA)^2$ value between 0.5 and 0.92. A slightly pessimistic value of 1.0 is used, to allow for any residual stresses. This then gives:

$$R = a/2$$

This interaction is illustrated in Figure 2.
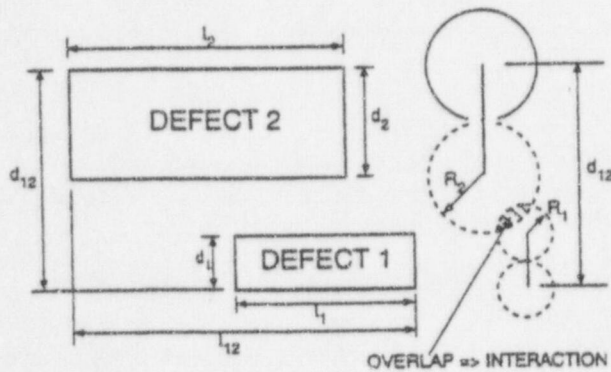
Figure 2. Interaction of Neighboring and Overlapping Defects

Defect 1 is removed and defect 2 is replaced with a new defect of length l_{12} and depth d_{12}.

Strictly, the influence zone as described above applies only to a surface-breaking defect. For a buried defect, the value of 'a' should be halved. However, given the question of possible residual stresses, it was assumed that all defects would have the same influence zone.

HAZ type defects are, however, treated differently than other defect types in assessing possible combination effects. They are assumed to have no influence zone; consequently, they cannot combine with any other defect type or with each other. This is because the overall nature of a HAZ defect is itself a network of small defects. While these could be thought of as a single defective area and hence one single defect, there would be no large influence zone outside the degraded area.

After seeding the weld with a series of defect types, inspection is then simulated. Inspections can be carried out at any time during the weld build. The simulation takes account of the time of the inspection. If two radiographic inspections are carried out over the lower part fill of the weld, they are considered as independent.

Finally, machining operations on either surface can be taken into account in the simulation, as can post weld heat treatment.

The outcome of this simulation is a density 'D' and distribution 'f(a)' of defect sizes entering service. In terms of the program definition, this would seem to be all that is required. However, if the data is to be used to assess a probability of failure, then a crack growth/fracture analysis will also be required. Such an analysis needs to know where the starting defect is located, i.e., surface-breaking or buried at some depth within the thickness of the weld. The simulation uniquely sizes and positions every defect, but unfortunately, this is too much information to handle in a fracture analysis. For welds less than four inches thick, the simulation categorizes the defects into five different default positions. The categories are as follows:

> surface-breaking inner or outer surface
> buried, near inner or outer surface
> buried, middle.

For the thicker pressure vessels, with and without cladding, the default categories were modified to:

> surface-breaking, inner surface
>
> inner crack tip, within one-eighth of the thickness from the inner surface
>
> inner crack tip, within one-eighth to one-quarter of the thickness from the inner surface
>
> inner crack tip, within one-quarter to one-half of the thickness from the inner surface
>
> inner crack tip, within one-half to three-quarters of the thickness from the inner surface
>
> inner crack tip, three-quarters of the thickness or more from the inner surface
>
> surface-breaking, outer surface.

5.0 Validation

It is questionable whether it is ever possible to validate a program of this type. One can carry out a quality assurance based verification that the model is reproducing what the experts wanted, and this has indeed been done; however, the question of validation still remains. Our attempt to validate the program can be split into two sections: the first is at the initial development stage of the program; the second is to compare the predictions of the model with data that was not part of the original knowledge base used to build the model, but that is within the scope of the model simulation.

5.1 Initial Validation

For the expert elicitations, two independent sets of experts were used. These two groups could be termed a theoretically based group and a practical group. Professional metallurgists made up the theoretical group, and welders made up the second, more practical, group.

The predictions of the model were compared with data from the pre-service inspections that were available. The nature of the model is such that it not only gives the probability of not detecting defects, but records the number of defects that would have been detected and hence repaired. It was therefore possible to compare the model predictions with the repair records from the build data. At first, the model predictions were somewhat low in comparison with the actual repair rate, a situation which caused considerable consternation. However, after some discussion it became clear that the majority of the recorded repairs and reworks were not for the type of crack-like defects that were being simulated, but were for a variety of other factors, more associated with basic quality assurance for less serious defects which were not crack-like. Unfortunately, the records were not detailed enough to sort out the differences, and the best estimate the inspection department could give was that for the type of defects being simulated, the predicted rate of occurrence was probably too high by a factor of two.

At the end of this initial period, the model produced no predictions that the experts who had generated the basic data were unhappy with, or that contradicted the limited practical data available, other than those highlighted in the previous paragraph.

5.2 Validation Against External Databases

This effort encompassed the most serious attempt to date at any meaningful independent validation. Four sources of data on thick section vessels were made available for comparison:

1) Nuclear Electric data from their extensive inspection of the Magnox ducting welds (Chapman 1993)

2) British Nuclear Fuels data from their pressure vessel weld inspection (Chapman 1993)

3) The Midland Reactor Pressure Vessel weld inspection (Lance et. al 1992)

4) The Pressure Vessel Research User Facility (PVRUF) data from nondestructive and destructive examinations.

The first three cases are analyzed below, and the fourth case is addressed in Appendix D.

The first two cases are for welds less than four inches thick, and the original RRA tables of values were used. For the Midland vessel prediction, the modified values given in Tables A.1 and A.2 of Appendix A were used. In each case, a probability density function (pdf) is plotted for the total defects within the weld, and the corresponding defect density per meter of finished weld is quoted. Since it has become popular to quote the defect density in terms of the volume of weld, the density per meter of finished weld is also converted to a defect density per cubic meter of laid weld.

It is also clear that defects at or near the inner surface of a weld are of considerable interest, as most often these defects dominate the probability of failure of a weld. Since the model separates the defect simulation into seven categories (see Section 4), the predicted defect

Validation

distribution and density for defects at or near the inner surface have also been included.

5.3 Nuclear Electric Ducts and Boiler Welds

With the co-operation of Nuclear Electric (NE), predictions of the simulation model have been compared with the results of ultrasonic inspection of NE ducts and boiler weld. Pulse echo techniques were used to size any defects found. The components inspected cover a range of weld types and section thicknesses. Because of the paucity of data, all the data were combined to give a single database.

A Gumbel Type II distribution was fitted by NE to the through-wall depths of the defects, for use in probabilistic assessments. It is used for all defect depths in the weld, although it should be noted that it is derived from defects with very limited through-wall extents.

This pdf for defect size, a, is given by:

$$p(a) = A^B Ba^{-(B+1)} \exp - (a/A)^{-B}$$

where the constants A and B are 1.285 and 2.857, respectively; a = defect depth (mm).

To obtain an early estimate of the model's predictive capability, it was decided to run just two reasonably representative welds, as follows:

Weld A

A 25.4 mm or one-inch thick single V, manual metal site weld.

Approximately 12 weld passes creating six layers approximately 4 to 4.5 mm deep.

Inspection: Root dye penetrant and single wall single image radiography.

Weld B

A 25.4 mm or one-inch submerged arc double V, automatic weld.

Four single passes, each approximately 6 to 6.5 mm deep.

Inspection: Single wall single image radiography.

Given that NE had combined the data from all their welds to produce the single database, the two simulations of the representative welds were combined in order to compare the model predictions with the NE database. Figure 3 is a plot of this combined pdf together with the NE extrapolated curve.
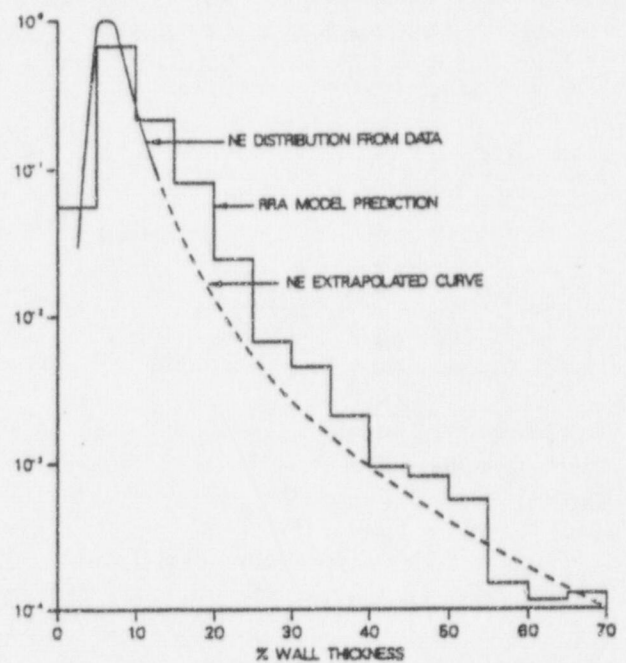
(Wall Thickness 25.4 mm or 1 in.)

Figure 3. Predicted Probability Density Function and the NE Probability Density Function Derived from the Data

It can be seen that the pdf is in exceptionally good agreement with that adopted by NE from the data. However, it should be remembered that the NE curve is itself only an extrapolation from the data, the form of which, i.e., the Gumbel Type II, is based on expert judgment.

We now turn our attention to the question of defect density. In determining the defect density, NE only considered indications that could be reasonably categorized

as crack-like, i.e., those that had a measurable through-wall dimension. This through-wall dimension was set at 4 mm. The density expressed per m³ of weld was estimated using the equation:

$$\text{Volume} = (0.4 \times \text{thickness})(\text{thickness})(\text{length})$$

The density obtained by NE was 12 defects per m³ (from 23 defects and the volume of examined weld metal).

The model prediction was 90 defects per m³ (see the end of Section 5.6 in connection with defect density).

It can be seen that the model predicts a defect density 7 to 8 times greater than that determined by NE.

It was said earlier that defects at or near the inner surface are of interest from the viewpoint of fracture mechanics and probability of failure. Figure 4 is a pdf of defects simulated by the model for the near inner surface and the inner surface-breaking region. Within this region, the defect density for defects greater than 4 mm drops from 90 defects per m³ to only 18 defects per m³.

5.4 British Nuclear Fuels Pressure Vessel Welds

With the co-operation of British Nuclear Fuels Limited (BNFL), the simulation model was used to predict the data generated by BNFL on their Magnox pressure vessel welds. Unlike the NE data, the BNFL data has the advantage of originating from just one thickness of weld, although there are a few variations of the weld preparation itself. The weld simulated was as follows:

A 51 mm or two-inch double and single V manual metal arc weld.

Approximately 30 weld passes, creating 12 layers, approximately 4 to 4.5 mm deep.

Inspection: Initial root of double V, dye penetrant and final weld single wall single image radiography.

The BNFL data was obtained from time-of-flight ultrasonic examination.
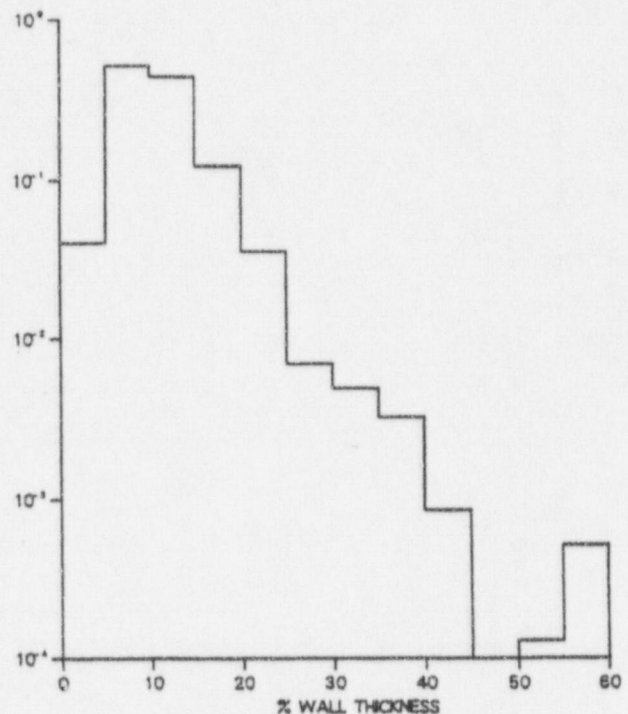
(Wall Thickness 25.4 mm or 1 in.)

Figure 4. Predicted Probability Density Function for Defects at or Near the Inner Surface: Nuclear Electric Weld

Like NE, BNFL split their data into two categories: the small defects that cannot be accurately categorized, and those for which a through-wall measurement can be assessed. To date, BNFL have inspected 46.8 m of weld. A total of 245 indications were recorded; however, all but three were less than 1 mm through-wall depth. These three defects were sized as 2.4, 4.0 and 6.8 mm.

It was not possible to derive a pdf from so few a number of defects and so, to compare the model, we simply predicted what we would expect to see from an inspection of 46.8 m of weld.

Figure 5 is a plot of the predicted pdf with a predicted total defect density of 1.46 defects per meter of completed weld. It can be seen that this pdf is quite similar to that for the NE pdf. If we ignore defects less than 5% of the wall thickness (1.3 mm) as those that could not be categorized, the defect density drops to 0.4 defects per meter
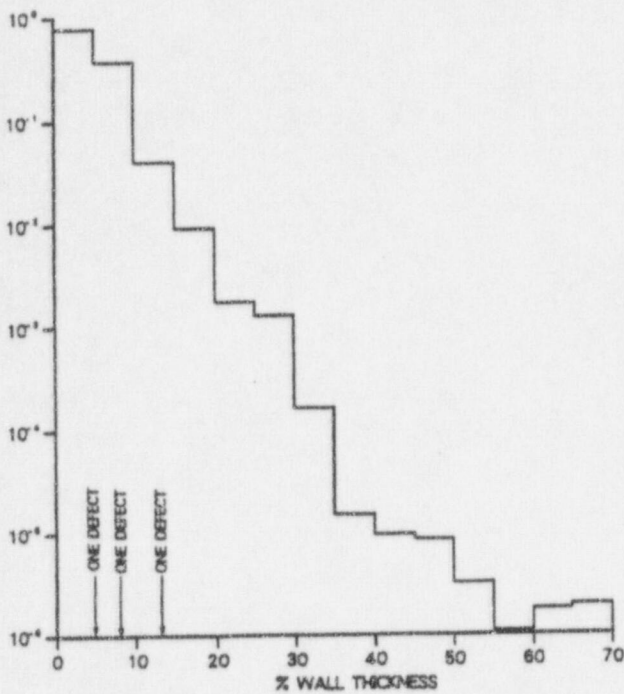
(Wall Thickness 51.4 mm or 2 in.)

Figure 5. Predicted Probability Density Function for the British Nuclear Fuels Weld

of weld. The defect density over the range 5 to 15% of the wall thickness is 0.39, leaving just 0.02 defects greater than 15% (7.6 mm). Thus the model would predict that, for 46.8 m of weld, there would be about a 90% chance of seeing a defect greater than 10 mm, with 18 to 19 defects expected over the range of 1.3 to 7.6 mm.

This shows that the model is again giving a very good general description of what has been observed but with an over-prediction of the number of defects by a factor of 6 to 7, which is very similar to the over-predictions of the NE simulation.

Figure 6 is a plot of the defects at or near the inner surface of the vessel weld. Again, a significant drop in defect density is seen, from 1.46 to 0.38 defects per meter of finished weld.
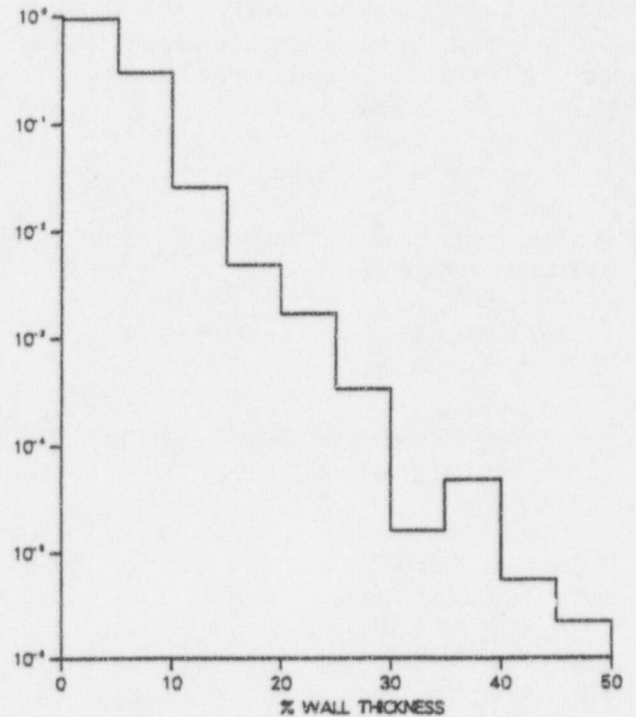
(Wall Thickness 51 mm or 2 in.)

Figure 6. Predicted Probability Density Function for Defects at or Near the Inner Surface: British Nuclear Fuels Weld

5.5 Preliminary Work for the Midland Reactor Pressure Vessel

The seam welds of the reactor pressure vessel (RPV) for the Midland plant were ultrasonically examined to locate regions containing indications. These regions were then subjected to destructive examination to establish the true nature of the indications. In this way, true crack-like defects can be identified and a very accurate sizing of the through-wall depth is obtained.

A total of 0.185 m^3 of the 8 $^9/_{16}$-in. thick seam weld were inspected. While a large number of small imperfections less than 1 mm have been found, only two crack-like

14

defects were observed (Lance 1992). These two defects were sized as 2.75 mm and 7.75 mm. As with the BNFL data, it is not possible to construct a pdf from this limited amount of data; we have, therefore, run the model again to predict what would be expected from an inspection of this volume of weld.

The simulation model used for this prediction contains the values in Tables 3 and 4 of Lance (1992), which are those values for the thicker vessel welds that were developed at the meetings held in Washington, D.C. with RPV welding engineers.

The weld was simulated as follows:

A 217 mm or 8-$^9/_{16}$-in. thick sub arc double V weld.

Approximately 34 weld layers containing 95 passes approximately 6 to 7 mm deep.

Inspection: Completed weld has a single wall single image radiography, and a final dye-penetrant inspection.

Figure 7 is a plot of the predicted pdf together with the Marshall pdf (see Marshall 1982). This plot, as it stands, is far too coarse to compare with the defects found. Furthermore, it is a pdf and we must include the defect density in order to make a comparison. The number of defects simulated per meter of finished weld was 1.25, which converts to 126 defects of any size per m^3 of weld.

The model predicted that approximately 20 to 22 defects up to 10 mm deep (approximately 1.5 beads deep) should have been observed within the volume of weld inspected. In fact, only two have been observed, which implies an over-prediction of about ten, consistent with the two earlier comparisons on the thinner section welds. However, it is interesting to break this comparison down further. If we look at the predicted number of defects up to 7 mm deep, i.e., up to one bead in depth, then the prediction is 18 to 20 defects as against only one measurable defect. However, the number of defects predicted between one and two beads deep is only 3 to 4, whereas one has been observed. Thus, going beyond the single bead depth, the prediction of defects seems to be quite good.

From the above, it would seem reasonable to conclude that the model has provided an acceptable prediction
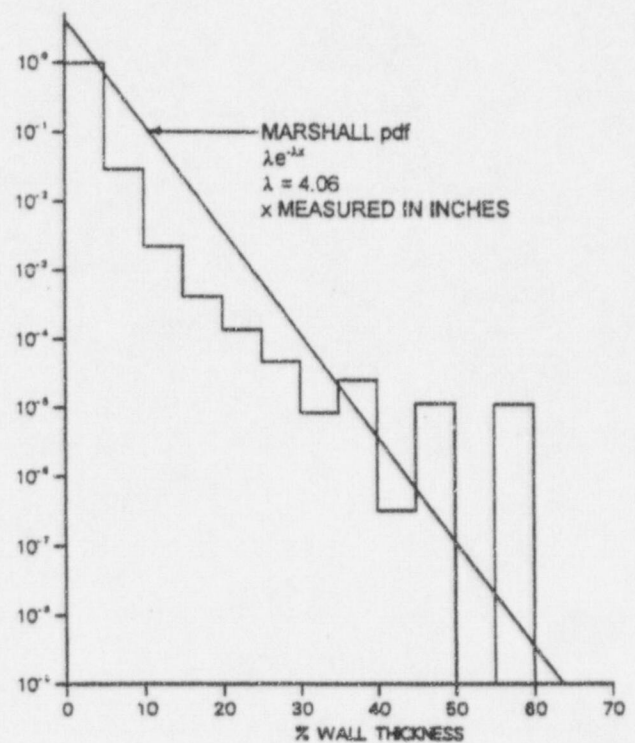
(Wall Thickness 217.5 mm or 8 $^9/_{16}$ in.)

Figure 7. Predicted Probability Density Function for the Midland RPV Seam Weld and the Marshall Probability Density Function

against the observed data, but with perhaps a consistent over-prediction of the number of defects, Figure 8.

Figure 9 is the pdf for the defects at or near the surface of a single V weld. The defect density depends on whether the weld prep is a single or double V. The single V weld, although it has a higher overall defect density, has fewer defects at or near the inner surface than the double V weld described above.

5.6 Comparison with the Marshall Distribution

While it should be clearly understood that the Marshall distribution is itself the result of an expert elicitation, the comparison with our model is of considerable interest. Figures 7 and 9 show that the Marshall exponential distribution passes fairly well through the model prediction;
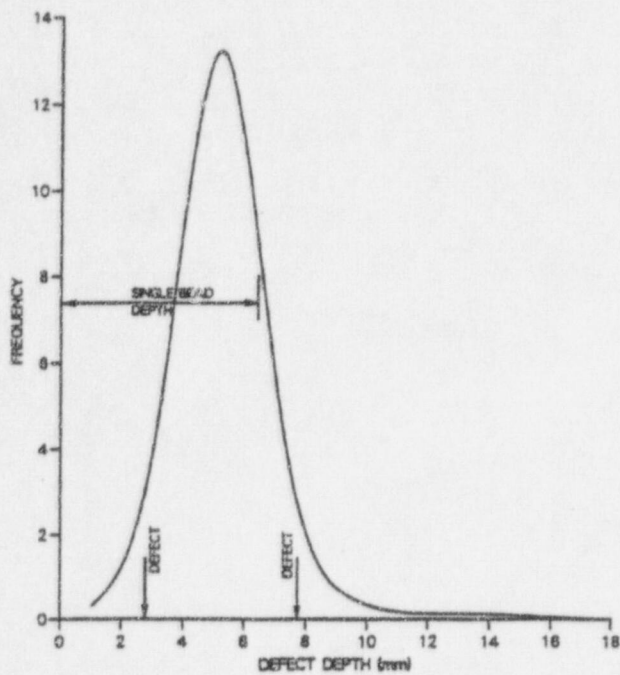
Figure 8. Predicted Frequency Plot for Small Defects for an Inspection Volume of 0.185 m³ (Midland Vessel) (8 ⁹/₁₆ in. thick)

but there is still the tendency for the model to predict a slight curvature, resembling more the Gumbel distribution discussed in Section 5.3. However, when we turn to the defect density, the difference is very dramatic. Marshall (1982) states that the Committee's value of 3.6 defects in the first report is for all sizes per vessel, and that in this case a single vessel contained approximately 3 m³ of weld. This then gives a defect density of 1.2 defects per m³ of weld, a value somewhat different from the model estimate of 390 defects per m³ of weld.

In the first Marshall report, published slightly earlier in 1976, it was stated that the Committee's information derives from both US and UK sources and indicates that, in 44 vessels, 12 defects were found having depths in the range of 0.5 to 1 in.; and that no defects of a depth greater than 1 in. were observed. If we assume that the value of 4.1 for λ as indicated in Figure 7 was derived independently, then the defect density to produce the given observation would be 2.1. Add to this the unspecified information from non-nuclear vessels, and we can justify the 3.6 defects per vessel and hence the 1.2 defects per m³ and the large discrepancy.

(Wall Thickness 217.5 mm or 8 ⁹/₁₆ in.)
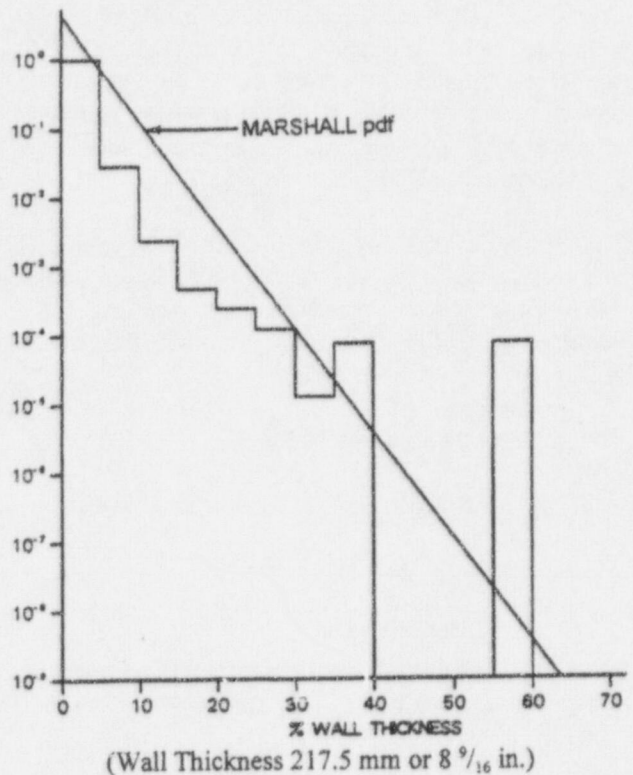
Figure 9. Predicted Probability Density Function for Defects at or Near the Inner Surface (Midland Vessel)

However, if we turn the question around, a different picture emerges. Instead of comparing the defect density per m³ of weld, let us see what the model predicts for the evidence the Marshall Committee were considering.

The first report was published in 1976, and if we allow time for the writing, etc., we must place the data acquisition in the early 1970s. The capabilities of ultrasonic inspection at that time would be significantly lower than today. Let us assume that the inspection was such that only defects greater than 0.5 in. could be clearly identified and recorded as defects. This would tie in with the fact that all the defects reported were in the range of 0.5 to 1 in. The model would then predict that for a vessel weld of 3 m³, we would expect to see eight or nine defects, that is, a factor of two or three more than quoted in the original report. The probability of seeing a defect greater than 1 in. would be about 0.25, so that over the full 44 vessels, the model would have predicted 11 such defects where none was seen. Viewed in this way, it can be seen that the model is in good agreement with the

Marshall report, but again gives this consistent over-estimate of the defect density.

5.7 Reevaluation of Slag Inclusions

In the early development of this simulation program, it was pessimistically assumed that all slag inclusions that remained in the weld would act as crack-like flaws. In this work, the welding experts at the two meetings held in the USA felt that such an assumption was unrealistic. However, none felt able to say that no slag inclusion could ever act as a crack-like flaw. The assumption has therefore been changed, and a probability is placed on any slag-type inclusion as to whether it will remain benign or will be crack-like. This probability is a function of its thickness, and effectively reduces the probability of crack initiation due to slag by a factor of about six to seven. However, the thickness of the slag also affects its inspection capability, which will act to offset the large number of thick slags.

Thus, the NE prediction drops from 90 to 18 as compared with a measured density of 12, i.e., an over-prediction of only 1.5. There would be little or no over-prediction for the BNFL results, and the Midland over-prediction would drop from ten to about two. However, in comparison with the Marshall defect density, the model predictions remain higher by a factor of 60 to 70.

6.0 Conclusions

The comparisons between the data sources and the original modeling assumptions (i.e., Chapman 1993) are consistently pessimistic in terms of the number of observed crack-like defects. Modifications made during this round of meetings with welding experts would appear to have addressed this overestimate, which was felt to stem from a pessimistic view with regard to the crack-like nature of embedded slag.

In terms of the distribution shape for very deep flaws, there is no meaningful data with which to compare the predictions of the model. The comparison with NE data is, however, interesting in that the distribution chosen by NE to extrapolate the data was a Gumbel Type II. While PRODIGAL makes no assumptions about the final distribution shape, it is interesting to note that it effectively identifies a series of different types of defects, each of which will presumably have its own distribution, and combines these to make the single 'total defect distribution.' It is the extremes of these individual distributions, together with their densities, that control the tail of the final 'total defect distribution;' which could in turn lead to an extremal form of distribution such as a Gumbel Type II! Thus, it could be argued that the individual defect type distributions are exponential, as per the Marshall assumption, but that the final distribution is a sum of such distributions which could be Gumbel in nature, as the model appears to predict.

The model has shown that experts can provide excellent relative and even absolute judgments within their areas of speciality and that this knowledge can then form the basic elements for a simulation model to predict what would happen in a variety of real situations. The key difference between the approach used here and others is that the experts are not required to make judgments outside their normal experience, i.e., judgments about rare events. Instead, they are asked to make judgments about the basic building blocks that make up the model, judgments which should be within their known experience. It is the simulation that then attempts to estimate the probability of a set of circumstances that lead to the rare event of a large defect.

7.0 References[a]

Chapman, O.J.V. 1993. "Simulation of Defects in Weld Construction," PVP-Vol 251 Reliability and Risk in Pressure Vessels and Piping, ASME 1993.

Lance, J., et al. 1992. "Flaw Distributions and Use of ISI Data in RPV Integrity Evaluations," Edited by M. J. Wittle, K. Iida, F. Ammirato and G. M. Light, ASM 11th International Conference on NDE in the Nuclear and Pressure Vessel Industry, Albuquerque, USA, April 30 - May 2, 1992.

Marshall, D. W. 1982. "An Assessment of the Integrity of PWR Pressure Vessels," Second Report by a Study Group under the Chairmanship of D. W. Marshall, published by the UKAEA, March 1982.

Simonen, F. A. 1994. "Meeting Minutes - NRC Flaw Distribution Workshop." December 7-8, 1994, Rockville, Maryland.

Simonen, F. A. 1996. "Meeting Minutes - NRC Meeting on Clad Region Flaws." Jul 29-30, 1996, Rockville, Maryland.

(a) Available in NRC PDR for inspection and copying for a fee.

Appendix A

Parameters for Thick Vessels Incorporated into RR-PRODIGAL Database

Appendix A

Parameters for Thick Vessels Incorporated into RR-PRODIGAL Database

This appendix details (Tables A.1 and A.2) the relative scorings and absolute conversion values assigned at the two workshops held in the USA. These workshops addressed the specific question of thick section vessels built for the US Nuclear Program. Table A.3 documents the parameters which describe the characteristics of the simulated defects. Figures A.1 thorugh A.16 are plots of the distribution functions listed in Table A.3.

The weightings shown in Tables A.1 and A.2 of Appendix A were allocated on a scale of 1 to 9. "1" represents a low probability of occurrence for the defect in question; for example, a weld is not prone to reheat cracking unless it is subjected to subsequent heat treatment. "9" represents a very high probability of occurrence for the defect in question; for example, a highly-restrained weld is extremely prone to shrinkage cracks and has been given a weighting of "9".

Table A.1. Effects of Welding Factors on the Probability of Defect Occurrence (Main Vessel)

		Type of Defect					
		Shrinkage Cracks	HAZ DHC	HAZ SRC	Lack of Fusion	Pores with Tails	Slag
Process	Manual Metal Arc (MMAW)	5	7	7	6	8	6
	Submerged Arc (SMAW)	7	6	6	4	6	4
	Manual TIG with Filler (GMAW)	4	4	4	3	4	0
	Automatic TIG with Filler (GTAW)	5	4	4	3	4	0
Restraint	High	9	9	9	5	5	5
	Medium	5	5	5	5	5	5
	Low	2	2	2	5	5	5
Material as Welded	Carbon or CMn Steel, SA 533 B	6	3	2	5	6	5
	Carbon or CMn Steel, SA 508	6	8	8	5	6	5
	Austenitic Stainless Steel, Ferrite Controlled	2	2	1	5	4	5
Location	Shop	5	5	5	6	6	6
	Field	7	7	7	7	7	7
Access	Good	3	3	3	3	3	3
	Average	5	5	5	5	5	5
	Restricted	7	7	7	7	7	7
Position	1G	5	5	5	5	5	5
	Conversion to Defect Density per mm of Weld Laid	1×10^{-10}	7×10^{-13}	3×10^{-13}	5×10^{-10}	2×10^{-10}	3×10^{-10}

Table A.2. Effects of Welding Factors on the Probability of Defect Occurrence (Clad)

		Type of Defect			
		Shrinkage Cracks	Lack of Fusion	Pores with Tails	Slag
Process	Submerged Arc	8	4	6	2
	Submerged Arc, Strip	2	4	8	2
	Manual TIG with Filler	4	4	4	0
	Shielded Metal Arc	6	6	6	6
Restraint	Low	2	5	5	5
Material as Welded	Austenitic Stainless Steel, Ferrite Controlled	2	5	4	5
Location	Shop	5	6	6	6
Access	Good	3	3	3	3
Position	1G	5	5	5	5
	Conversion to Defect Density per mm of Weld Laid	2.5×10^{-11}	1.5×10^{-10}	2×10^{-10}	1×10^{-10}

Table A.3. Parameters for the Defects that Occur During Welding (Vessel and Clad)

Defect Type	Defect Width[a] (Beta)[b]		Defect Depth[c] Initiation (Weibull)[d]	Length to Depth Ratio (Weibull)	Defect Angle[e] (Beta)		Probability of Forward Propagation
Shrinkage Cracks (associated with individual weld passes)	Min = 0.05, a = 3	Max = 0.5mm b = 5	Min Size = 0 η = 0.7 Weld Run β = 3.0	Min Length = Depth η = 6 x Depth β = 1.5	Range ± 15° of vertical line through weld a = 2	b = 2	Zero
Heat Affected Zone (HAZ) cracks DHC	Min = 0, a = 2	Max = 0.5mm b = 7	Min Size = 0 η = 0.25 Weld Run β = 2.0	Min Length = Depth η = 4 x Depth β = 2.0	Range ± 5° of side wall a = 2	b = 2	0.7
Heat Affected Zone (HAZ) cracks SRC	Min = 0, a = 2	Max = 0.5mm b = 7	Min Size = 0 η = 3.5 Weld Run β = 2.0	Min Length = Depth η = 4 x Depth β = 2.0	Range ± 5° of side wall a = 2	b = 2	0.0
Lack of Fusion (Side Wall Weld Fill)	Min = 0, a = 3	Max = 0.5mm b = 6	Min Size = 0.5mm η = 1 Weld Run β = 5.5	Min Length = 3 x Depth η = 9 x Depth β = 2.0	Range ± 5° of side wall a = 2	b = 2	0.2
Lack of Fusion between Runs (weld Fill)	Min = 0, a = 3	Max = 0.5mm b = 6	Min Size = 0 η = 0.6 Weld Run β = 5.5	Min Length = 5 x Depth η = 12 x Depth β = 2.0	Min = 70°, Max = 90° vertical line through weld a = 5	b = 3	0.02
Pores with Tails	Not needed		Min Size = 0 η = 0.64 Root Run β = 5.0	Min Length = 0.3 x Depth η = 0.2 x Depth β = 3.0	Not Needed		Zero
Slag Between Runs	Min = 0.5, a = 3	Max = 4mm b = 8	Min Size = 0 η = 0.6 β = 5.5	Min Length = 3 x Depth η = 12 β = 2.0	Min = 70°, Max = 90° vertical line through weld a = 5	b = 3	0.02
Slag Against Side Wall	Min = 0.5, a = 3	Max = 4mm b = 8	Min Size = 0 η = 0.6 β = 5.5	Min Length = 3 x Depth η = 12 β = 2.0	Range ± 5° of side wall a = 2	b = 2	0.5

(a) Defect Width = Separation between opposite surfaces of flaw.

(b) A beta random variable X on [0,1] has the density; $f(x) = x^{a-1}(1 - x)^{b-1}/B(a,b)$ beta random variables on [Min,Max] are obtained by the transformation Min + (Max - Min) X.

(c) Defect Depth = Through-wall dimension of flaw.

(d) If X has a Weibull distribution, then $f(x) = \beta\eta^{-\beta} x^{\beta-1}\exp(-(x/\eta)^{\beta})$ for x > 0.

(e) Defect Angle = Angle between plane of flaw and a line normal to vessel surface.

SHRINKAGE DEFECT
DEFECT WIDTH BETA DISTRIBUTION
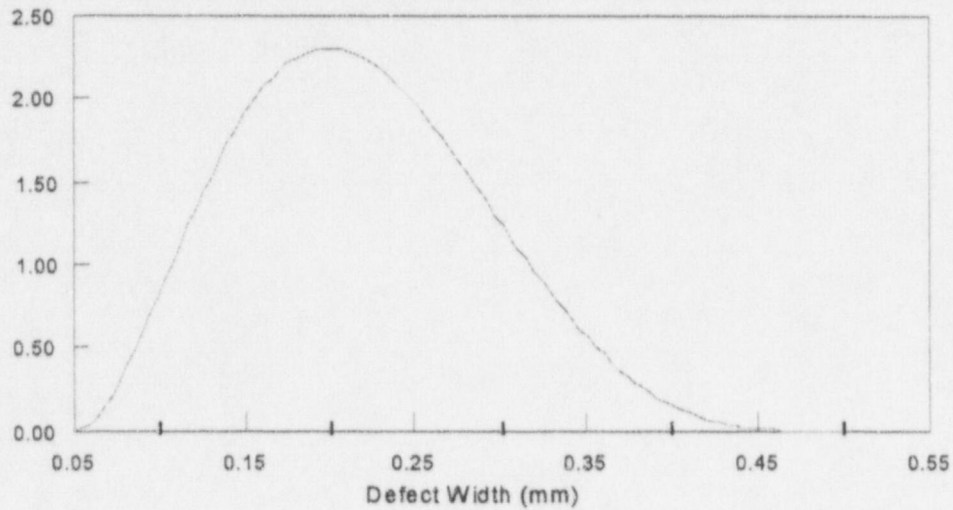
HEAT AFFECTED ZONE (DHC & SRC) DEFECT
DEFECT WIDTH BETA DISTRIBUTION
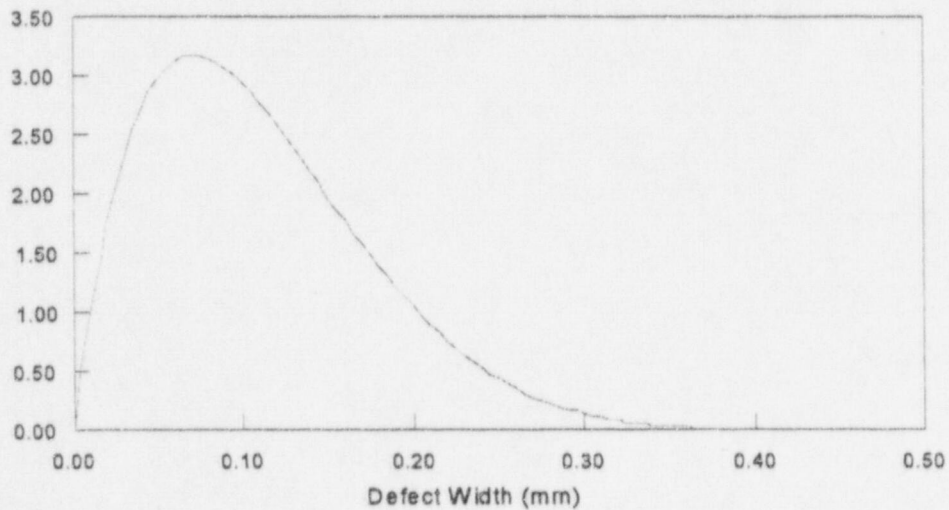
Figure A.1. Probability Density Functions Describing Defect Widths for Shrinkage Defects and Heat Affected Zone Defects

LACK OF SIDEWALL FUSION DEFECT
DEFECT WIDTH BETA DISTRIBUTION
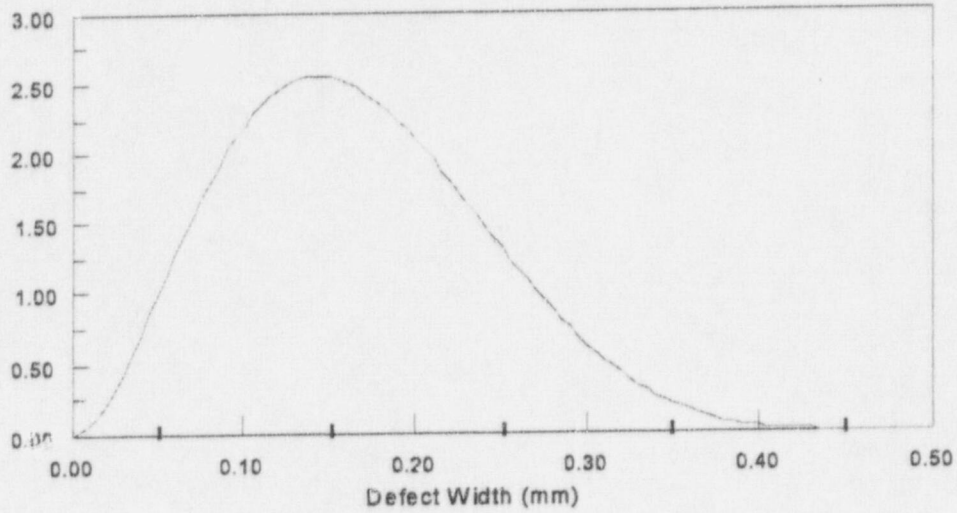
LACK OF INTERRUN FUSION DEFECT
DEFECT WIDTH BETA DISTRIBUTION
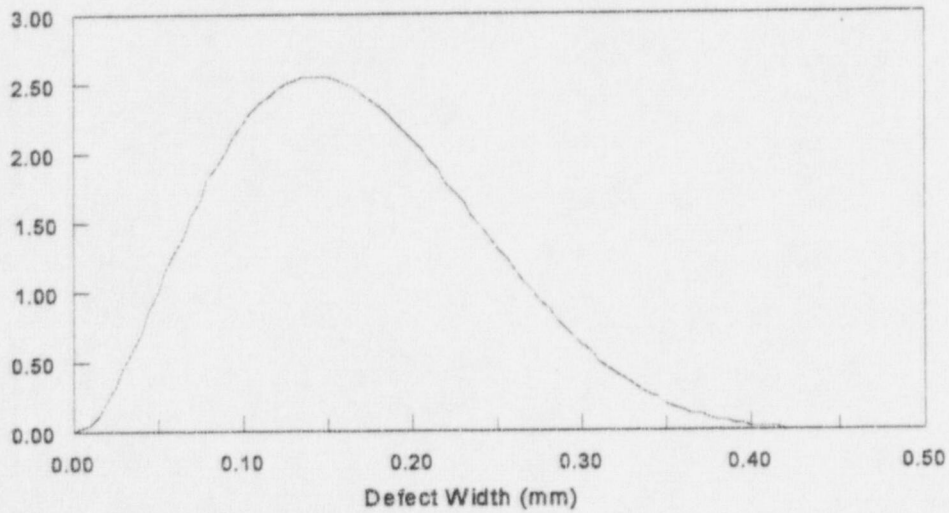
Figure A.2. Probability Density Functions Describing Defect Widths for Lack of Sidewall
Fusion Defects and Lack of Interrun Fusion Defects

INTERRUN SLAG DEFECT
DEFECT WIDTH BETA DISTRIBUTION
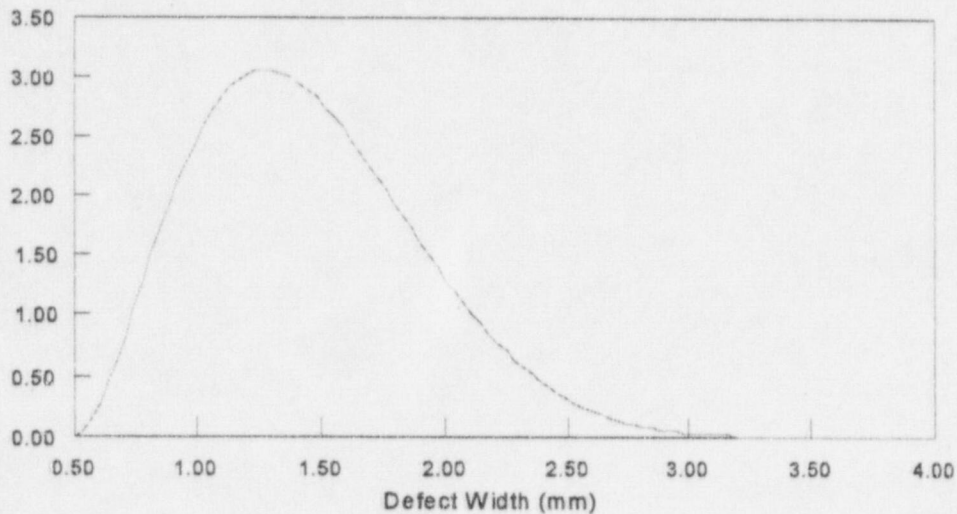
SIDEWALL SLAG DEFECT
DEFECT WIDTH BETA DISTRIBUTION
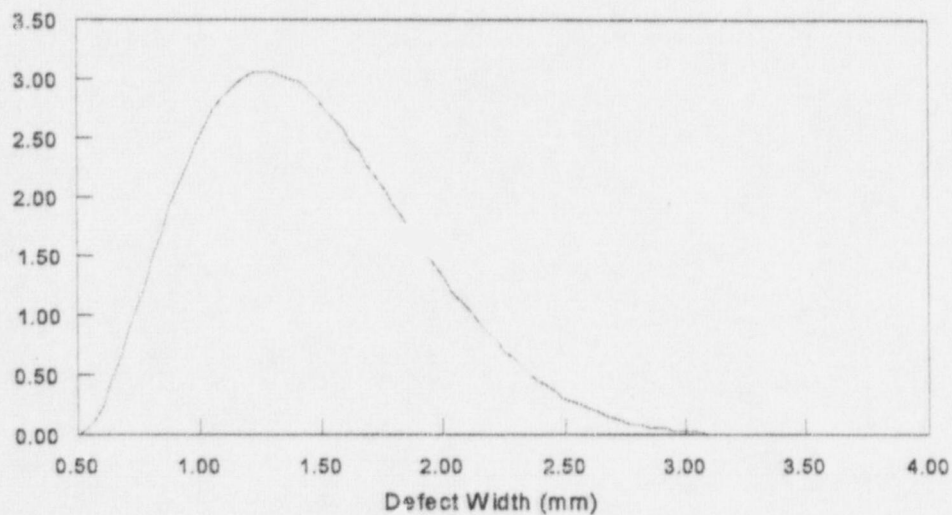
Figure A.3. Probability Density Functions Describing Defect Widths for Interrun Slag Defects and Sidewall Slag Defects

SHRINKAGE DEFECT INITIAL DEFECT SIZE
WEIBULL DISTRIBUTION
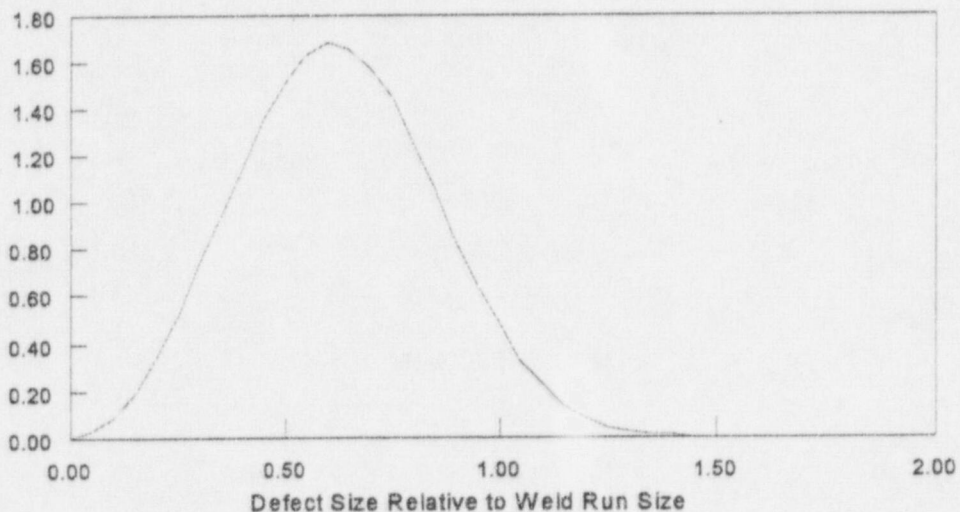
HEAT AFFECTED ZONE DEFECT (DHC) - INITIAL DEFECT
WEIBULL DISTRIBUTION
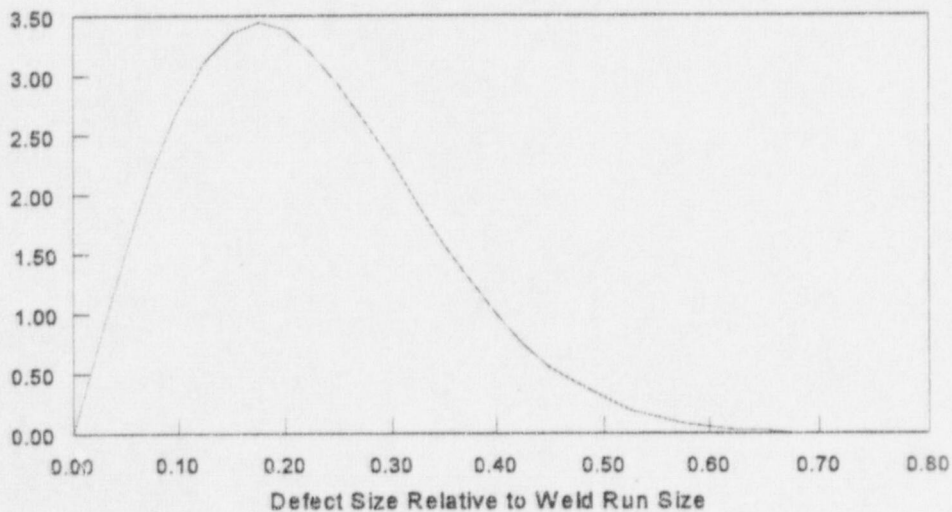
Figure A.4. Probability Density Functions Describing Defect Depths for Shrinkage Defects and Heat Affected Zone (Delayed Hydrogen Cracking) Defects

HEAT AFFECTED ZONE DEFECT (SRC) - INITIAL DEFECT
WEIBULL DISTRIBUTION
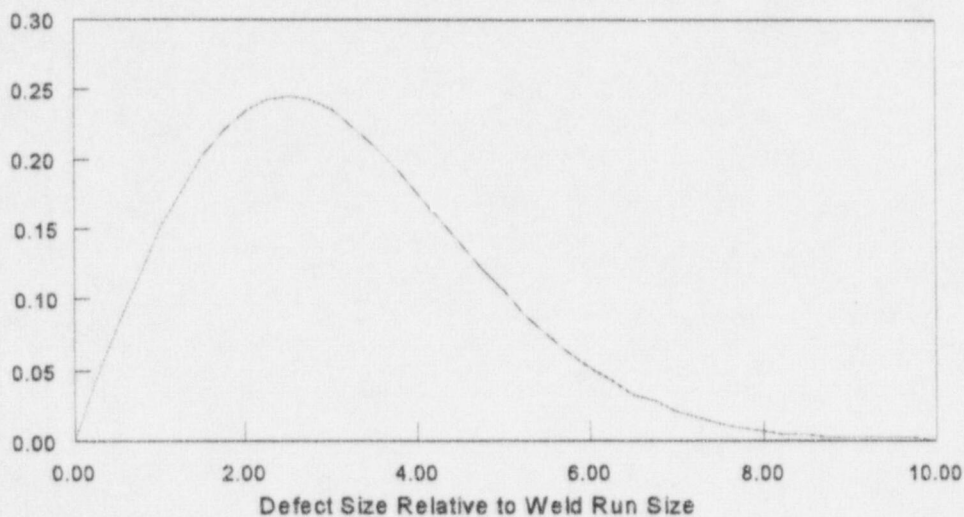
LACK OF SIDEWALL FUSION DEFECT - INITIAL DEFECT
WEIBULL DISTRIBUTION
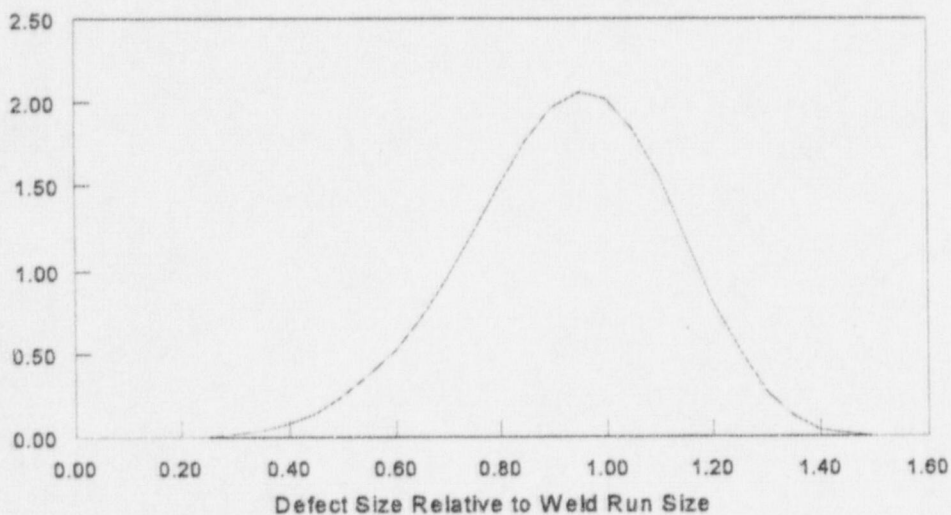
Figure A.5. Probability Density Functions Describing Defect Depths for Heat Affected Zone
(Stress Relief Crack) Defects and Lack of Sidewall Fusion Defects

LACK OF INTERRUN FUSION DEFECT - INITIAL DEFECT SIZE
WEIBULL DISTRIBUTION

Defect Size Relative to Weld Run Size
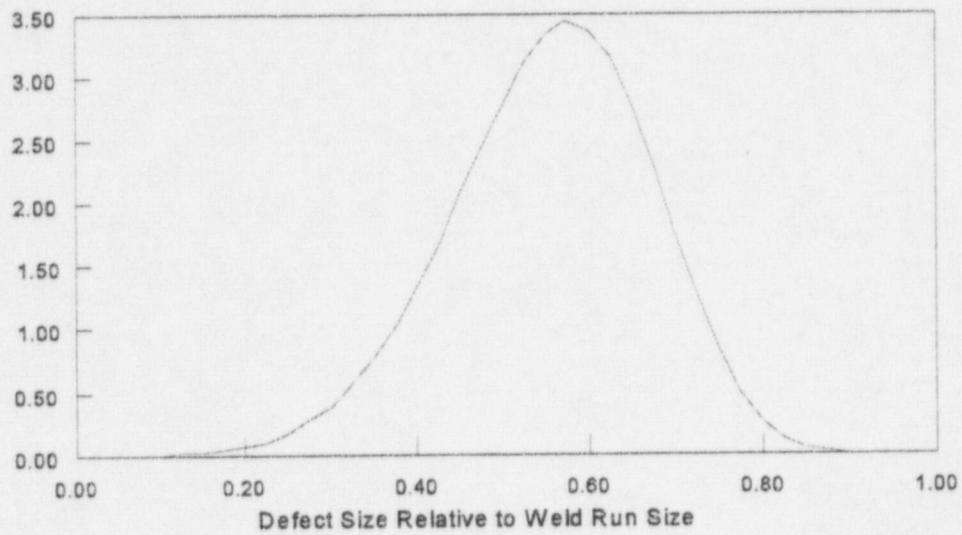
PORES WITH TAIL DEFECT - INITIAL DEFECT SIZE
WEIBULL DISTRIBUTION

Defect Size Relative to Weld Run Size
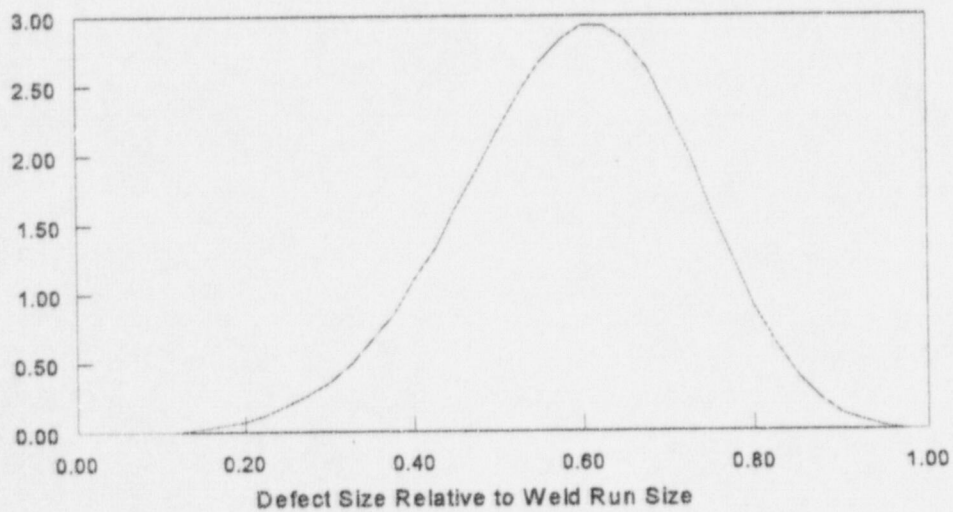
Figure A.6. Probability Density Functions Describing Defect Depths for Lack of Interrun Fusion Defects and Pores with Tails Defects

INTERRUN SLAG DEFECT - INITIAL DEFECT SIZE
WEIBULL DISTRIBUTION
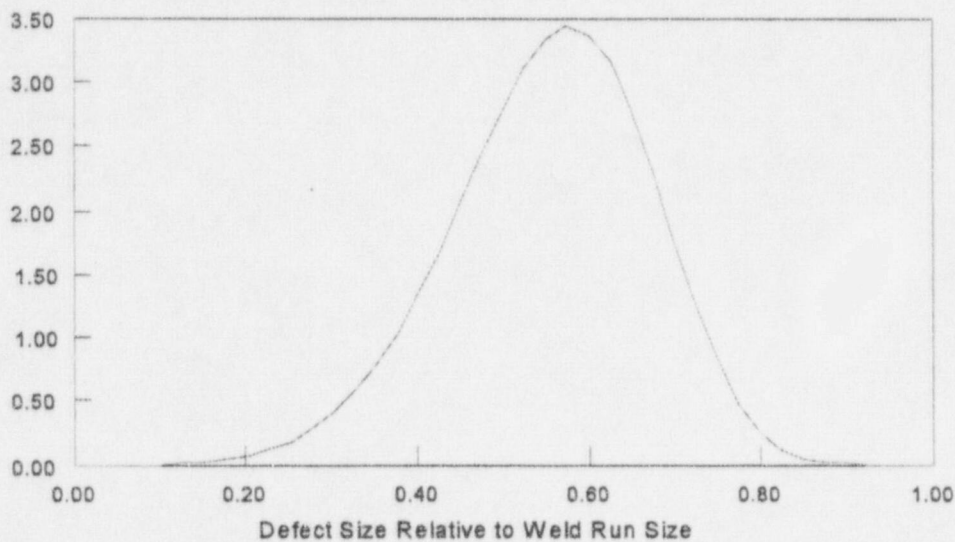
SIDEWALL SLAG DEFECT - INITIAL DEFECT SIZE
WEIBULL DISTRIBUTION
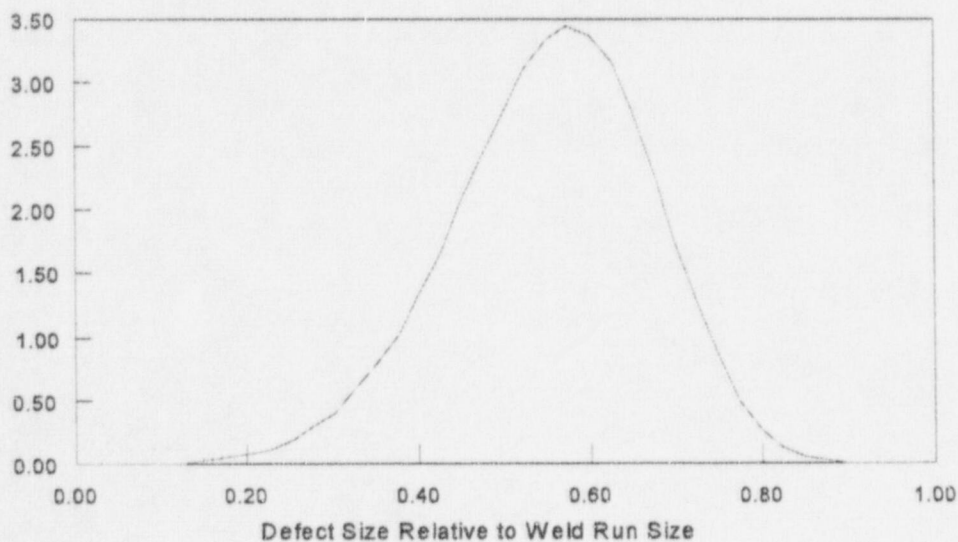
Figure A.7. Probability Density Functions Describing Defect Depths for Interrun Slag Defects and Sidewall Slag Defects

SHRINKAGE DEFECT
ASPECT RATIO WEIBULL DISTRIBUTION
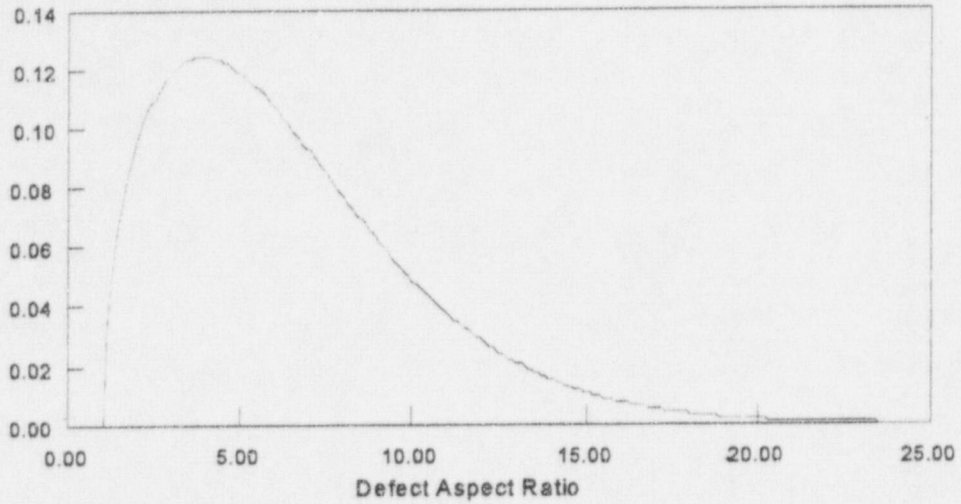
HEAT AFFECTED ZONE DEFECTS (DHC & SRC)
ASPECT RATIO WEIBULL DISTRIBUTION
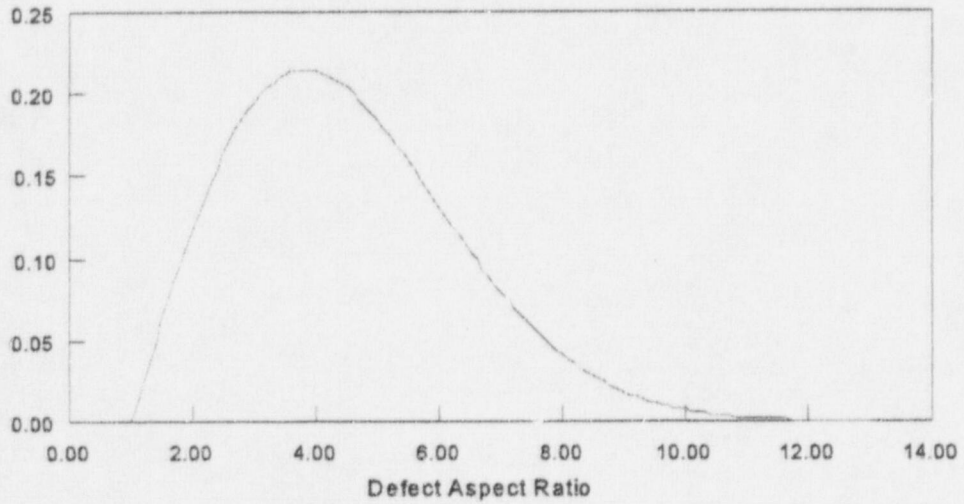
Figure A.8. Probability Density Functions Describing Defect Aspect Ratios for Shrinkage Defects and Heat Affected Zone Defects

LACK OF SIDEWALL FUSION DEFECT
ASPECT RATIO WEIBULL DISTRIBUTION
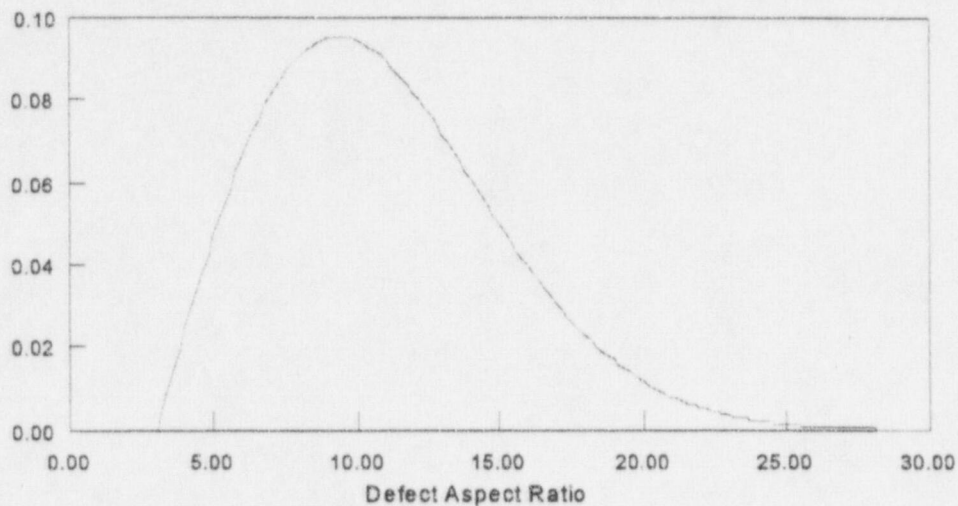
LACK OF INTERRUN FUSION DEFECT
ASPECT RATIO WEIBULL DISTRIBUTION
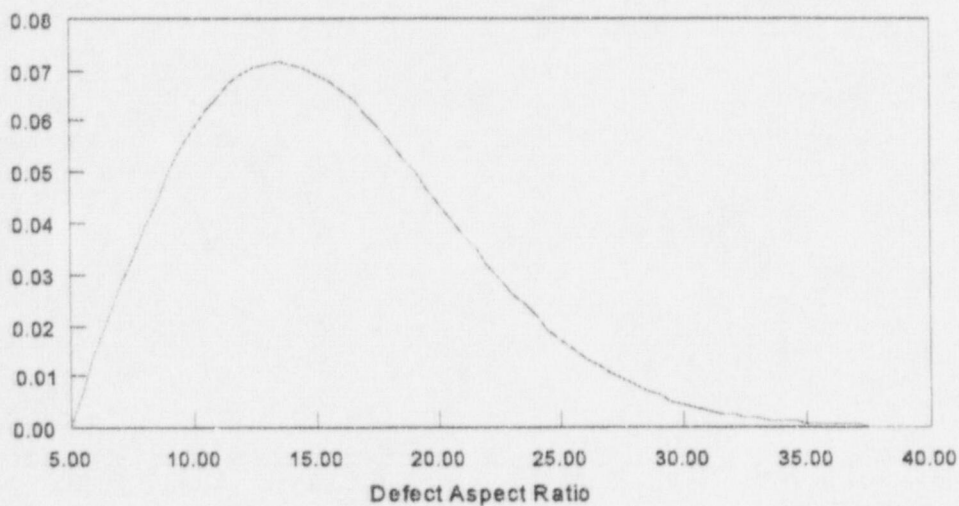
Figure A.9. Probability Density Functions Describing Defect Aspect Ratios for Lack of
Sidewall Fusion Defects and Lack of Interrun Fusion Defects

PORES WITH TAILS DEFECT
ASPECT RATIO WEIBULL DISTRIBUTION

Defect Aspect Ratio
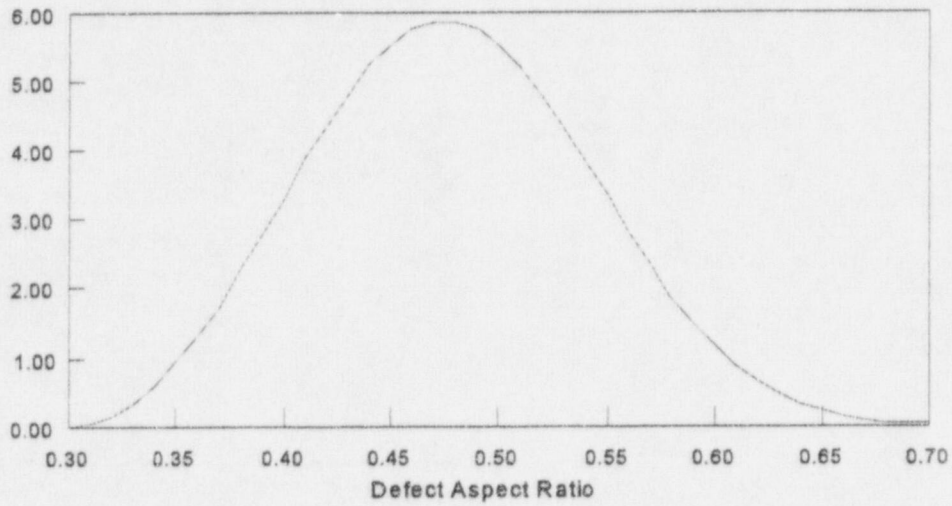
INTERRUN SLAG DEFECT
ASPECT RATIO WEIBULL DISTRIBUTION

Defect Aspect Ratio
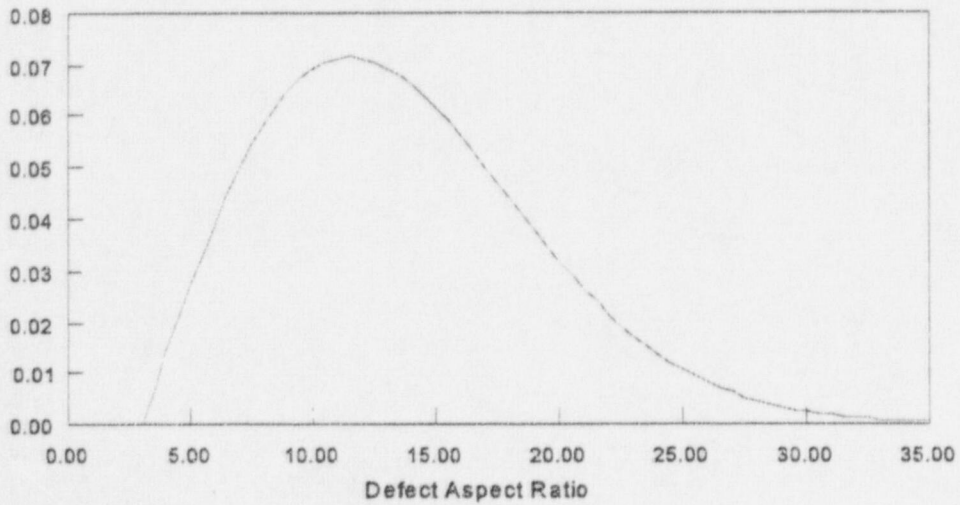
Figure A.10. Probability Density Functions Describing Defect Aspect Ratios for Pores with Tails Defects and Interrun Slag Defects

SIDEWALL SLAG DEFECT
ASPECT RATIO WEIBULL DISTRIBUTION
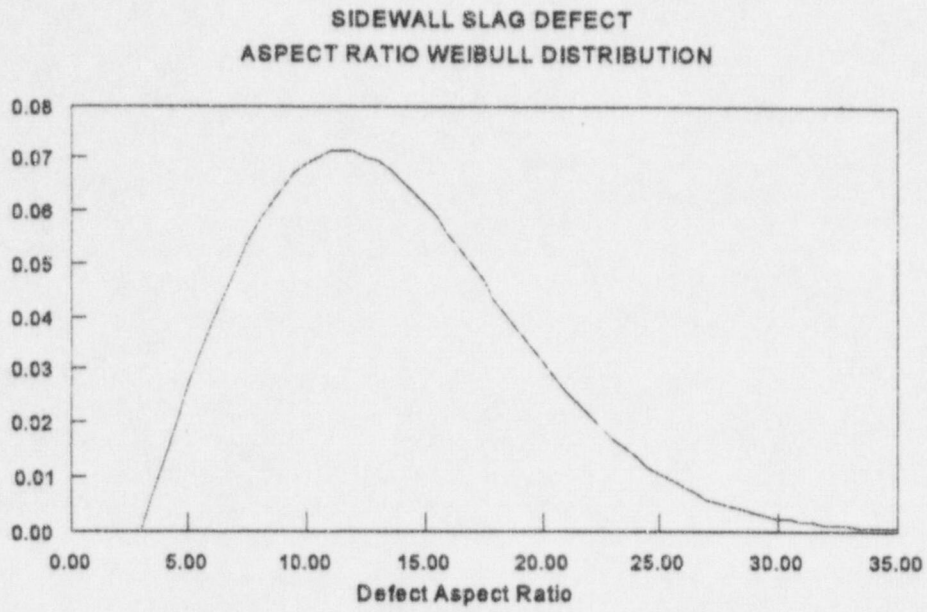
Figure A.11. Probability Density Function Describing Defect Aspect Ratio for Sidewall Slag Defects

SHRINKAGE DEFECT
DEFECT ANGLE BETA DISTRIBUTION
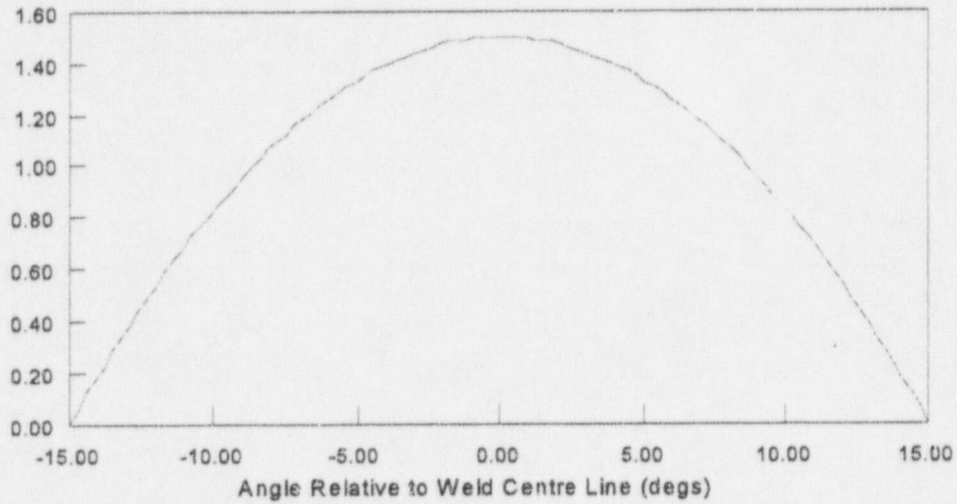
HEAT AFFECTED ZONE DEFECTS (DHC & SRC)
DEFECT ANGLE DISTRIBUTION
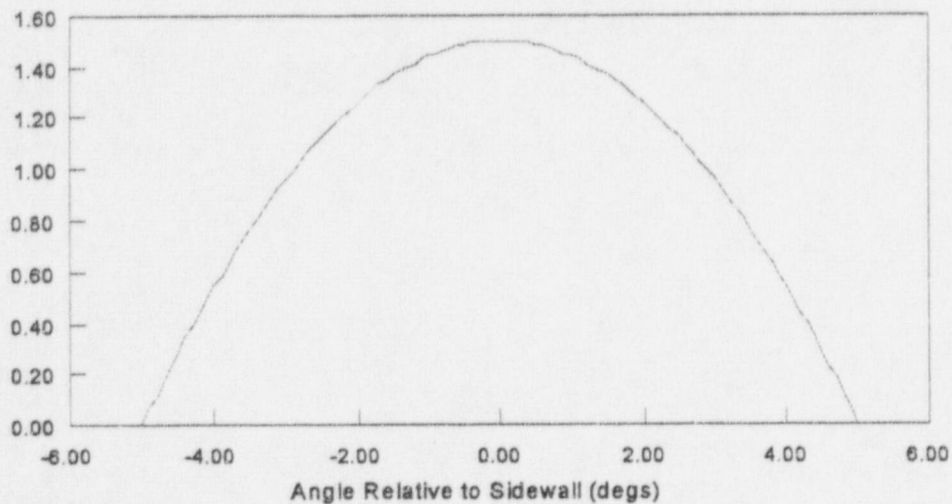
Figure A.12. Probability Density Functions Describing Defect Angles for Shrinkage Defects and Heat Affected Zone Defects

LACK OF SIDEWALL FUSION DEFECT
DEFECT ANGLE BETA DISTRIBUTION
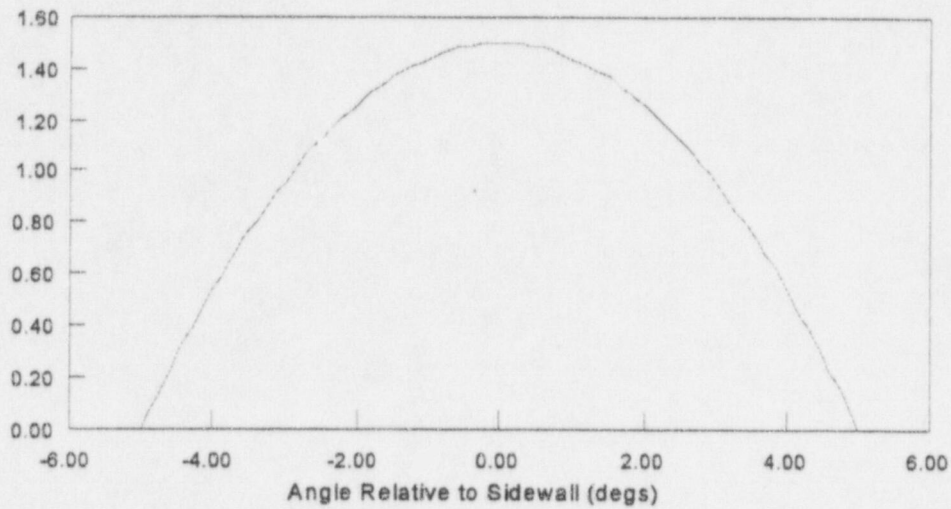
LACK OF INTERRUN FUSION DEFECT
DEFECT ANGLE BETA DISTRIBUTION
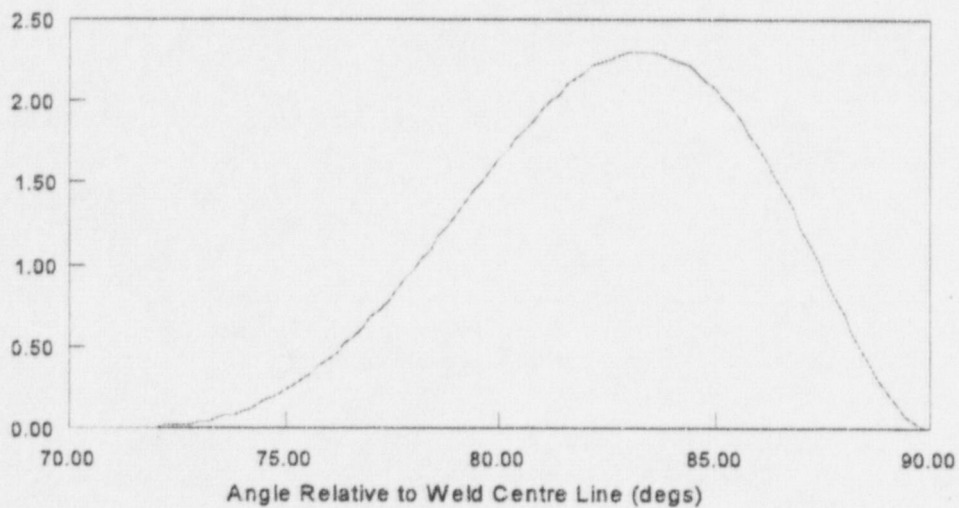
Figure A.13. Probability Density Functions Describing Defect Angles for Lack of Sidewall
Fusion Defects and Lack of Interrun Fusion Defects

INTERRUN SLAG DEFECTS
DEFECT ANGLE BETA DISTRIBUTION
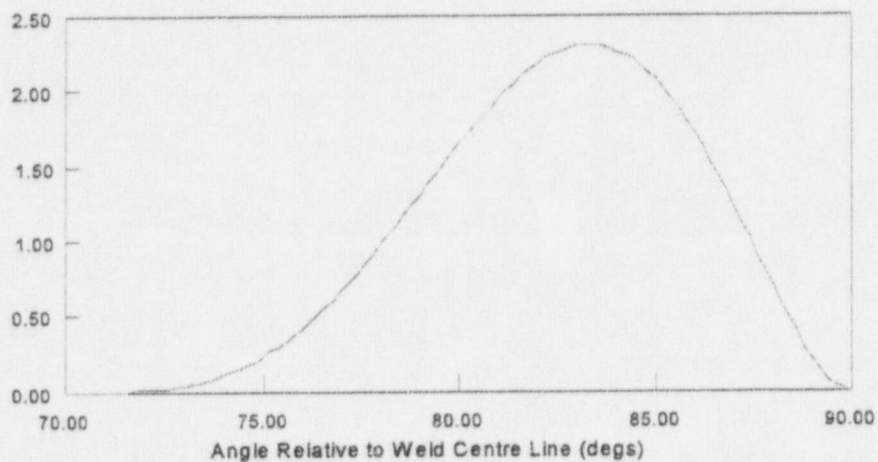
SIDEWALL SLAG DEFECT
DEFECT ANGLE BETA DISTRIBUTION
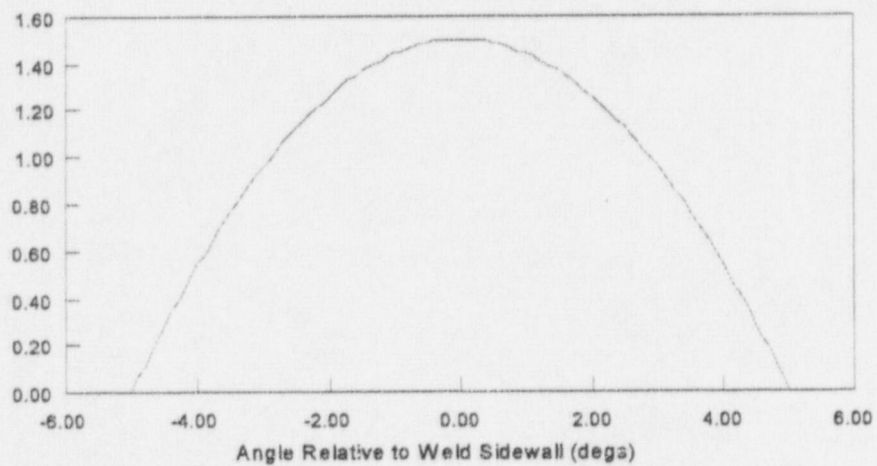
Figure A.14. Probability Density Functions Describing Defect Angles for Interrun Slag Defects and Sidewall Slag Defects

POST WELD HEAT TREATMENT - PROPAGATION POWER
WEIBULL DISTRIBUTION
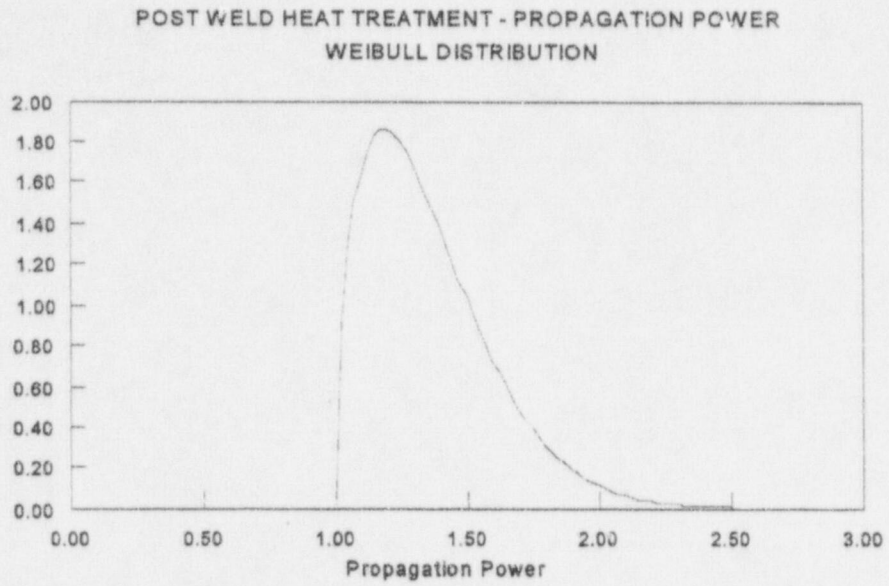
Figure A.15. Probability Density Function Describing Post Weld Heat Treatment Propagation Power

WELD PROPAGATION FACTOR
WEIBULL DISTRIBUTION
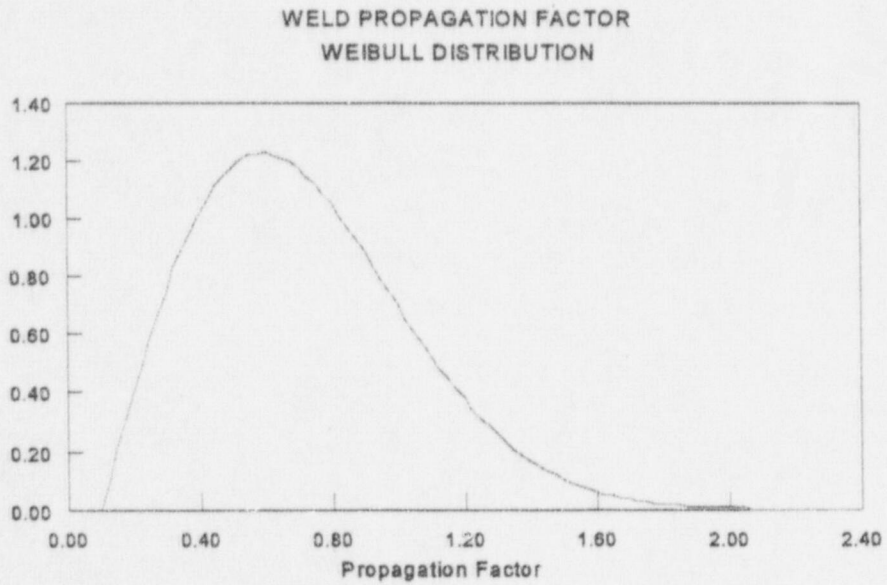
Figure A.16. Probability Density Function Describing Weld Propagation Factors

Appendix B

Defects that Occur in Pressure Retaining Welds and the Factors that Influence Them

Appendix B

Defects that Occur in Pressure Retaining Weld
and the Factors that Influence Them

This appendix gives a more detailed account of the types of defects and welding processes considered for the simulation within the RR-PRODIGAL computer program.

B.1 Glossary of Welding Abbreviations

EBW - Election Beam Welding - Fusion welding in which the joint is made by the impact of a focused beam of electrons.

FCAW - Flux-Cored Arc Welding - A variation of the MIG process in which the arc is formed in a stream of shielding gas between a continuously-fed electrode wire and the workpiece. The wire is flux-cored, and with certain "self-shielded" consumables, no additional shielding gas is necessary.

LW - Laser Welding - Fusion welding in which the joint is made using a focused laser beam as the heat source.

MIG - Metal Inert Gas Welding - Also known as GMAW or gas-shielded metal arc welding. Inert gas-shielded arc welding using a consumable electrode.

MMA - Manual Metal Arc Welding - Also known as SMAW or shielded metal arc welding. An arc welding process using short lengths of flux-covered consumable electrode which are applied by the operator without automatic or semi-automatic means of replacement. No protection in the form of a gas or mixture of gases from a separate source is applied to the arc or molten pool during welding.

SAW - Submerged Arc Welding - Metal-arc welding in which a bare wire electrode or electrodes are used; the arc or arcs are enveloped in a flux, some of which fuses to form a removable covering of slag on the weld.

TIG - Tungsten Inert Gas Welding - Also known as GTAW or gas-shielded tungsten arc welding. Inert gas shielded welding using a non-consumable electrode of pure or activated tungsten.

B.2 Introduction

This appendix covers work on a probability-based vulnerability assessment for welds. In order to make this assessment, a set of figures was required to represent the effects of variable welding conditions (such as process, location, the materials involved, and the joint geometry) on the likelihood of defect occurrence.

No attempt was made to incorporate the effects of repairs or rewelding; only defects produced during "original" welding were considered. Nine major defect types were included in the assessment:

Centerline cracks
Lamellar tears
Transverse cracks
Heat-affected zone cracks
Lack of penetration
Lack of fusion
Non-metallic inclusions
Porosity
Metallic inclusions.

After discussions among the welding, metallurgy, inspection and stress departments, the following types of defects were excluded:

1. Lamellar tears - the weld geometry required for this type of defect did not occur in the welds of interest to nuclear plant.

2. Transverse cracks - the welds were cleared off after each layer and any defects in weld were deemed too small to worry about.

3. Lack of penetration - no welds producing this type of defect occur in naval or commercial nuclear plants.

4. Metallic inclusions - an experimental program indicated that these inclusions were not crack initiators.

Minor defects such as weld overfill, underfill, excessive concavity or convexity were not included, as generally such defects are remedied during production as a matter of course, and lead to no further problems.

The effects of a variety of welding factors were considered, but several were omitted on the basis that they could not be quantified for individual welds. For example, welder skill exerts a major influence on the occurrence of several types of defects, but although a welder's skill may be assessed from details of previous experience and qualifications, no individual rating could be allocated to a single welder producing a weld on a given day. Instead the "degree of difficulty" of a weld has been accounted for by the incorporation of sections relating to welding position, location, and degree of access.

Brief notes follow in the next few sections on the reasoning behind the defect likelihood assessments.

B.3 Centerline Cracking

As a weld bead solidifies and contracts, any impurities present tend to collect at the top center of the bead. The stresses present may then cause a centerline crack along the weld bead due to the presence of low strength or low melting point phases, Figure B.1.

Process

There is greater risk of centerline cracking when welding by autogenous TIG (see Glossary for explanation of abbreviations) or by any other process producing a weld bend with an undesirable width-to-depth ratio. Also, automatic high speed welding (SAW, EBW, LW, automatic TIG) techniques show a greater tendency to centerline segregation (and therefore to centerline cracking) than do manual techniques.

Geometry

The higher the level of weld joint restraint, the higher is the risk of centerline cracking. Tacks and single-pass welds are more susceptible than the roots of multipass welds. The fill runs of large multipass welds are generally the least susceptible. Poorly-fitting joints resulting in a loss of weld section are also susceptible.

Materials

Particularly susceptible materials include Type 347 stainless steel, ferrous alloys contaminated by sulphur and/or phosphorus, monel and cupronickel. Nickel alloys are also prone to sulphur pickup, leading to centerline cracking.

Welding Location

Laboratory welds are assumed to be deposited under virtually ideal controlled conditions by skilled welders. Welds produced by vendors are taken as intermediate, and boat welds as the most prone to defects, depending on welder skill and environment. Thorough cleaning of the weld preparation is required to avoid contamination, and this is entirely dependent upon the welder. Undesirable width-to-depth ratios may also be welder-generated, and may lead to centerline cracking.

Welding Position and Access to Weld

Centerline cracking is not dependent on these factors.

B.4 Heat-Affected Zone Cracking

HAZ defects can occur at two periods during the manufacturing process. The first occasion occurs just after the welding process when the metal starts to cool below approximately 100°C. During this period, hydrogen can diffuse from the weld metal into the hardened heat-affected zones and cause cracking. The hydrogen may come from moisture in or on the welding consumable or on the joint faces or from other contaminants. This type of HAZ cracking is called delayed hydrogen cracking (DHC). The second form of HAZ cracking is called reheat or stress relief cracking (SRC). These cracks form after post-weld heat treatment (PWHT) and are caused by the dissolution of the material in the HAZ, and its grain structure becoming coarsened. Subsequently during PWHT, precipitation may occur from within the grains in this region, causing them to strengthen so that residual stress relaxation occurs only by sliding of the grain boundaries, with virtually no grain deformation; thus causing cracking, Figure B.1.

Process

The higher the hydrogen potential of the welding process, the greater the chances of HAZ cracking. The critical level is 10 ml of hydrogen per 100 g of metal in the weldpool. Also, the lower the heat input, the greater the risk of HAZ cracking, due to the lower level of diffusivity of any hydrogen gas present.

Geometry

The thicker the joint sections, the larger the heat sink and the higher the chances of HAZ cracking. Multirun welds are more susceptible than single runs. The higher the level of weld joint restraint, the higher the risk of HAZ cracking.

Materials

The higher the carbon equivalent value of ferritic steels, the more likely is the occurrence of HAZ cracking. Stainless steels and cupronickel are virtually immune to this type of defect; Cr-Mo and Mn-Mo steels are quite high risk materials.

Welding Location

It is assumed that laboratory welds are deposited under virtually ideal controlled conditions by skilled welders. Production welds made by vendors are taken to be intermediate, and site welds as the most prone to defects, depending on welder skill and environment.

Failure to ensure the correct level of preheat or postheat is highly welder-dependent and leads to higher chances of HAZ cracking.

Welding Position and Access to Weld

These factors are unlikely to affect the chances of HAZ cracking.

B.5 Lack of Fusion

The lack of fusion defect is a lack of union between the weld metal and the parent plate or (in multirun welds) between successive weld runs, Figure B.1.

Process

For TIG processes, and oxyacetylene welding in particular, insufficient oxide removal may lead to lack of fusion. Excessive inductance in dip-transfer MIG may also be a problem.

Geometry

The narrower the weld preparation and/or the deeper the nose, the greater is the chance of lack of root fusion. The thicker the weld section, the more chance there is of lack of sidewall fusion.

Materials

Lack of fusion defects are not dependent upon material type.

Welding Location, Position and Access to Weld

Any access difficulty preventing the use of the correct electrode angle will increase the chance of lack of fusion. Welder skill is vital in helping to ensure sufficient fusion when using manual processes. A vertical or overhead workpiece position may lead to slag flooding and lack of fusion.

B.6 Non-Metallic Inclusions

Linear slag inclusions are normally due to incomplete slag removal between weld runs but may occasionally be caused by slag laminations within the parent plate. Isolated slag inclusions can be caused by mill scale or rust on the plate, or by

damaged electrode coatings which denude the weld metal of slag-forming elements of adequate floatability, i.e., slag is left within the weld bead rather than floating to the top for removal, Figure B.1.

In the original work, started in the early eighties, the assumption was made that all non-metallic inclusions should be treated as crack-like defects. While this assumption was believed to be pessimistic even then, at the time there was felt to be insufficient evidence to contradict this assumption. Since that time, the latest expert panel meetings have concluded that there is sufficient knowledge available today for this assumption to be relaxed. The simulation program has therefore been modified, and a function has been introduced that relates the simulated inclusion thickness to the probability of crack initiation.

Process

Slag inclusions are common in MMA and SAW deposits. Oxide inclusions are common in TIG deposits. Turbulent arc conditions in any arc welding process may lead to entrapment between welding runs.

Geometry

The tighter the weld preparation (narrow "V" joint, deep nose, narrow gap) and the thicker the joint, the greater is the likelihood of entrapped inclusions. Single pass welds are less prone to slag inclusions than are multipass welds.

Materials

A dirty base material or an oxidized surface will lead to a greater likelihood of non-metallic inclusions; however, in general the occurrence of non-metallic inclusions is not dependent on factors which will be known about the material prior to welding.

Welding Location

It is assumed once more that laboratory welds are produced under virtually ideal controlled conditions and by skilled and conscientious welders. Welds produced by vendors are taken as intermediate, and boat welds as the most prone to defects which are dependent on welder skill and environment.

Thorough removal of slag between the runs of multipass welds is important - and highly welder-dependent - in avoiding non-metallic inclusions.

Welding Position and Access to Weld

Vertical or overhead working positions may lead to slag flooding the weld. Any access difficulty likely to prevent the use of the correct electrode angle is likely to lead to the occurrence of non-metallic inclusions.

B.7 Porosity

A welded joint will usually contain gas-forming elements. These evolve into phases as the temperature decreases and result in the formation of cavities or porosity. Porosity which occurs uniformly along the weld may be caused by moisture, rust or grease on the plate surface, oxygen or nitrogen contamination from the atmosphere, or oxygen contamination from the shielding gas, Figure B.1.

Where porosity occurs in isolated groups, its most likely cause is the existence of unstable conditions as the arc is being struck. Weld metal may be deposited before the gas shield is established. Isolated porosity which is strung out is more likely to be caused by incorrect electrode angle or strikeout.

Interdendritic porosity or shrinkage porosity may occur at weld stop-start positions and may be linked with solidification cracking.

Process

Fluxless processes such as TIG are more susceptible to porosity than are the fluxed processes such as SAW or MMA. This is because the gas-shielded (fluxless) processes may be prone to loss or contamination of the gas cover (for example, due to excessive electrode stickout in MIG welding), or to entrapment of the shielding gas in the molten welding pool.

Geometry

A narrow weld preparation may lead to turbulence and corresponding loss of cover in the gas-shielded processes.

Materials

Cleanliness of the base material is extremely important, but this may not be either known or controllable prior to welding. A damp or contaminated workpiece or consumables is a frequent cause of porosity. Certain materials such as cast irons and some carbon steels are particularly prone to porosity when welded.

Welding Location

Assumptions regarding the effect of various locations on the occurrence of defects which are dependent upon welder skill and environment are given in Tables A.1 and A.2 of Appendix A. Poor starting/finishing techniques in MMA welding may lead to interdendritic porosity.

Inadequate cleaning of base materials, and damp workpiece, flux, or shielding gas are all factors likely to lead to porosity. On site welds, air drafts may blow away the gas shield.

Welding Position and Access to Weld

Any access difficulty that prevents the welder from maintaining the correct electrode/nozzle - workpiece distance may lead to the occurrence of porosity in the weld.

Pore with Tail

Centreline Crack

Lack of Interrun Fusion
Interrun Slag

HAZ Crack

Lack of Sidewall Fusion
Sidewall Slag
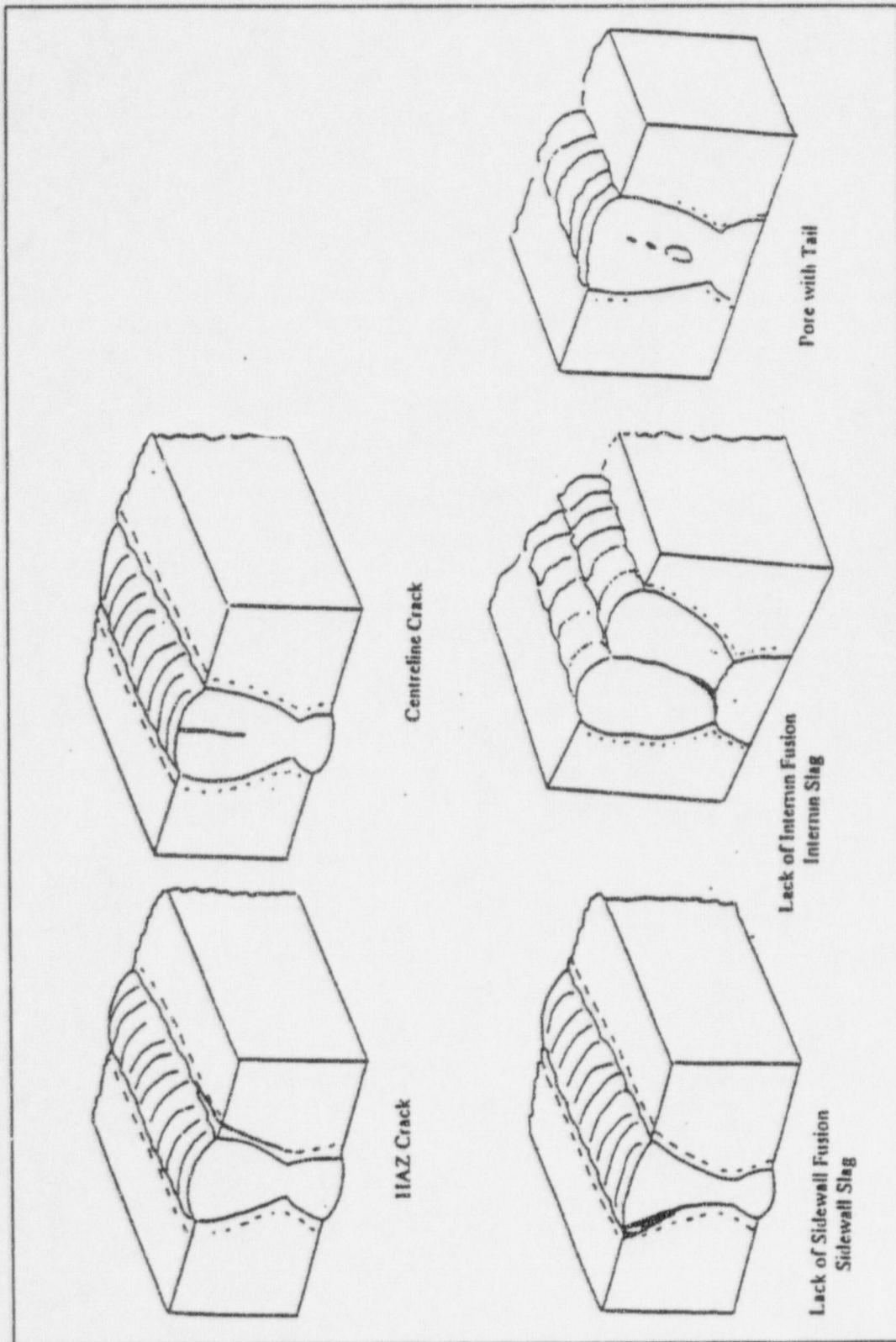
Figure B.1. Types of Crack-Like Defects

Appendix C

Radiographic Inspection Efficiency

Appendix C

Radiographic Inspection Efficiency

This appendix gives a brief description of the theoretical analysis and judgmental decisions that were applied to derive a probability of detection for the different types of defects subject to radiographic inspection.

C.1 Introduction

RAD 96-3d is a FORTRAN computer program which models radiographic inspection. A radiation source beams down through the inspection piece and onto a film to record the optical density, which may indicate the presence of a defect. The defects of interest in this work are narrow crack-like defects, which are modelled by a rectangular slot. This appendix summarizes the theoretical details behind this analysis.

C.2 The Source

A rectangular source is assumed, with its face parallel to the film. The finite size of the source gives rise to a lack of geometric sharpness in the film image. The types of source modelled are x-ray, gamma ray, iridium, cesium, cobalt, and ytterbium.

The source energy level, source-to-film distance and exposure time are chosen so as to produce an optimal exposure of the film. An optical density of about 2.0 is usually sought.

C.3 The Film

The program includes a curve fit to a typical film characteristic. This enables optical densities to be calculated. The film contrast parameter can be found by differentiation, which enables a calculation of the change in optical density due to a defect.

The source-to-film distance, source intensity, and time of exposure are chosen in practice so as to produce an optimum optical density D^* in the range of 2.0 to 2.4 for a test piece of thickness x^*. The program calculates the optical density D corresponding to a thickness x from D^* and x^*, without needing the source intensity and time of exposure.

The defect image on the film is covered by a pre-set mesh of squares, with nodes defined by their corner points. Optical densities are calculated at the nodes.

C.4 Change in Optical Density Due to a Defect

The change in density due to a gap of length Δx in the path of the direct radiation is taken from the work of Halmshaw and Hunt (1975).

$$\Delta_D = (G_D \log_{10} e \, (e^{\mu \Delta x} - 1))/B(\mu, x)$$

where:

G_D is the film contrast coefficient, which is derived from the film sensitometric curve

μ is the attenuation coefficient, which is calculated by interpolation in tables given in McMaster (1959)

B   is the build-up factor, which is calculated from μ and the path length through the metal, from a curve fit given in Halmshaw and Hunt (1975).

The program uses an adaptive integration scheme over the source surface. From each integration point, a ray is traced to the film node under consideration, and the path length Δx through the defect is calculated. It follows that the geometric unsharpness is accurately modelled. After the calculation has been done for all the nodes, the density distribution is modified to take account of inherent unsharpness.

C.5 Inherent Unsharpness

The impact of an x-ray photon on the film causes a blurring over a region of diameter U_i, the inherent unsharpness. U_i is calculated from a curve fit given in Halmshaw and Hunt (1975). The effect of the inherent unsharpness is to reduce the optical density of the point under consideration, and to distribute the excess density to neighboring nodes within a circle of diameter U_i. In return, contributions will be similarly returned from neighboring nodes. The redistributed density reduces nearly to zero on the circumference of the image.

C.6 Defect Representation

Halmshaw & Hunt's (H&H) analysis for a 5 mm deep, 0.025 mm width slot has been reproduced at various angles of flaw misorientation relative to the x-ray path. The resulting optical density profiles are given in Figures C.1 to C.4. As would be expected, the signal gets broader as the angle of misorientation increases, while its maximum strength reduces.

Correlations by H&H of their experiments and analytical results suggest that the limit of detection by the human eye is at an optical density of about 0.006. Experimental work carried out by RRA agrees with this conclusion. It can be seen from Figure C.3 that at an angle of 12 degrees the optical image falls above this level, while at 16 degrees, Figure C.4, it is just below, suggesting that for this slot, the limit of detection is between 12 and 16 degrees misorientation.

Analytical runs for deeper slots, 10 and 15 mm, have also been carried out. As one could predict from the theory, the maximum signal from a misoriented slot does not depend upon this increasing depth. Figures C.5 to C.6 show the optical image for the 10 and 15 mm slots at 12 degrees and, although the width of the optical image has increased for the 15 mm slot, the plateau value remains at just above 0.006.

While the optical image from a straight slot-like defect may be considered representative for some naturally occurring manufacturing defects, i.e., a 'shrinkage crack' or small 'lack of fusion,' it is not representative of the full range of naturally occurring defects. For example, one would believe that a large 'lack of sidewall fusion' defect, which by definition would traverse two or three weld passes, would take on a complex faceted shape that reflects the weld passes!

In order to see the effect of this faceting, the 12 mm deep by 0.025 mm width slot was split into three curved segments as shown in Figure C.7. The resulting optical density plot, Figure C.8, shows three peaks some way above the 0.006 value associated with the simple slot. The peak optical densities of this plot would be much more visible to the inspector, and we can suggest that such a defect would be identified. However, the question becomes how would such an indication be interpreted and consequently sentenced by the inspector?

The authors suspect a high probability that such an indication would be interpreted as three separate stringers each of no structural significance. Thus, an inspection efficiency curve, i.e., one that is interpreted as the probability of removing defects of structural relevance, is a combination of the probability of identifying that a defect exists and then correctly diagnosing that the defect is in need of removal.

At this stage, the authors do not know of sufficient data to aid this second decision; and so it is assumed that radiographic inspection efficiency is related to the optical image associated with an equivalent slot at a given angle. The implication of this is that a defect, misoriented at an angle of 16 degrees to the radiographic beam, with a width or gap between its faces of 0.025 mm, would not be detected, regardless of the defect depth through the wall thickness. This assumption is clearly pessimistic in that it ignores the probability of detection and repair of larger defects with irregular profiles.

C.7 Probabilistic Interpretation of Inspection

The value of 0.006 as an optical density that can just be seen is in the nature of a deterministic statement: i.e., below 0.006, no detection; above 0.006, 100% detection. Clearly, such a situation is unrealistic, and so the detection is described as a probability which is a function of the optical image given by the artificial slot-like defect. This function has been established based on judgment, and is as follows:

$$\text{Probability of Detection} = 0.995 - \exp(-1000\Delta_D^2)$$

Translating this to the 0.025 mm slot gives the following probabilities of detection versus angles:

Table C.1

5 mm deep by 0.025 mm Width Defect	Defect Angle, Degrees	0	4	8	12	16
	Probability of Detection, %	95.1	39.7	17.3	7.8	4.3

C.8 References

1. Halmshaw, R., and Hunt, C. A. 1975. "Can Cracks be Found by Radiography?" *British Journal of NDT*. May 1975.

2. McMaster, R. C. 1959. "Non-Destructive Testing Handbook," Vol I.
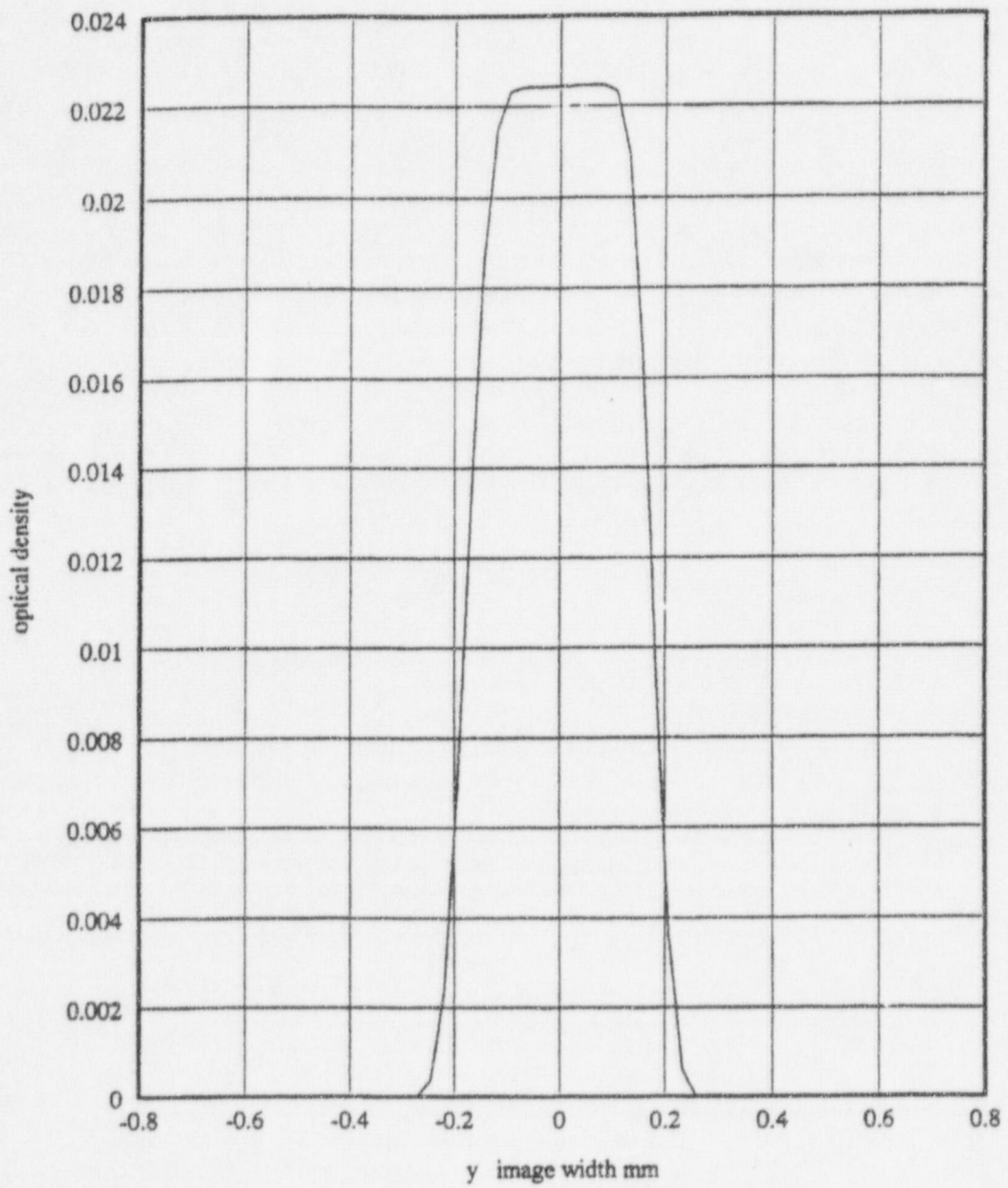
Figure C.1. Optical Density of 5 mm Deep by 0.025 mm Width Slot at 4° Misorientation
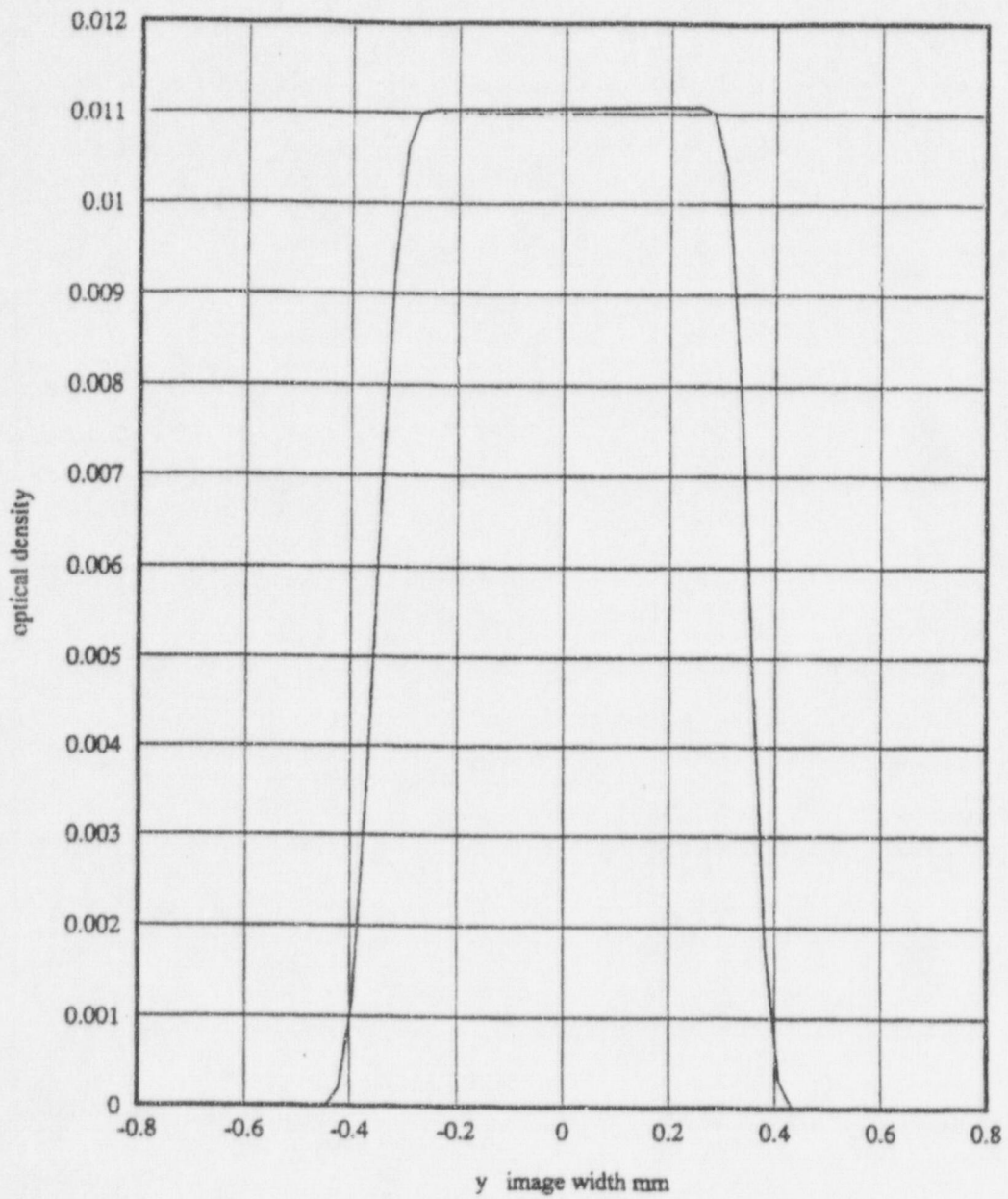
Figure C.2. Optical Density of 5 mm Deep by 0.025 mm Width Slot at 8° Misorientation
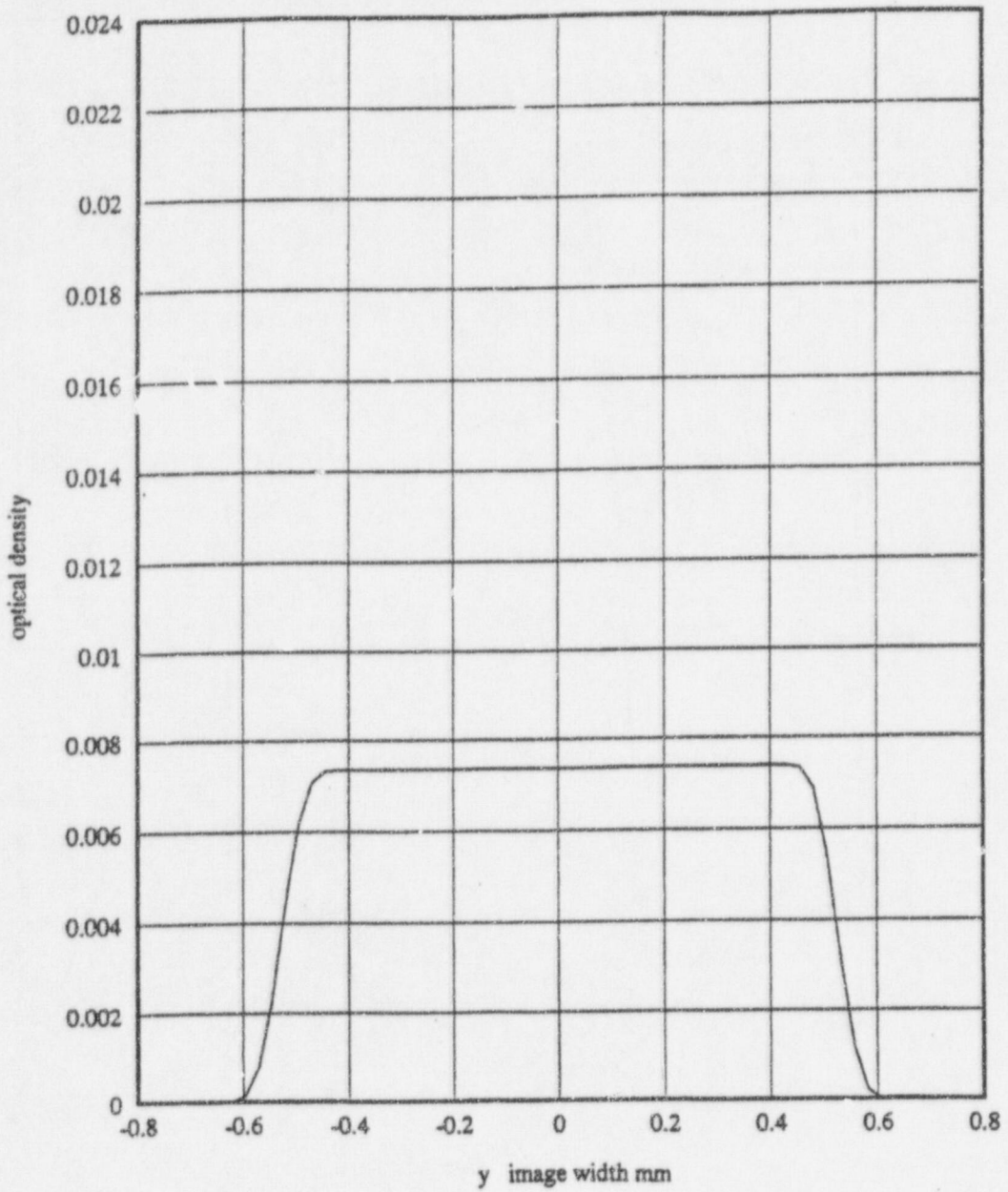
Figure C.3. Optical Density of 5 mm Deep by 0.025 mm Width Slot at 12° Misorientation
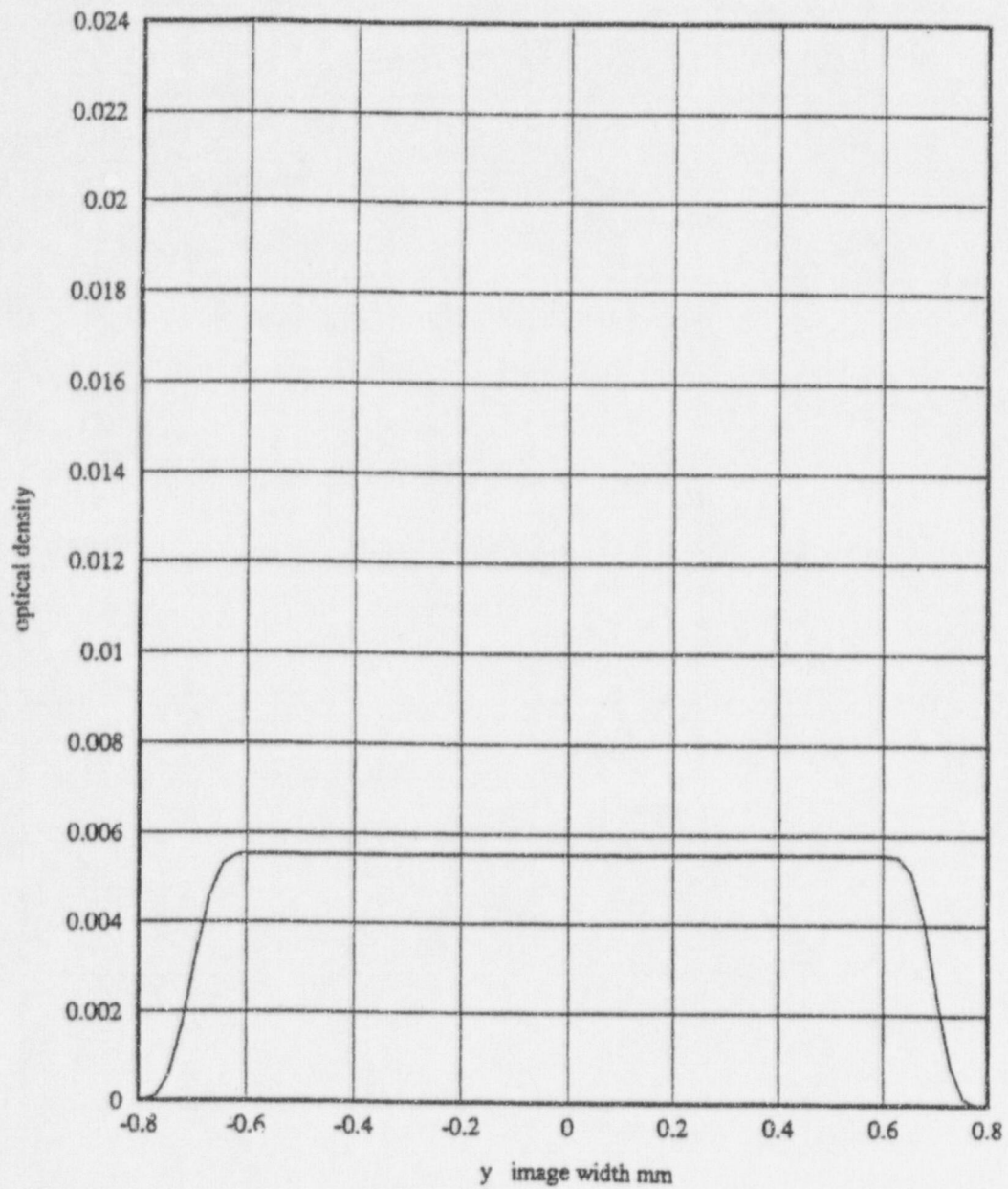
Figure C.4. Optical Density of 5 mm Deep by 0.025 mm Width Slot at 16° Misorientation
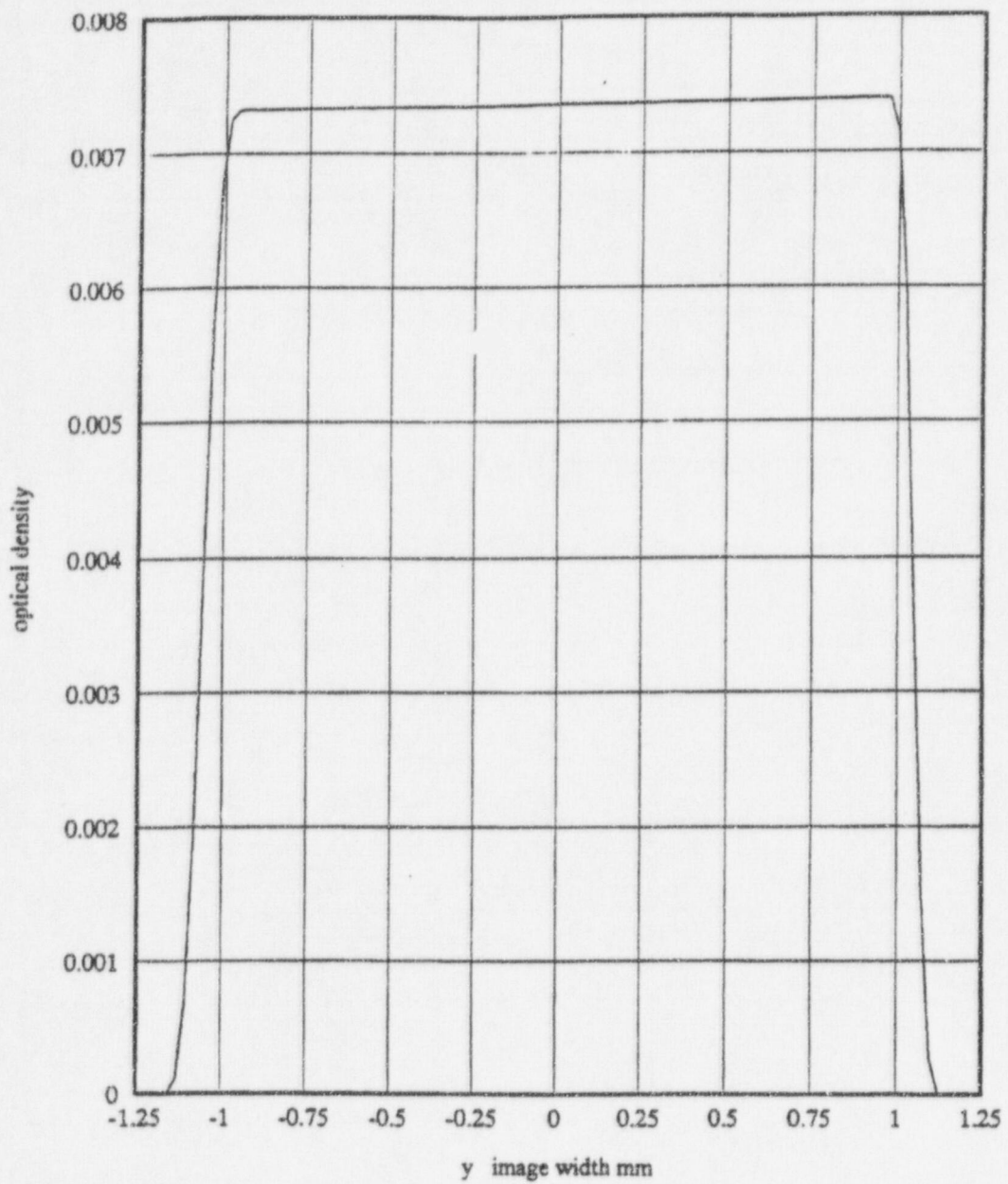
Figure C.5. Optical Density of 10 mm Deep by 0.025 mm Width Slot at 12° Misorientation
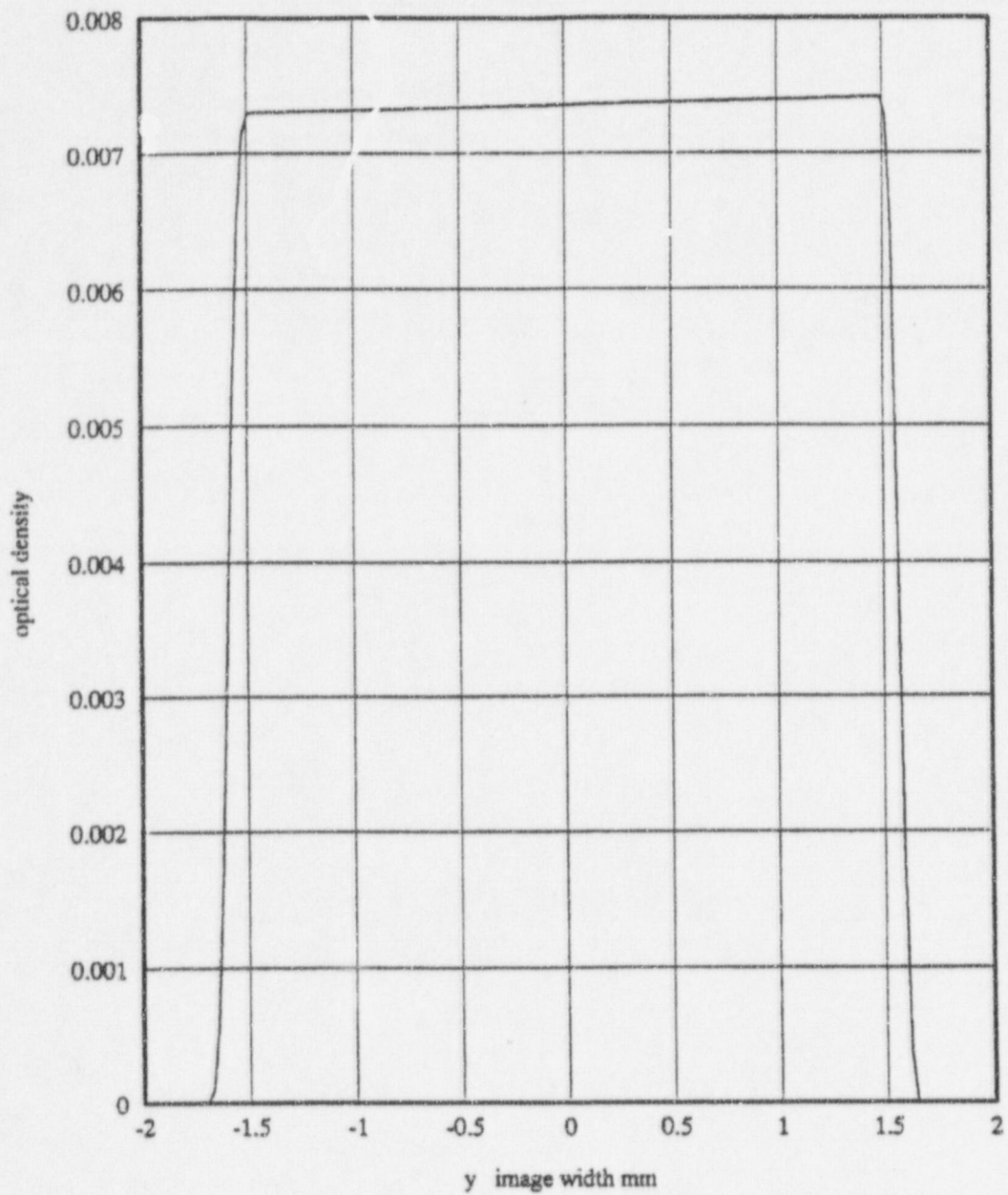
Figure C.6. Optical Density of 15 mm Deep by 0.025 mm Width Slot at 12° Misorientation

Figure C.7. 12 mm Deep Defect by 0.025 mm Width with 3 Curved Segments
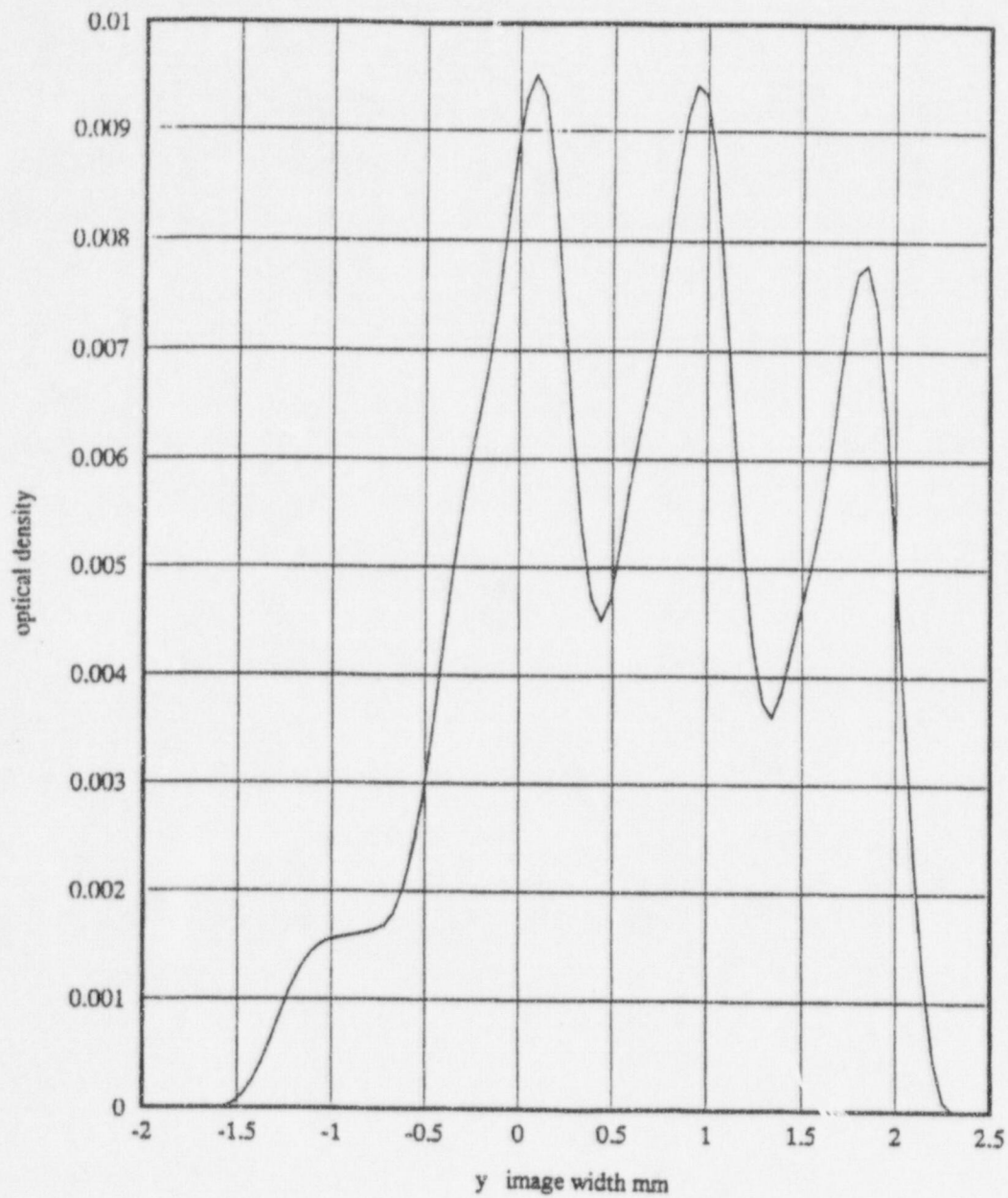
Figure C.8. Optical Density for 3 Curved Segments Shown in Figure C.7

Appendix D

**Application of RR-PRODIGAL to the Simulation of Flaws
in the PVRUF Reactor Pressure Vessel Welds**

Appendix D

Application of RR-PRODIGAL to the Simulation of Flaws
in the PVRUF Reactor Pressure Vessel Welds

D.1 Introduction

Pacific Northwest National Laboratory (PNNL) under contract to the U.S. Nuclear Regulatory Commission (NRC) has performed nondestructive and destructive examinations of welds taken from reactor pressure vessels which were manufactured for cancelled nuclear power plants. One such vessel was located at the Pressure Vessel Research User Facility (PVRUF) at the Oak Ridge National Laboratory. The objective of the PNNL research (Schuster, Doctor, and Simonen 1996; Schuster, Doctor, and Pardini 1997) was to determine the numbers and sizes of flaws in the vessel welds, and to develop empirical estimates of fabrication flaw rates for use in structural assessments based on fracture mechanics. This appendix describes simulations performed with RR-PRODIGAL to predict the numbers and sizes of flaws in the PVRUF vessel welds. The twofold objective of these calculations was to 1) illustrate the use of the RR-PRODIGAL code, and 2) validate the code by comparing predicted and observed flaw distributions. The present comparison of this prediction with the data from destructive flaw verification is a tentative one, because the report on destructive tests is presently being finalized and reviewed.

D.2 Background on PVRUF Vessel Studies

The PVRUF pressure vessel, Figure D.1, was assembled by Combustion Engineering in 1980 for a nuclear power plant that was not completed. The pressure vessel has a diameter of 4.39 m (173 in.), a height of approximately 13.34 m (525 in.), and is made out of A533B steel. The wall thickness varies from one region to the next, but within 25 cm (10 in.) of the beltline welds it is 22 cm (8.6 in.) thick.

Subsequently, the vessel was moved to the Oak Ridge National Laboratory to be used for research studies. One such study performed detailed examination of the welds to determine the density and size distributions for the fabrication flaws within the welds. These examinations used the very sensitive SAFT-UT (Synthetic Aperture Focusing Technique for Ultrasonic Testing) to detect and characterize flaws. Data were obtained from three types of examinations:

SAFT-UT Examinations Performed Onsite - PNNL staff moved the SAFT-UT system to the Oak Ridge site and examined 100 percent of the beltline region welds with access from the vessel inner surface. The data collected at Oak Ridge were then sent to PNNL for detailed analyses. The results of these analyses were documented in technical papers (Schuster, Doctor, and Simonen 1996; Schuster, Doctor, and Pardini 1997) and provided a preliminary description of the estimated flaw population, which consisted of about 2500 indications.

SAFT-UT Examinations Performed at PNNL - Sections of welds were removed from the PVRUF vessel and shipped to PNNL for detailed examinations. This material amounted to roughly 50 percent of the vessel beltline welds and included all of the largest indications detected by the onsite SAFT-UT examinations. SAFT-UT examinations were performed at PNNL on the individual segments of the vessel, Figure D.2. With access from the various sectioned

surfaces of the segments, it was possible to achieve an enhanced level of sensitivity and resolution. In a number of cases, some flaws which had been conservatively characterized by the preliminary examinations to be a single large flaw were more accurately determined to be several closely spaced smaller flaws.

Destructive and Radiographic Examinations - Small cubes containing the larger indications were cut from the weld segments. The sizes and locations of the defects within the cubes were confirmed by radiography. The final step was to section the cubes to obtain metallographic confirmation of selected defects, as shown by the example of Figure D.3.

A complete list of flaws in the PVRUF vessel welds was compiled on the basis of the above examinations. The total number of flaws was about 2500, with most of these flaws having through-wall dimensions of less than 3 mm. All of the larger flaws were confirmed and characterized on the basis of the detailed SAFT-UT, radiographic examination, and destructive examinations. The sizes of the flaws in the material which remained at Oak Ridge were reestablished, using sizing rules developed on the basis of experience gained from the detailed examinations.

D.3 Description of Weld

Figures D.4 and D.5 show metallographic cross sections of the two PVRUF weld geometries which were examined. Approximately 67.5% of the examined welds were of the uniform thickness single-V configuration shown in Figure D.4. The remaining 32.5% of the examined weld length was of the thickness transition configuration, Figure D.5. In both cases, the weld was made by the submerged metal arc process. The root passes of the single-V welds were removed by back gouging and welded from the inside surface. It was assumed that this welding also used the submerged metal arc process. A stainless steel cladding was then applied over the inner surface of weld, using a multi-wire welding process.

Figure D.6 shows the configuration of weld beads in a typical weld cross section. In producing this figure, the interfaces between adjacent weld beads were visually located using special lighting and magnification. The interfaces were then marked with a felt tip pen for identification. It is seen that the thicknesses of the weld passes were smallest within the rewelded zone located at the inner surface of the vessel.

D.4 Input Data for RR-Prodigal

Table D.1 summarizes the input data used to specify the weld build up, the welding process, and the inspection process. These inputs were provided to the RR-PRODIGAL code through interactive screen menus. Appendix E provides an example of printed output from RR-PRODIGAL. Part of this output is a detailed description of input specifications.

D.4.1 Weld Bead Configuration

Figures D.7 and D.8 were developed as a preliminary step prior to the interactive session with RR-PRODIGAL. These figures describe idealized geometries of the two weld configurations. The weld prep geometry, number of weld layers, and number of weld beads were determined directly from the metallographic cross sections. If such precise weld configuration information had not been available, the analysis could have been based on estimates of the weld configuration, making use of vessel construction drawings and knowledge of typical practices used to make such welds. It is worth noting that the numbers and sizes of weld beads in the outer part of the weld were consistent with the trends of other data available at PNNL for similar welds. However, generic information on welding practices would not have provided the same quality of data as shown in Figure D.5 regarding the configuration of weld passes for the rewelded region at the inner surface. Without the metallographic information, a common weld bead size would have been assumed for all weld passes.

D.4.2 Welding Parameters

Table D.1 and the example output of Appendix E describe the inputs used to simulate the welding process. The vessel material was A533B low alloy steel, and the welding process was the submerged metal arc process. Specification of the build circumstances (welding location, position, access, joint geometry and restraint) for the weld were generic (or default) values applicable to welds in reactor pressure vessels.

D.4.3 Inspection and Processing Parameters

After completion of the welds, the vessel was given a reheat treatment. The inner and outer surfaces were then machined. Surface examinations of the inner and outer surfaces were performed, followed by an X-Ray examination of the completed weld. In the RR-PRODIGAL simulation, all material with flaws detected by the surface and X-ray examinations was assumed to be replaced by defect-free material. The final operation after inspection was the application of cladding to the inner surface of the weld, with no inspection or repair of the cladding.

The selected parameters for the X-ray examination corresponded to typical or standard practice for the fabrication of US vessels. An energy level of 2.5 Mev and a source diameter of 4 mm were specified. An access factor of 1.0 was specified to indicate that 100 percent of the weld length was radiographed. The film was assumed to be at the inner surface of the vessel, with an X-ray source-to-film distance of 2 m.

A second RR-PRODIGAL simulation was then performed as a sensitivity study, which assumed that no X-ray examination or repairs to the vessel were conducted. Results of these simulations provided insights into the effectiveness of the X-ray examinations. The results also provided a basis on which to evaluate the implications of the simplified approach used by RR-PRODIGAL, which optimistically assumed that all detected flaws are repaired, including flaws smaller than the sizes of the code flaw acceptance criteria.

D.4.4 Output Zones

Output from RR-PRODIGAL describes the radial locations of simulated flaws relative to the inner clad surface of the vessel, with the "flaw location" being defined as the radial coordinate of the inner flaw tip. Part of the input to RR-PRODIGAL allows the user to define a convenient set of zones for this output. Table D.1 indicates the zones used for the present calculations. One zone addresses flaws located within the cladding material. The next two zones address flaws outside the clad region but within 1.0 in. of the vessel inner surface. These zones together correspond to the flaws reported in the PNNL examinations of the PVRUF vessel to be within the "near surface zone." The final four zones cover the region of the vessel wall described as "remainder of vessel wall."

D.5 Results from RR-PRODIGAL

Appendix E consists of printed output files generated by RR-PRODIGAL. Each run with RR-PRODIGAL generates a collection of output files which includes the following files:

Input for weld specification: *dancer.weld.00062*

Input for clad specification: *dancer.clad.00062*

Output for predicted flaw distribution: *dancer.waltzer.00062.*

The file names for each RR-PRODIGAL run differ only with respect to the numerical identifier (e.g., 00062).

Plots can be displayed interactively with RR-PRODIGAL to show predicted distributions of flaw depths and flaw locations within the vessel wall. These plots are useful for interpreting and reviewing results, but are not suitable for comparing results of RR-PRODIGAL simulations with data on observed flaw rates. For this purpose, the output file (e.g., dancer.waltzer. 00062) was downloaded to a personal computer and then read into a spreadsheet program so that the flaw distribution data could be manipulated and plotted.

Figures D.9-D.11 show the distributions of simulated flaw depths which were predicted by RR-PRODIGAL. These plots indicate the number of flaws per meter of weld as a function of the flaw depth dimension. Figure D.9 addresses the uniform thickness weld (see Figure D.7) whereas Figure D.10 addresses the thickness transition weld (see Figure D.8). Figure D.11 indicates essentially no difference in the predicted flaw depths for the two weld configurations.

Figures D.9 and D.10 show that there are more outer region flaws than inner region flaws, by a factor between 10 and 100. This ratio is consistent with the large differences between the volumes of weld metal for the two regions. In Figures D.9 and D.10, the definition of an inner region flaw is any flaw with its inner tip located within 1.0 in. of the wetted inner surface of the vessel (but excluding flaws within the clad material). All other flaws with inner tips more than 1.0 in. removed from the vessel inner surface are described as outer region flaws.

The plots of Figures D.9 and D.10 also show the effects of X-ray examinations (which also include the effects of repairing all of the detected flaws). The results indicate that the X-ray examinations will detect most flaws, failing to detect only about one out of 10 to one out of 100 flaws. However, simulations of inspections in RR-PRODIGAL rather simplistically assume that all material with detected flaws is replaced with material free of flaws. In reality, small flaws will be accepted without repair. Also, repaired welds are as likely (or more likely) to contain flaws than the original weld metal. Therefore, the true distribution of flaws for inspected welds will fall somewhere between the two limiting curves of Figures D.9 and D.10. Nevertheless, it is expected that more of the large flaws rather than the small flaws will be repaired. However, it should be noted that radiographic indications are related to flaw lengths, which are only loosely correlated with flaw depths. Therefore, repair criteria may result in some deeper cracks being left without repair, while less deep but longer flaws may be repaired.

D.6 Comparison of Simulated and Observed Flaw Distributions

The SAFT-UT field system was used to inspect all of the beltline welds of the PVRUF vessel and approximately half of the circumferential weld of the intermediate to upper shell course weld, for a total of 20 m (800 in.) of inspected weld, using 10 inspection modes. Based on the nominal cladding thickness of 6 mm (0.24 in.) and the weld cross sections from the construction drawings, Table D.2 gives the volumes and surface areas for the SAFT-UT inspections at PVRUF.

Detailed results of the examination of the PVRUF vessel will be documented in a future report (NUREG/CR-6471) to be prepared by PNNL. Preliminary results have been described in a previous paper (Schuster, Doctor, and Pardini 1997), and more recent results were available to support the present objective of comparing predictions by RR-PRODIGAL with observed flaw occurrence rates. The plots of Figures D.12-D.17 make such comparisons, based on the observed flaw data described in Tables D.3 and D.4.

D.6.1 Treatment of Calculated Flaw Rates

All calculated flaw rates were normalized to give the number of flaws per meter of weld having depth dimensions greater than a given value. Whereas the RR-PRODIGAL code was applied to two weld configurations (Figures D.7 and D.8), the data on observed flaws were combined for the two configurations. Therefore, the RR-PRODIGAL results for the two configurations were combined as a weighted average, in accordance with 67.5 percent of the welds being of the uniform thickness type and 32.5 percent of the thickness transition type.

D.6.2 Treatment of Observed Flaw Rates

In the data on observed flaws, flaws are classified according to the zones where they occur within the vessel wall. These zones are clad material, weld material, base metal, and repair weld material. Flaws in clad material and base metal material are excluded from consideration in the present discussion. The flaw data for repair welded material was first included with the data for weld material. In a second evaluation the flaws for repair welds were excluded, because the RR-PRODIGAL code does not simulate the effects of repair welding.

The observed flaw data also lists separate categories for planar flaws and volumetric flaws. Because the RR-PRODIGAL code addresses only crack-like flaws and not volumetric flaws (e.g., fat slags), one treatment of the observed data was limited to planar flaws. Because the definitions of volumetric flaws may not be the same in the PVRUF and RR-PRODIGAL evaluations, a second treatment combined the planar and volumetric flaws. In the end, the method of treating volumetric flaws made little difference, because most of the larger PVRUF flaws were planar flaws.

The size categories with the largest number of flaws were those with a through-wall extent of less than 5 mm (outer region flaws) and 3 mm (inner region flaws). The sizing capabilities of SAFT-UT did not permit more definitive measurements of flaw size. In the present evaluations, the <3 mm flaws and <5 mm flaws were arbitrarily treated as having depths of 2 mm and 4 mm, respectively.

The data on observed flaws for the PVRUF vessel gave total flaw counts for all the examined welds. These flaw counts were converted to flaws per meter of weld by dividing the observed flaw counts by the total length of weld examined (20.32 m).

D.6.3 Comparison Including Flaws in Repair Welds

Figures D.12-D.14 show simulated versus observed flaw size distributions from PVRUF vessel examinations. These plots include flaws in the original weld metal along with some relatively large and significant flaws which were detected in regions of repair welding. The various plots address flaws in the inner region (Figure D.12), flaws in the outer region or remainder of the vessel wall (Figure D.13), and flaws in all regions of the vessel wall (Figure D.14). RR-PRODIGAL predictions are given both for simulations of X-ray examinations and without X-ray examinations.

The observed PVRUF data show a much larger number of flaws of very small size than are predicted by the RR-PRODIGAL simulations. This lack of agreement is not a significant concern. These flaws are too small to be important to structural integrity, and are also below the size domain addressed by the RR-PRODIGAL model (i.e., flaw depths much less than the weld bead dimension are excluded).

The observed and predicted flaw depth distributions are in better agreement when the flaw depths approach 5 mm, which is roughly the radial dimension of the weld bead. For flaw depths greater than 5 mm, Figures D.12-D.14 show that the observed flaw rates from RR-PRODIGAL agree best with predicted rates which exclude the effects of the X-ray examinations. This trend holds even though the PVRUF welds were given a relatively high quality X-ray examination. Potential reasons for this inconsistency include:

1) The RR-PRODIGAL model may systematically underestimate flaw frequencies.

2) The RR-PRODIGAL model was developed to predict the expected number of flaws for a large population of vessel welds with given attributes, and does not address random differences for individual welds. Accordingly, the PVRUF vessel could be a vessel which has more weld flaws than the average for such vessels.

3) The RR-PRODIGAL model was developed to address only crack-like flaws and excludes volumetric types of flaws. The inclusion of volumetric flaws into the model would roughly double the predicted flaw frequencies and would, in part, resolve the differences between the predicted and observed flaw distributions.

4) The RR-PRODIGAL model assumes that a repair is made for all flaws detected by X-ray examinations. In practice, repairs are not made for small indications. While unrealistic estimates of repair rates would explain inconsistencies in the predictions for smaller flaw sizes, this factor should not apply to the larger flaws (10 to 15 mm).

An additional consideration is the effect of flaws in repair welded material, which is addressed in the following section.

D.6.4 Comparison Excluding Flaws in Repair Welds

Figures D.15-D.17 show simulated versus observed flaw size distributions from the PVFUF vessel examinations, with flaws in repair welded material excluded from the population of flaws. Although the PVRUF data included only a few cases of such flaws, the relatively large sizes of these flaws produced a disproportionate effect on the flaw size distribution curves.

Figures D.16 and D.17 show interesting trends. For flaw depths of about 5 mm, the observed flaw rates are consistent with results predicted by RR-PRODIGAL without X-ray examination. This suggests that 5-mm flaws can be detected but would not be repaired, in accordance with flaw acceptance standards. For flaw depths of 10 mm, the observed flaw rates are consistent with predicted flaw rates which include the effects of X-ray examinations. This could imply that flaws with depths in the 10 mm range are typically repaired in practice.

In summary, there is relatively good agreement between the predicted and observed flaw rates, given that flaws associated with repair welding are excluded from the PVRUF data. Evidently, repair welded regions can have significantly higher rates of occurrence for the larger flaws. Such repairs in the PVRUF vessel required deep grindouts to the vessel wall, along with the manual deposition of weld metal deep within the narrow gap of these grindouts. The difficulty of such welding would be poorly represented by the process used to make the original weld (i.e., machine welding by the submerged metal arc process).

D.7 Discussion and Conclusions

The evaluations described above indicate relatively good agreement between the observed flaw rates for the PVRUF vessel and the flaw rates predicted by the RR-PRODIGAL code. Differences between the two rates are believed to be within the level of accuracy associated with uncertainties in the predictive model, and to be consistent with the expected random vessel-to-vessel variations in flaw occurrence rates.

Future refinements to the RR-PRODIGAL model, which could offer the potential to reduce the level of differences between the predicted and observed flaw rates, include:

1) Modification of the flaw prediction model to better represent the very small flaws which have depths much less than the weld bead dimensions. While such modifications would provide improved correlations with observed flaw rates, the associated increases in the numbers of smaller flaws would have little significance relative to the structural integrity of welds.

2) Improved modeling of weld repair practices. Such improvements would exclude the repair of those detected flaws which give radiographic indications having lengths less than those of the governing flaw acceptance criteria. An improved model should also simulate the potential for higher flaw occurrence rates associated with material in weld repair regions.

In conclusion, the relatively good agreement between the model and the PVRUF data enhances the level of confidence in the ability of the RR-PRODIGAL model to predict the numbers and sizes of flaws in reactor pressure vessel welds. This agreement also enhances the value of the PVRUF data, because the RR-PRODIGAL model is based on an extensive body of knowledge regarding welding flaws and the factors that contribute to their occurrence. The fact that flaw rates for the PVRUF welds agree with expected trends indicates that the PVRUF vessel is representative of a larger population of vessels, rather than being an outlier relative to flaw occurrence rates.

D.8 References

Schuster, G.J., S.R. Doctor, and F.A. Simonen. 1996. "A Methodology for Determining Fabrication Flaws in a Reactor Pressure Vessel," pp. 187-194, *Proceedings of ASME-JSME International Conference on Nuclear Engineering 1996 - ICONE-4 - Volume 1 - Part A - Basic Technological Advances*, American Society of Mechanical Engineers.

Schuster, G.J., S.R. Doctor, and A.F. Pardini. 1997. "Validation of Reactor Pressure Vessel Fabrication Flaws," Electric Power Research Institute, Proceedings of NDE Damage Assessment Workshop, October 6-7, 1997, La Jolla, California.

Table D.1. Input Parameters Used with RR-PRODIGAL to Simulate Flaws in Welds of PVRUF Vessel

Parameter	Uniform Thickness Weld	Transition Thickness Weld
Material type	A533B	A533B
Welding process	Submerged arc	Submerged arc
Weld angle	4.10 degree	3.18 mm
Upper (outer) weld width	50.8 mm	52.1 mm
Lower (inner) weld width	48.8 mm	64.7 mm
Weld passes	Layers 0-14 6.01-mm thick 2 runs per layer Layers 15-29 7.53-mm thick 3 runs per layer Layers 30-34 3.56-mm thick 2 runs per layer	Layers 0-16 6.09-mm thick 2 runs per layer Layers 17-32 5.97-mm thick 3 runs per layer Layer 33 4.0-mm thick 3 runs Layer 34 4.0-mm thick 4 runs Layer 35 4.0-mm thick 5 runs Layer 36 4.0-mm thick 6 runs
Clad material	Stainless steel Fe controlled	Stainless steel Fe controlled
Clad weld	In-line orientation 2 layers each 5.5-mm thick 5 runs per layer Each pass 0.74-mm wide	In-line orientation 2 layers each 4.0 mm thick 7 runs per layer Each pass 0.98-mm wide
X-ray	Energy level = 2.5 Mev Source diameter = 4 mm Source to film distance = 2 m Inspection mode = SWSIROOT Access factor = 1.0	Energy level = 2.5 Mev Source diameter = 4 mm Source to film distance = 2 m Inspection mode = SWSIROOT Access factor = 1.0

Table D.1. (contd)

Parameter	Uniform Thickness Weld	Transition Thickness Weld
Output zones	Clad 0-4.74 percent wall	Clad 0-3.58 percent wall
	Weld 4.74-7.84 percent wall	Weld 3.58-7.94 percent wall
	Weld 7.84-10.95 percent wall	Weld 7.94-11.39 percent wall
	Weld 10.95-25.0 percent wall	Weld 11.39-25.0 percent wall
	Weld 25.0-50.0 percent wall	Weld 25.0-50.0 percent wall
	Weld 50.0-75.0 percent wall	Weld 50.0-75.0 percent wall
	Weld 75.0-100.0 percent wall	Weld 75.0-100.0 percent wall

Table D.2. Amount of Material Inspected by SAFT-UT in the PVRUF Vessel

Near Surface Zone	
Clad	0.027m^3 (0.95ft^3)
Clad to Base Metal Interface	4.6m^2 (50ft^2)
Weld Metal	0.015m^3 (0.53ft^3)
HAZ	0.005m^3 (0.18ft^3)
Base Metal	0.073m^3 (2.58ft^3)
Remainder of Vessel Wall	
Weld Metal	0.15m^3 (5.3ft^3)
HAZ	0.051m^3 (0.18ft^3)
Base Metal	1.0m^3 (35.3ft^3)

Table D.3. PVRUF: Flaw Frequency in the Near Surface Zone

Zone	<3 mm	3 mm V	3 mm P	4 mm V	4 mm P	5 mm V	5 mm P	6 mm V	6 mm P	7 mm V	7 mm P	8 mm V	8 mm P	Total >2 mm V	Total >2 mm P
Clad	1148	3	0	1	0	0	0	0	0	0	0	0	0	4	0
Weld	191	1	6	0	3	1	2	0	0	0	0	0	0	2	11
Base	180	4	6	0	3	0	0	0	0	0	0	0	0	4	9
Total	1519	8	12	1	6	1	2	0	0	0	0	0	0	10	20

Total Number Characterized >2 mm	30
V = Volumetric — Total Number <3 mm	1519
P = Planar — Total Number	1549

Table D.4. PVRUF: Flaw Frequency in Remainder of Vessel Wall
(All confirmed flaws and unconfirmed flaws)

Zone	<5 mm	5-6 mm		7-8 mm		9-10 mm		11-12 mm		13-14 mm		15-16 mm		17-18 mm		Total >5 mm	
		V	P	V	P	V	P	V	P	V	P	V	P	V	P	V	P
Repair	--	0	9	0	2	0	0	0	1	0	0	0	0	0	0	0	13
Weld	653	2	17	0	7	0	1	0	0	0	0	0	0	0	0	2	25
Base	365	3	8	0	2	0	0	1	1	0	0	0	0	0	0	4	11
Total	1018	5	34	0	11	0	1	1	2	0	0	0	0	0	0	6	49

Through-Wall Extent of Flaw (DZ)

Total Number Characterized >5 mm	55
V = Volumetric — Total Number <5 mm	1018
P = Planar — Total Number	1073
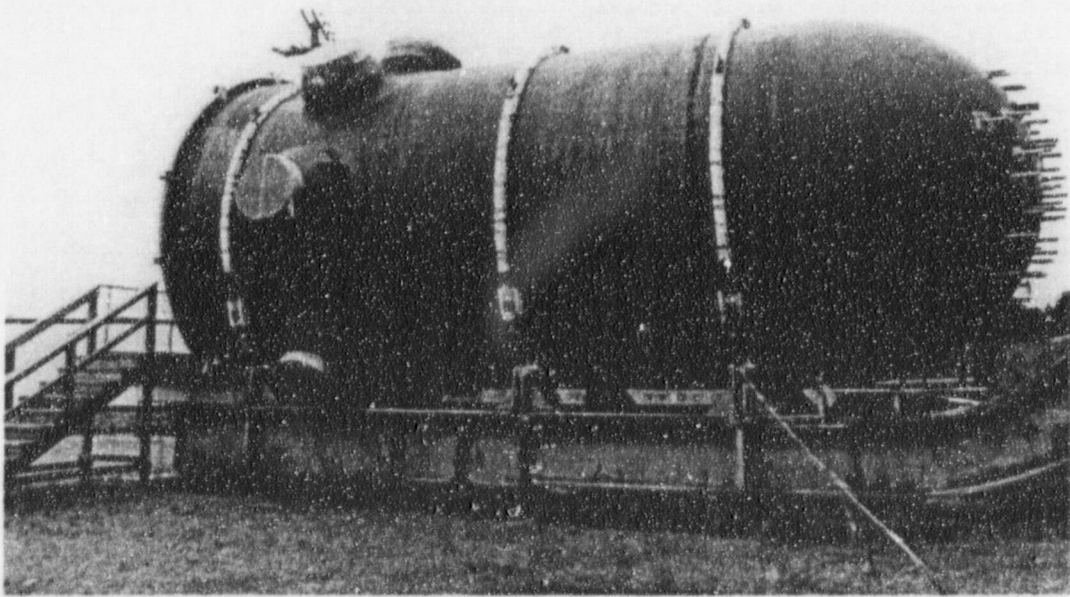
Figure D.1. PVRUF Vessel at Oak Ridge National Laboratory
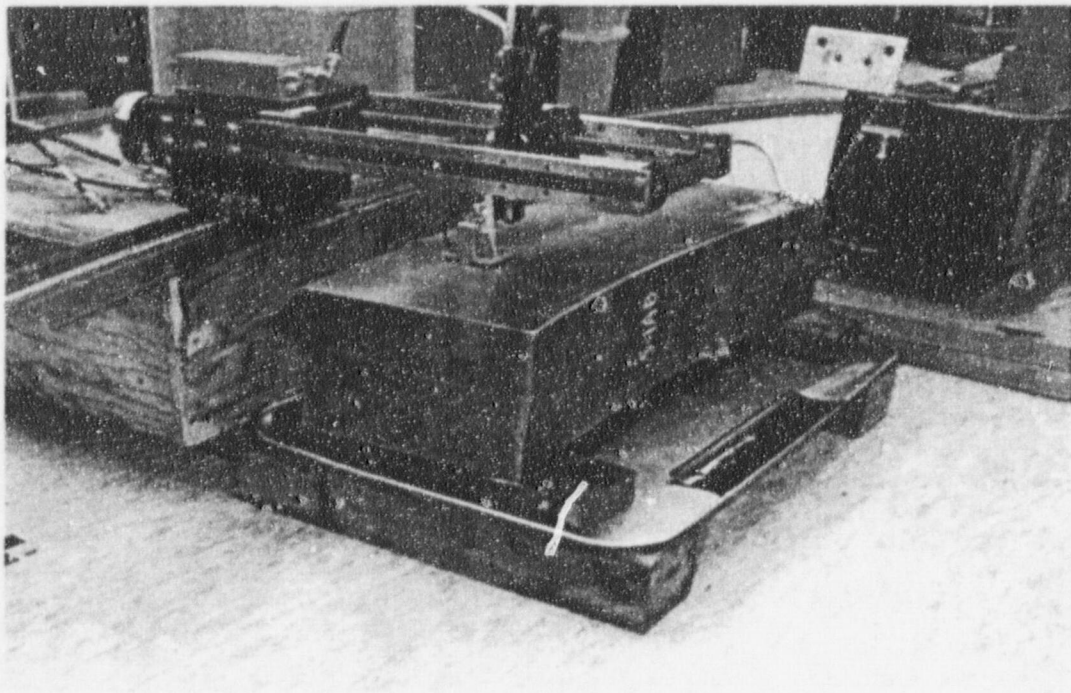
Figure D.2. Segment of PVRUF Vessel During Examination with UT-SAFT System
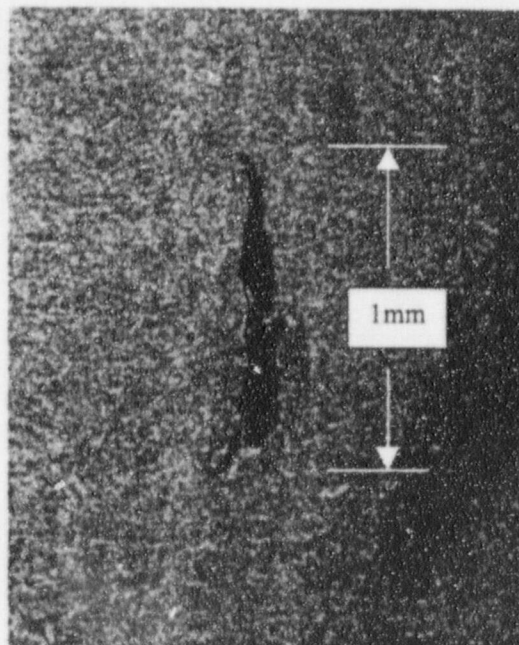
Figure D.3. Micrograph of 1-mm Flaw

~15 Passes

3 Pass Weld
11.3 cm

~15 Passes

2 Pass Weld
8.8 cm

2 cm

22.75 cm

1:1 Scale

Clad 5 to 10 cm

7 Clad Beads Over Weld
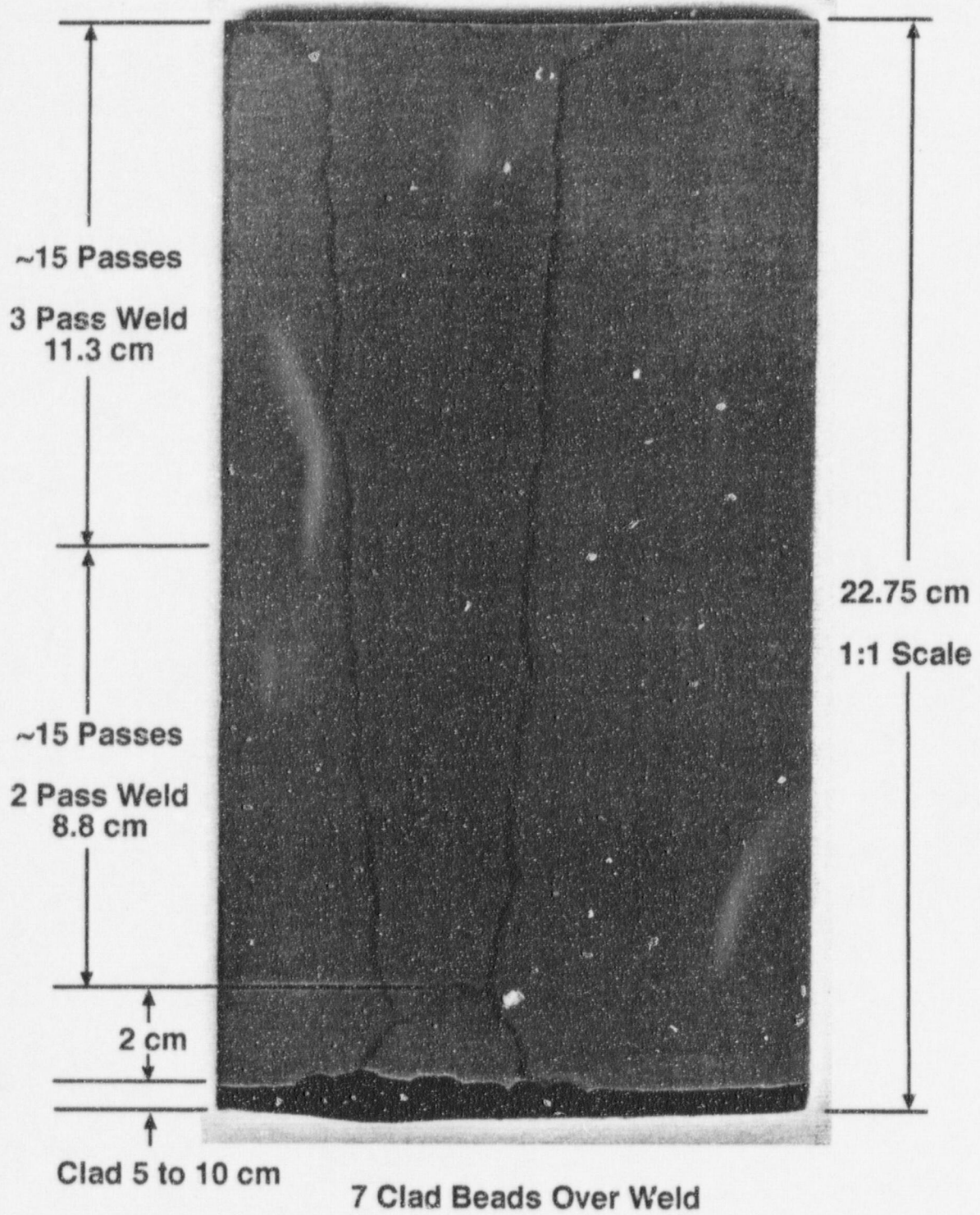
Figure D.4. Cross Section of Uniform Thickness Single V Weld

7.9 cm
12 or 13
Layers
3 Rows

9 Layers
3.9 cm
2 to 3 Rows

22 cm

13 Layers
8.4 cm
2 Rows

16 cm

4 to 5 Layers

Clad = 8mm   Clad = 5mm
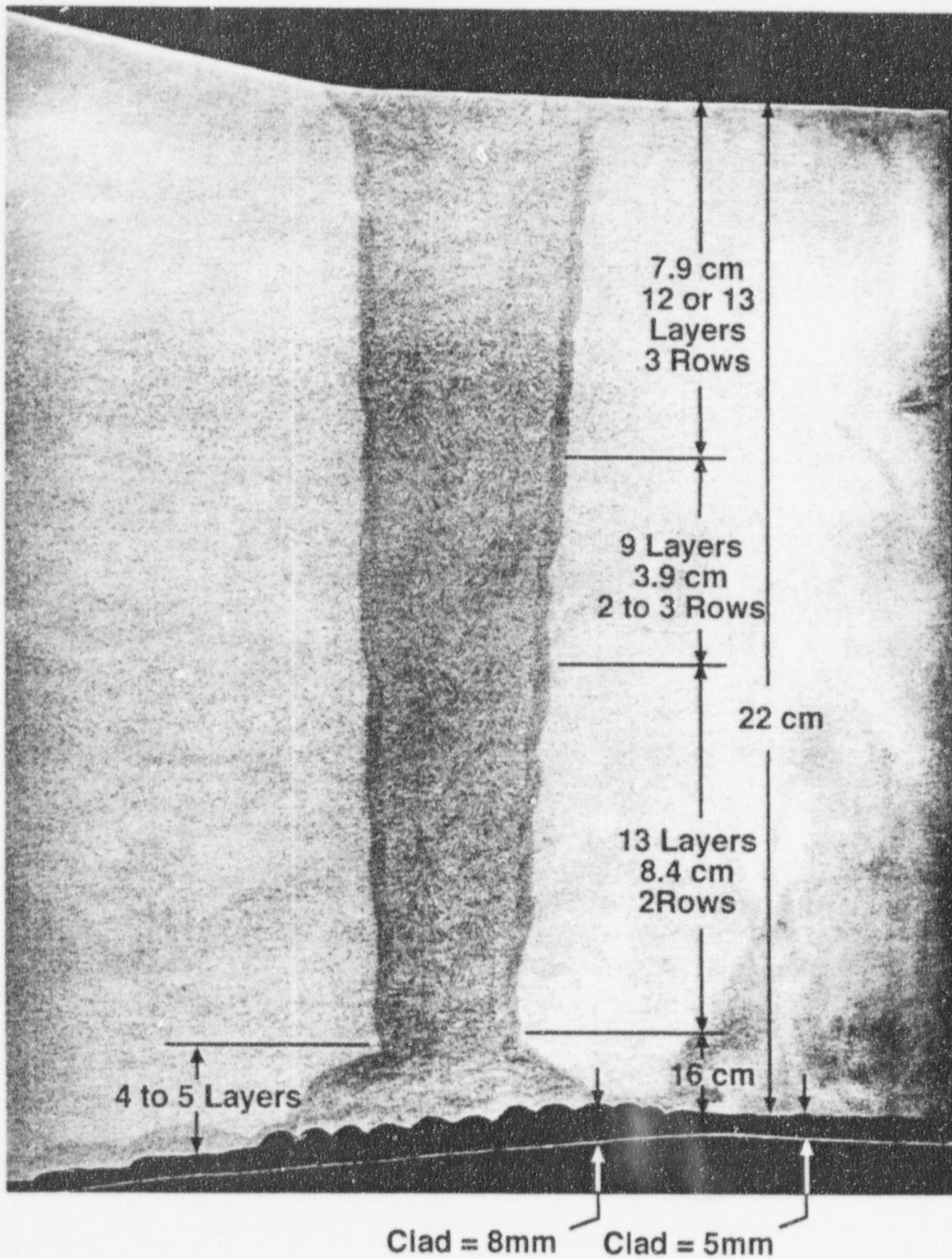
Figure D.5. Cross Section of Thickness Transition Single V Weld
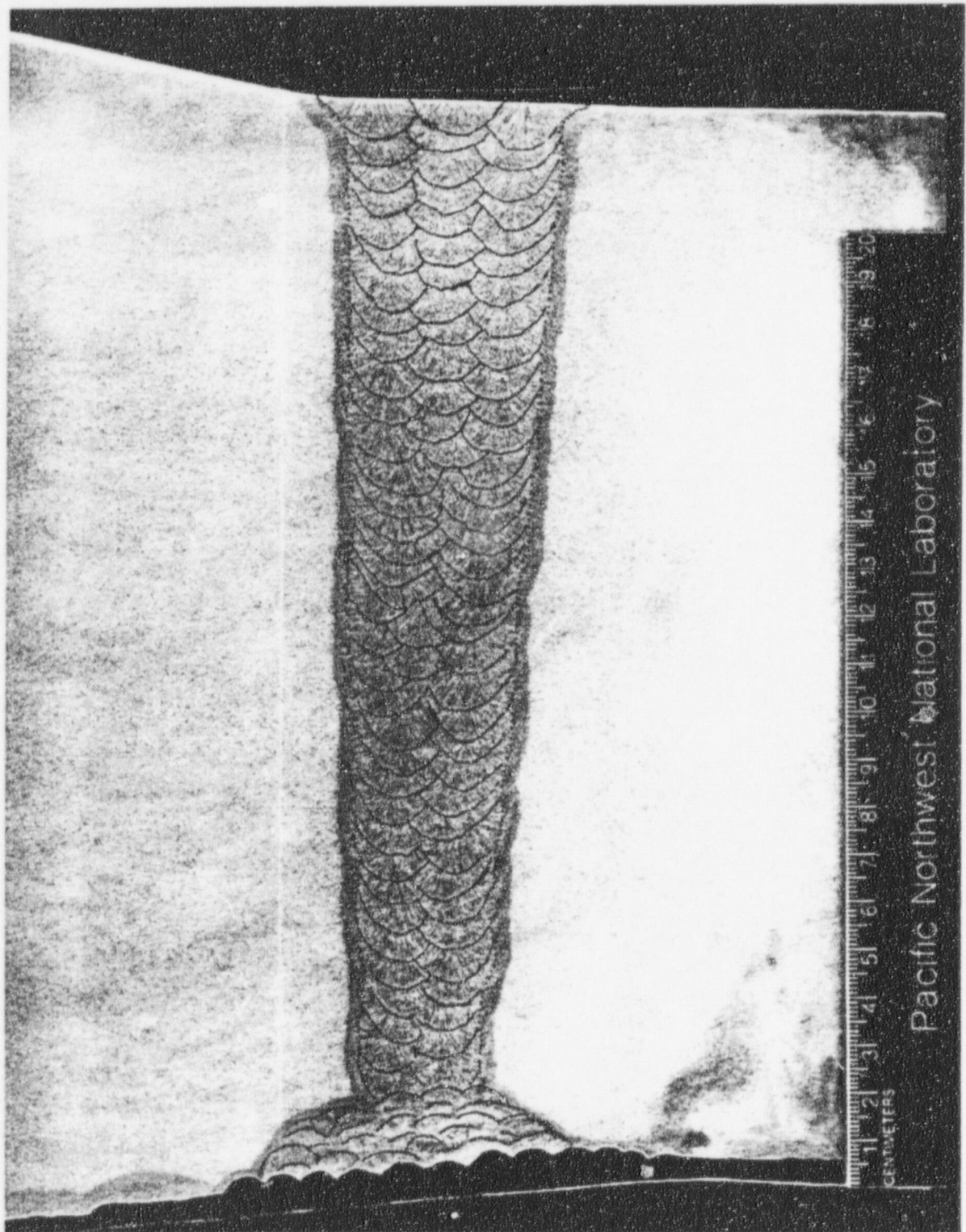
Figure D.6. Single V Weld with Highlighted Weld Passes
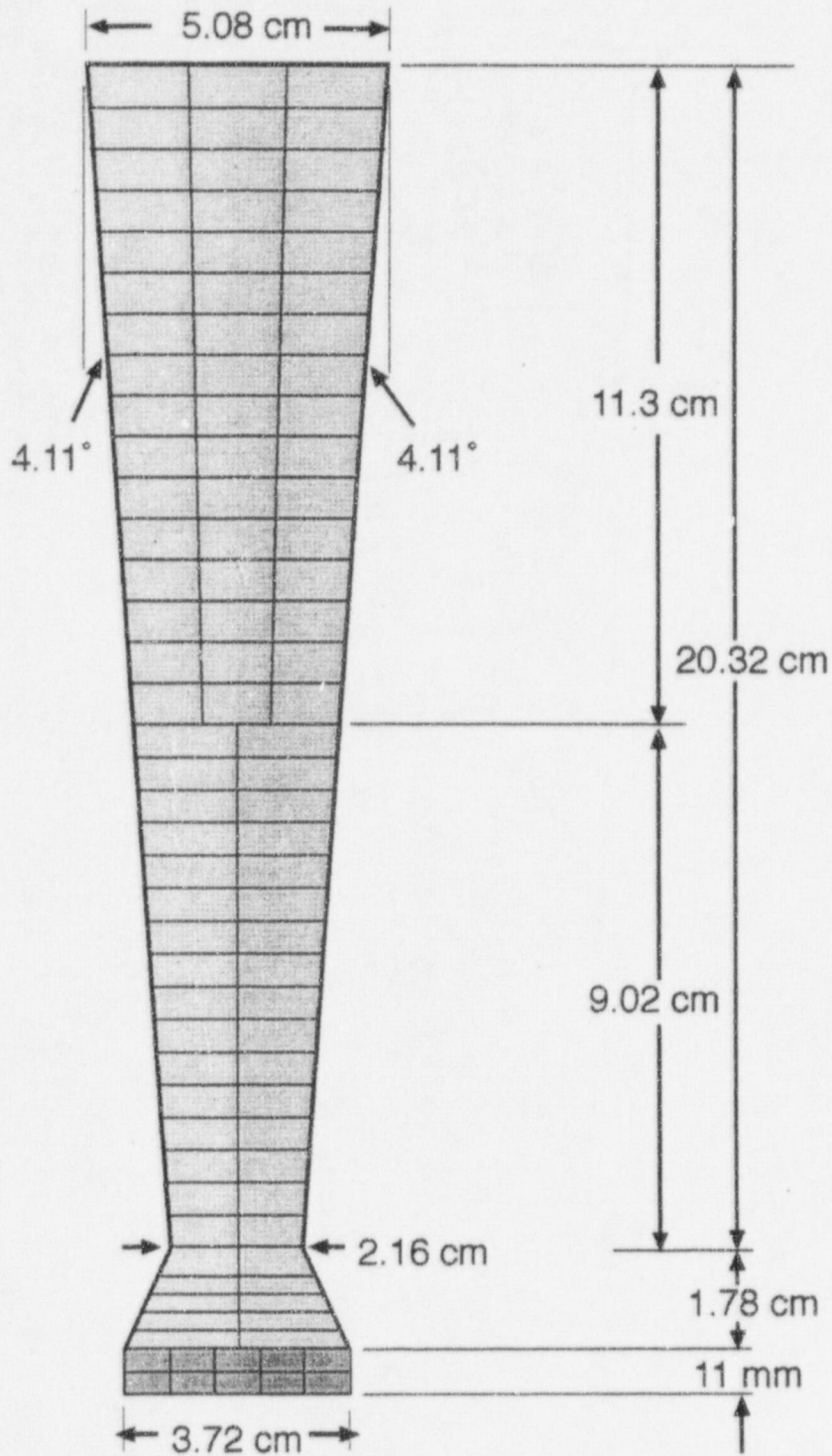
Figure D.7. Model of Uniform Thickness Single V Weld
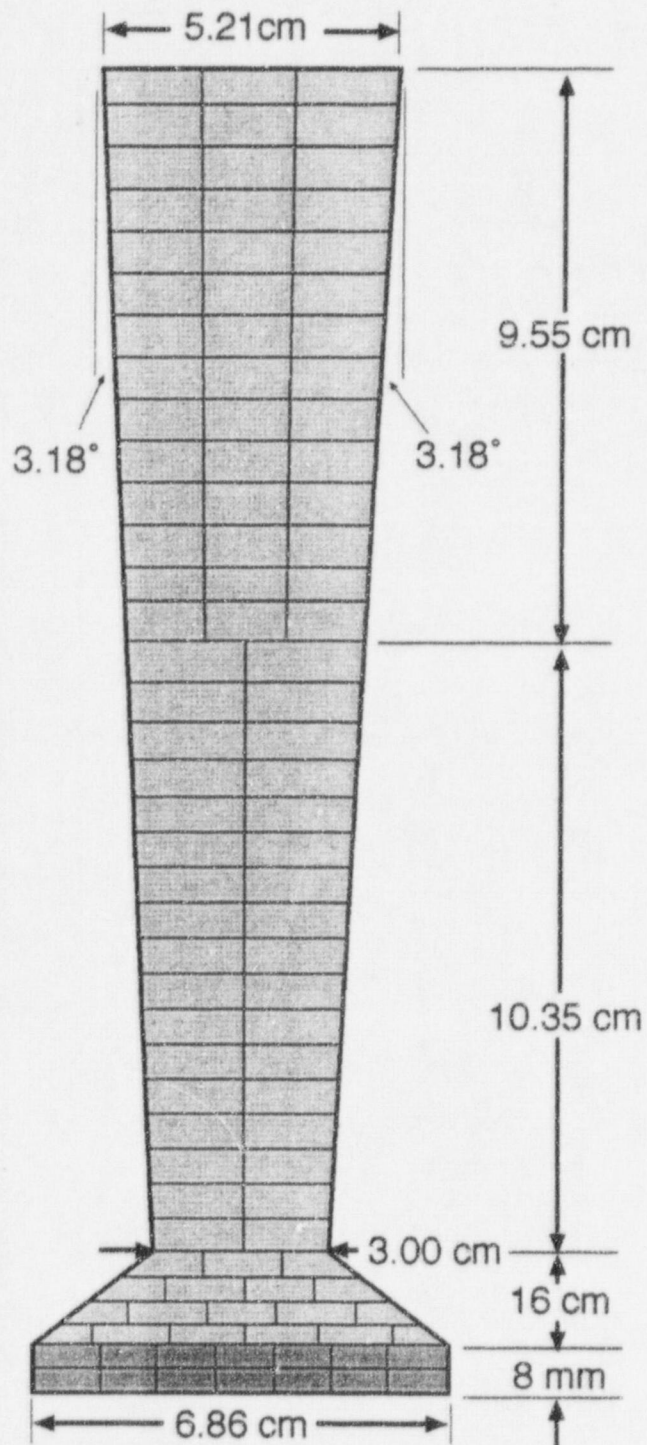
Figure D.8. Model of Thickness Transition Single V Weld
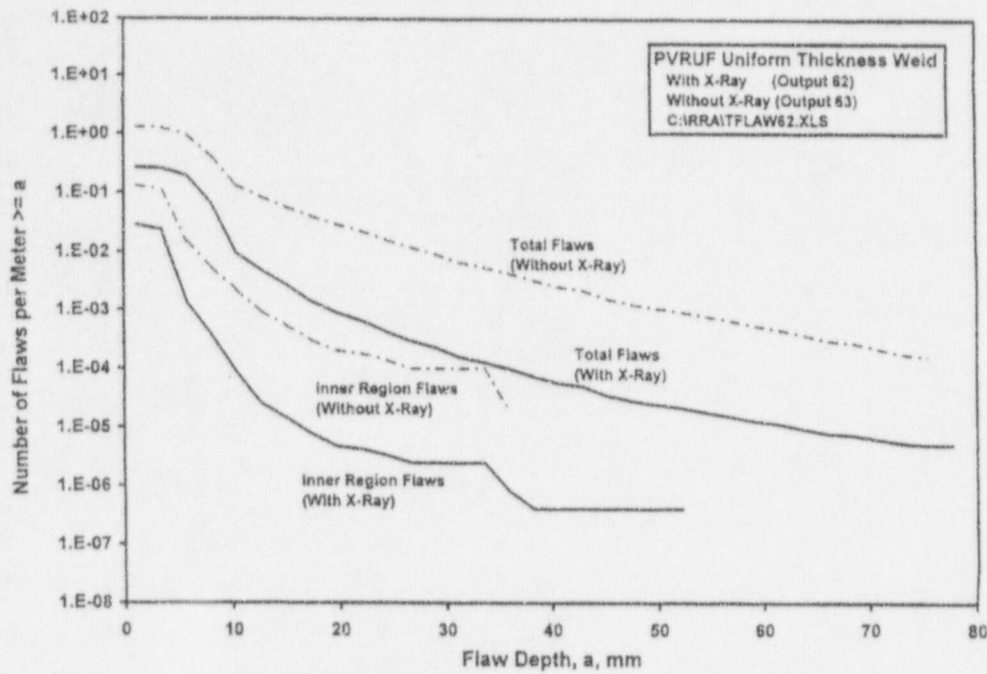
Figure D.9. Calculated Flaw Frequencies for Uniform Thickness Single V Weld Showing Effect of X-Ray Examination
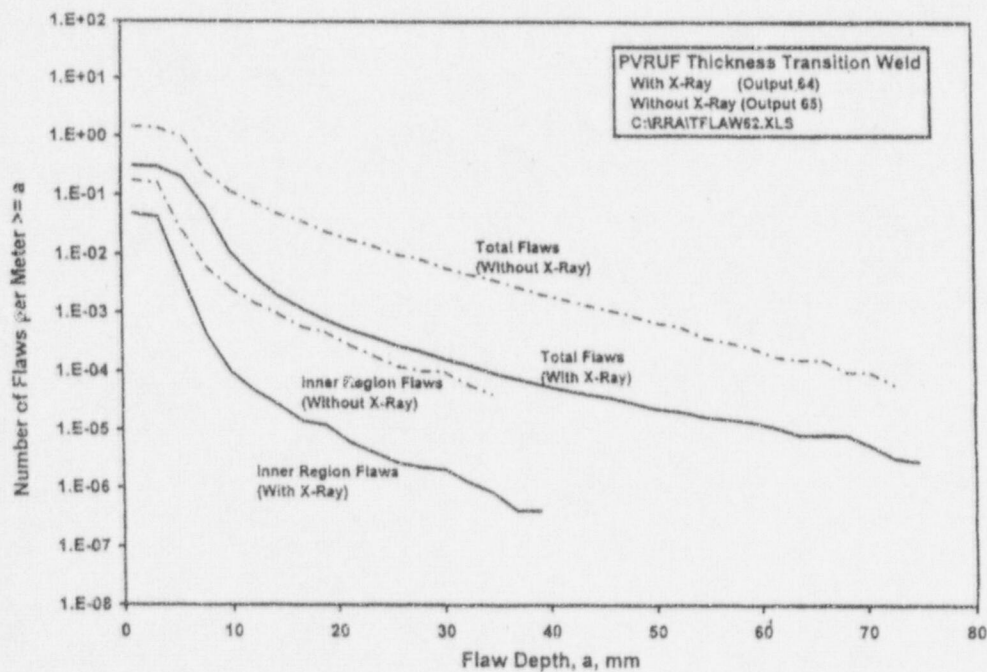
Figure D.10. Calculated Flaw Frequencies for Thickness Transition Single V Weld Showing Effect of X-Ray Examination
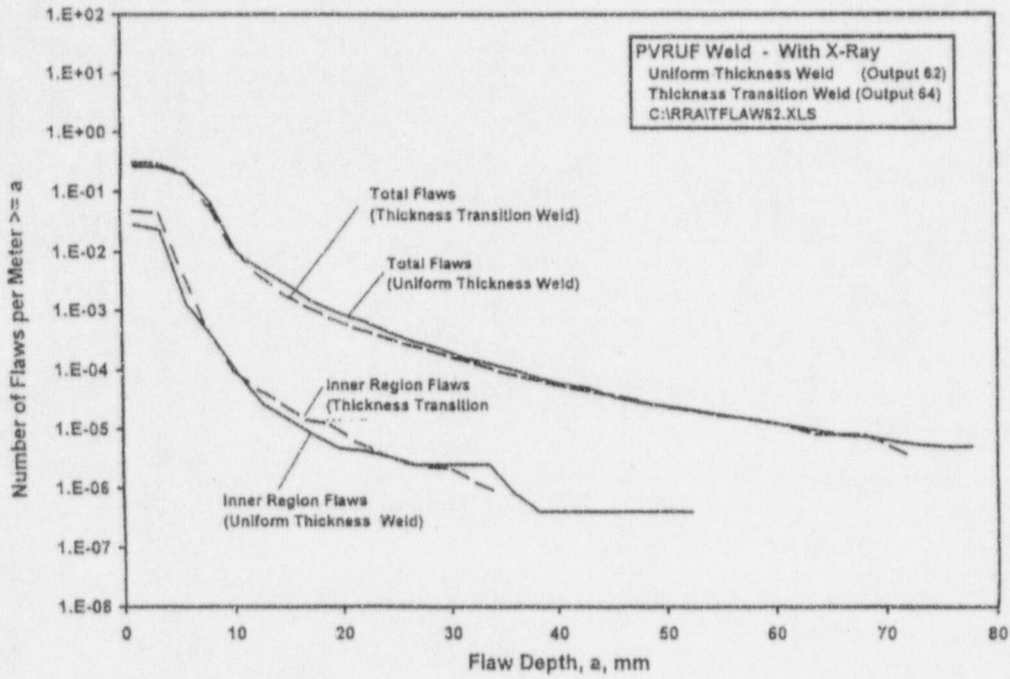
Figure D.11. Calculated Flaw Frequencies for Single V Weld Showing Effect of Weld Configuration
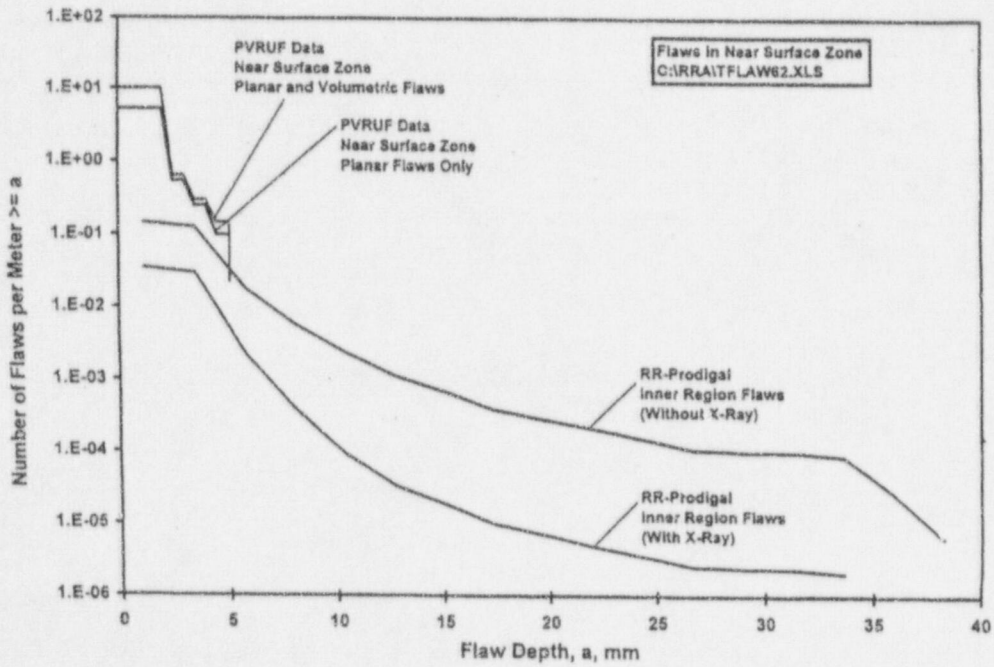
Figure D.12. Simulated Versus Observed Flaws in Near Surface Zone Including Flaws Due to Repair Welding
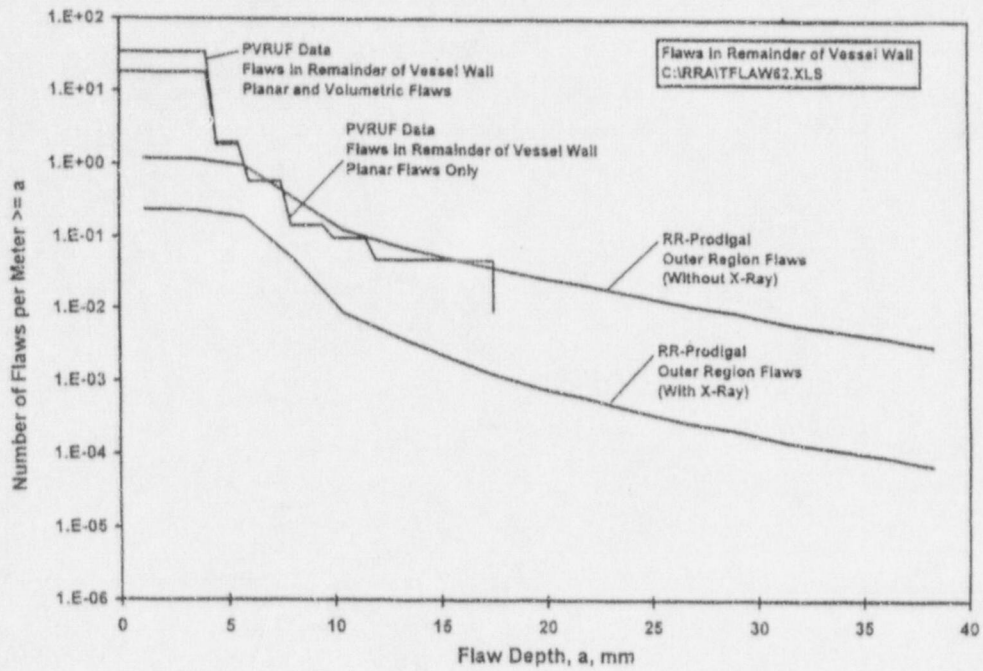
Figure D.13. Simulated Versus Observed Flaws in Remainder of Vessel Wall Including Flaws Due to Repair Welding
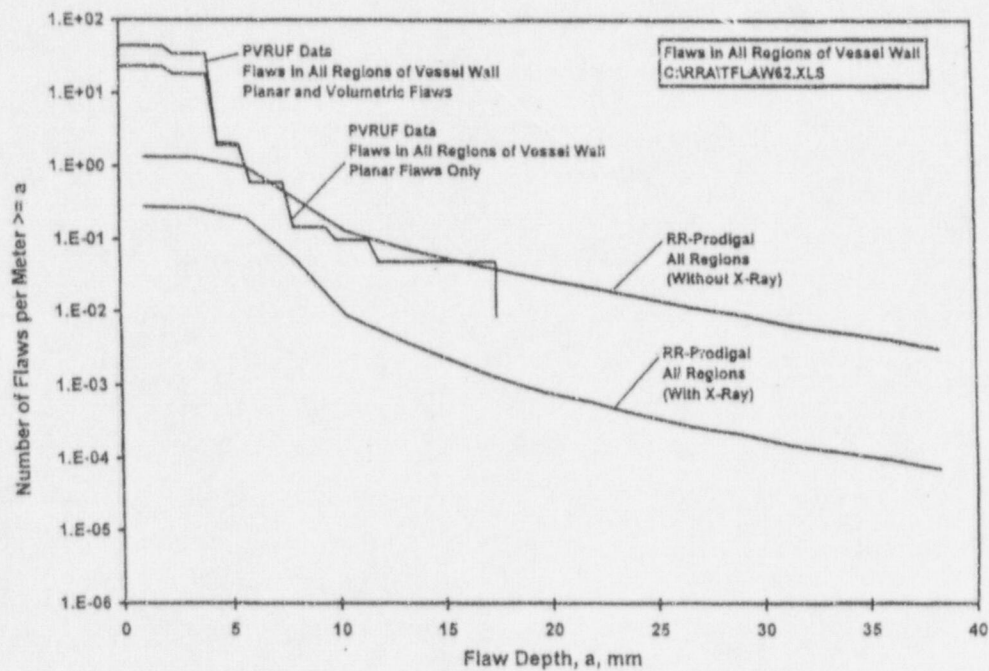
Figure D.14. Simulated Versus Observed Flaws in All Regions of Vessel Wall Including Flaws Due to Repair Welding
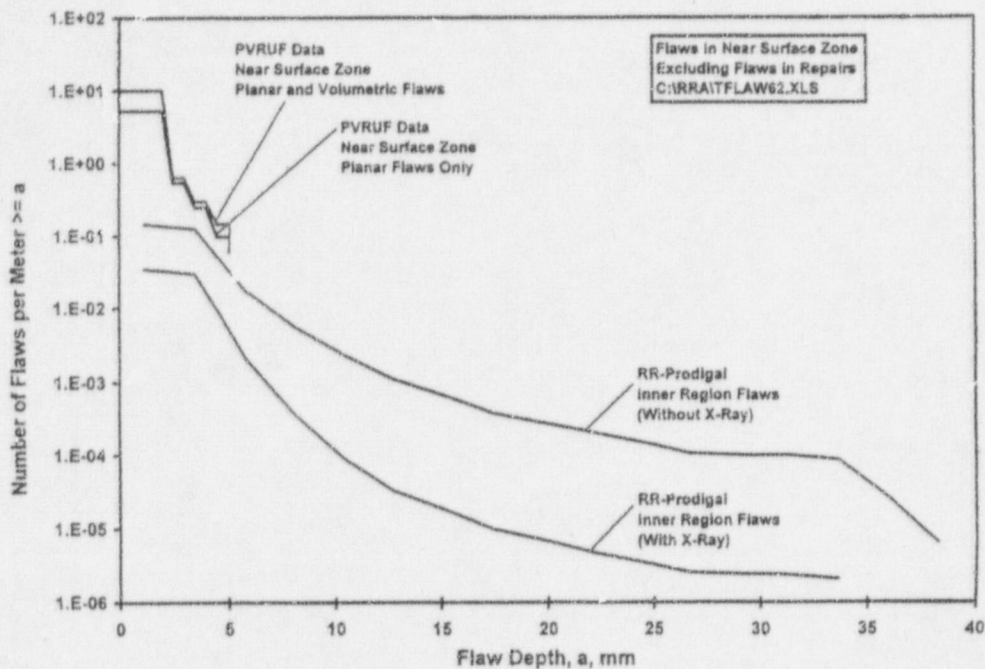
Figure D.15. Simulated Versus Observed Flaws in Near Surface Zone Excluding Flaws Due to Repair Welding
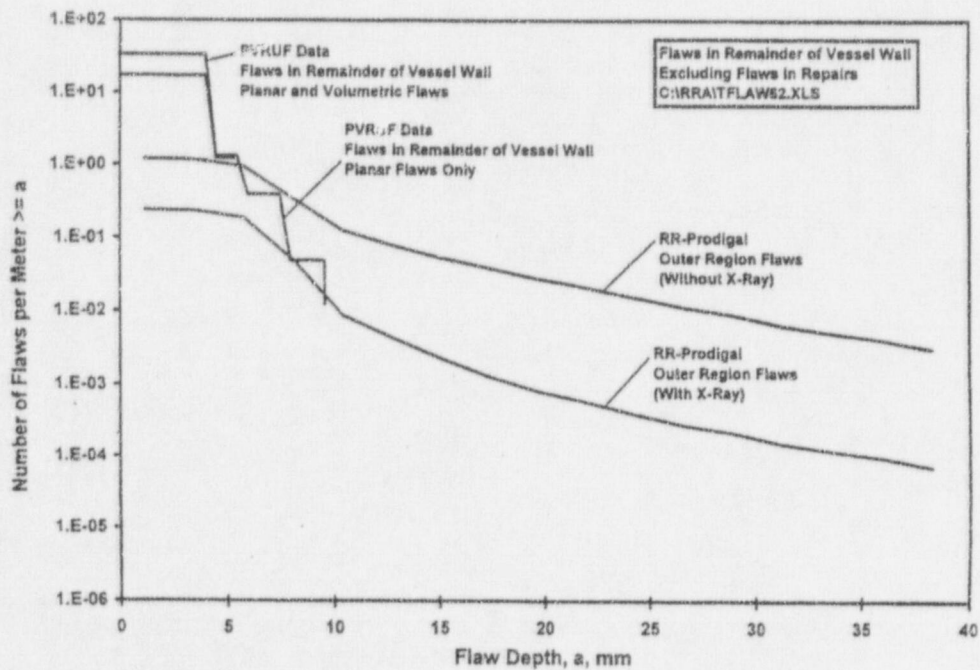
Figure D.16. Simulated Versus Observed Flaws in Remainder of Vessel Wall Excluding Flaws Due to Repair Welding
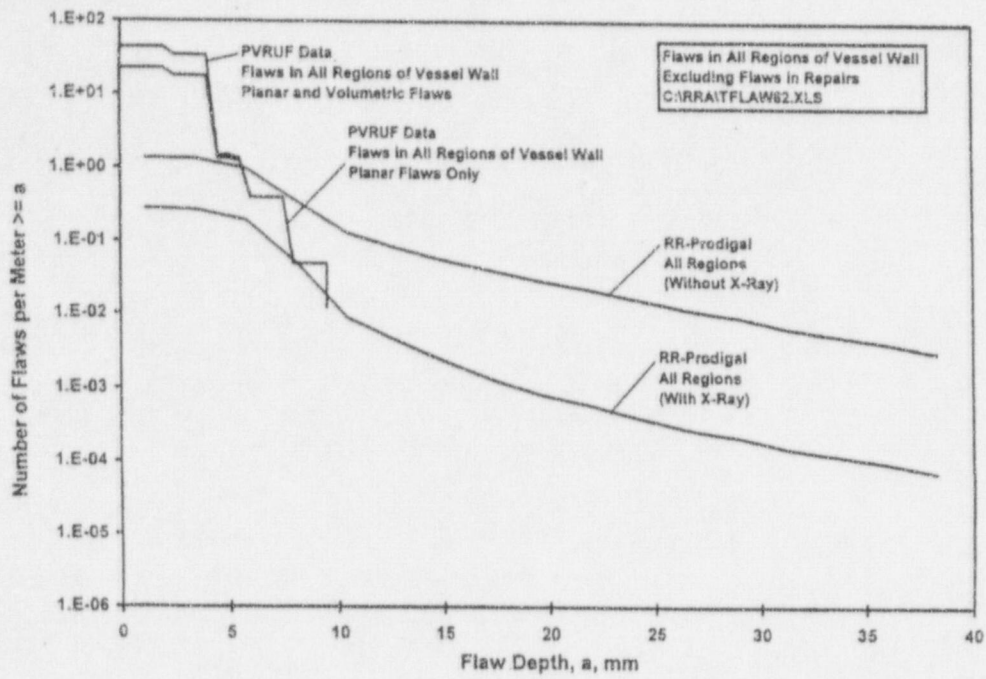
Figure D.17. Simulated Versus Observed Flaws in All Regions of Vessel Wall Excluding Flaws Due to Repair Welding

Appendix E

Example of RR-PRODIGAL Output File

Appendix E

Example of RR-PRODIGAL Output File

```
JULY 16, 1998
C:\RRA\WELD.4
UNIFORM THICKNESS WELD - WITH X-RAY
RERUN WITH JUNE VERSION OF RR-PRODIGAL
INPUT FILE = 5.1   OUTPUT FILE = WELD.4 = DANCER.WELD.00004
TITLE = UWELD1

  STRUCTURE DESCRIPTION
  ********************** ****

                STRUCTURE NAME = LONG
                ...............

                STRUCTURE TYPE : WELD
                ...............

                DATABASE TITLE : PNNLvessel
                ...............

                 ZONES TITLE : Customised
                ...............

                STRUCTURE DEPTH :  217.382
                ...............

                STRUCTURE LENGTH :   1000.00
                ...............

                UPPER STRUCTURE WIDTH :   50.800
                .....................

                LOWER STRUCTURE WIDTH :   24.368
                .....................

                STRUCTURE WALL ANGLE :    4.110
                .....................


  BUILD DESCRIPTION :
  ..................

                NUMBER OF STRUCTURE LAYERS :  25
                ..........................

                    NUMBER OF RUNS IN LAYER(  1) :   2

                    NUMBER OF RUNS IN LAYER(  2) :   2

                    NUMBER OF RUNS IN LAYER(  3) :   2

                    NUMBER OF RUNS IN LAYER(  4) :   2

                    NUMBER OF RUNS IN LAYER(  5) :   2

                    NUMBER OF RUNS IN LAYER(  6) :   2

                    NUMBER OF RUNS IN LAYER(  7) :   2

                    NUMBER OF RUNS IN LAYER(  8) :   2

                    NUMBER OF RUNS IN LAYER(  9) :   2

                    NUMBER OF RUNS IN LAYER( 10) :   2

                    NUMBER OF RUNS IN LAYER( 11) :   2

                    NUMBER OF RUNS IN LAYER( 12) :   2

                    NUMBER OF RUNS IN LAYER( 13) :   2

                    NUMBER OF RUNS IN LAYER( 14) :   2
```

```
NUMBER OF RUNS IN LAYER( 15)  :   2

NUMBER OF RUNS IN LAYER( 16)  :   3

NUMBER OF RUNS IN LAYER( 17)  :   3

NUMBER OF RUNS IN LAYER( 18)  :   3

NUMBER OF RUNS IN LAYER( 19)  :   3

NUMBER OF RUNS IN LAYER( 20)  :   3

NUMBER OF RUNS IN LAYER( 21)  :   3

NUMBER OF RUNS IN LAYER( 22)  :   3

NUMBER OF RUNS IN LAYER( 23)  :   3

NUMBER OF RUNS IN LAYER( 24)  :   3

NUMBER OF RUNS IN LAYER( 25)  :   3

NUMBER OF RUNS IN LAYER( 26)  :   3

NUMBER OF RUNS IN LAYER( 27)  :   3

NUMBER OF RUNS IN LAYER( 28)  :   3

NUMBER OF RUNS IN LAYER( 29)  :   3

NUMBER OF RUNS IN LAYER( 30)  :   3

NUMBER OF RUNS IN LAYER( 31)  :   2

NUMBER OF RUNS IN LAYER( 32)  :   2

NUMBER OF RUNS IN LAYER( 33)  :   2

NUMBER OF RUNS IN LAYER( 34)  :   2

NUMBER OF RUNS IN LAYER( 35)  :   2
```

```
NUMBER OF START-STOPS :   0
........................


BUILD CIRCUMSTANCES :
.....................
           FILL :
           ......

                PROCESS = SUB
                MATERIAL = 533
                LOCATION = VENDOR
                POSITION = 1G
                ACCESS = GOOD
                JOINT GEOMETRY = STAN
                RESTRAINT = HIGH
```

ACTIVITY DEFINITIONS :
****

        NUMBER OF ACTIVITIES = 40
        ....

                ACTIVITY(1) = LAYER

                THICKNESS   =   6.01   INNER/OUTER LAYER = OUTER

                ACTIVITY(2) = LAYER

                THICKNESS   =   6.01   INNER/OUTER LAYER = OUTER

                ACTIVITY(3) = LAYER

                THICKNESS   =   6.01   INNER/OUTER LAYER = OUTER

                ACTIVITY(4) = LAYER

                THICKNESS   =   6.01   INNER/OUTER LAYER = OUTER

                ACTIVITY(5) = LAYER

                THICKNESS   =   6.01   INNER/OUTER LAYER = OUTER

                ACTIVITY(6) = LAYER

                THICKNESS   =   6.01   INNER/OUTER LAYER = OUTER

                ACTIVITY(7) = LAYER

                THICKNESS   =   6.01   INNER/OUTER LAYER = OUTER

                ACTIVITY(8) = LAYER

                THICKNESS   =   6.01   INNER/OUTER LAYER = OUTER

                ACTIVITY(9) = LAYER

                THICKNESS   =   6.01   INNER/OUTER LAYER = OUTER

                ACTIVITY(10) = LAYER

                THICKNESS   =   6.01   INNER/OUTER LAYER = OUTER

                ACTIVITY(11) = LAYER

                THICKNESS   =   6.01   INNER/OUTER LAYER = OUTER

                ACTIVITY(12) = LAYER

                THICKNESS   =   6.01   INNER/OUTER LAYER = OUTER

                ACTIVITY(13) = LAYER

                THICKNESS   =   6.01   INNER/OUTER LAYER = OUTER

                ACTIVITY(14) = LAYER

                THICKNESS   =   6.01   INNER/OUTER LAYER = OUTER

```
ACTIVITY( 15) = LAYER
THICKNESS   =    6.01    INNER/OUTER LAYER = OUTER

ACTIVITY( 16) = LAYER
THICKNESS   =    7.53    INNER/OUTER LAYER = OUTER

ACTIVITY( 17) = LAYER
THICKNESS   =    7.53    INNER/OUTER LAYER = OUTER

ACTIVITY( 18) = LAYER
THICKNESS   =    7.53    INNER/OUTER LAYER = OUTER

ACTIVITY( 19) = LAYER
THICKNESS   =    7.53    INNER/OUTER LAYER = OUTER

ACTIVITY( 20) = LAYER
THICKNESS   =    7.53    INNER/OUTER LAYER = OUTER

ACTIVITY( 21) = LAYER
THICKNESS   =    7.53    INNER/OUTER LAYER = OUTER

ACTIVITY( 22) = LAYER
THICKNESS   =    7.53    INNER/OUTER LAYER = OUTER

ACTIVITY( 23) = LAYER
THICKNESS   =    7.53    INNER/OUTER LAYER = OUTER

ACTIVITY( 24) = LAYER
THICKNESS   =    7.00    INNER/OUTER LAYER = OUTER

ACTIVITY( 25) = LAYER
THICKNESS   =    7.63    INNER/OUTER LAYER = OUTER

ACTIVITY( 26) = LAYER
THICKNESS   =    7.53    INNER/OUTER LAYER = OUTER

ACTIVITY( 27) = LAYER
THICKNESS   =    7.53    INNER/OUTER LAYER = OUTER

ACTIVITY( 28) = LAYER
THICKNESS   =    7.53    INNER/OUTER LAYER = OUTER

ACTIVITY( 29) = LAYER
THICKNESS   =    7.53    INNER/OUTER LAYER = OUTER

ACTIVITY( 30) = LAYER
THICKNESS   =    7.53    INNER/OUTER LAYER = OUTER
```

```
ACTIVITY( 31) = LAYER

THICKNESS   =   3.56    INNER/OUTER LAYER = INNER


ACTIVITY( 32) = LAYER

THICKNESS   =   3.56    INNER/OUTER LAYER = INNER


ACTIVITY( 33) = LAYER

THICKNESS   =   3.56    INNER/OUTER LAYER = INNER


ACTIVITY( 34) = LAYER

THICKNESS   =   3.56    INNER/OUTER LAYER = INNER


ACTIVITY( 35) = LAYER

THICKNESS   =   3.56    INNER/OUTER LAYER = INNER


ACTIVITY( 36) = REHEAT


ACTIVITY( 37) = MACHINE    ACTIVITY NUMBER( 37) =    0


             AMOUNT TO BE MACHINED FROM UPPER SURFACE = 2.00
             AMOUNT TO BE MACHINED FROM LOWER SURFACE = 1.00


ACTIVITY( 38) = DYEPEN    ACTIVITY NUMBER( 38) =    0


             SURFACE TO BE INSPECTED = LOWER


ACTIVITY( 39) = DYEPEN    ACTIVITY NUMBER( 39) =    1


             SURFACE TO BE INSPECTED = UPPER


ACTIVITY( 40) = XRAY      ACTIVITY NUMBER( 40) =    0


             NO OF SIDEWALL INSPECTIONS = 1
             ENERGY LEVEL = 2.5000E+00
             SOURCE DIAMETER = 4.00
             SOURCE TO FILM DISTANCE = 2000.00
             SOURCE INCLINATION = 0.000
             SOURCE INSPECTION MODE = SWSIROOT
             ACCESS FACTOR = 1.00

AMOUNT OF INSPECTION REQUIRED : 1.0000
--------------------------------


RANDOM NUMBER GENERATOR SEED :   0
--------------------------------
```

```
*** INSPECTION CATEGORY LOWER SURFACE BREAKING         ***

*** INSPECTION EFFICIENCY CURVE FOR CENTRE CRACK          ***
.......................................................................

DEFECT DEPTH =    206.513 EFFICIENCY =    0.976723
DEFECT DEPTH =    10.8691 EFFICIENCY =    0.776723
DEFECT DEPTH =    5.43455 EFFICIENCY =    0.976678
DEFECT DEPTH =    2.71727 EFFICIENCY =    0.967737
DEFECT DEPTH =    1.35864 EFFICIENCY =    0.857197
DEFECT DEPTH =   0.679319 EFFICIENCY =    0.503425
DEFECT DEPTH =   0.339659 EFFICIENCY =    0.181754
DEFECT DEPTH =   0.169830 EFFICIENCY =    5.16609E-02
DEFECT DEPTH =   0.679319 EFFICIENCY =    0.503425
DEFECT DEPTH =    1.01898 EFFICIENCY =    0.735523
DEFECT DEPTH =    206.513 EFFICIENCY =    0.976723
DEFECT DEPTH =    10.8691 EFFICIENCY =    0.976723
DEFECT DEPTH =    5.43455 EFFICIENCY =    0.976678
DEFECT DEPTH =    2.71727 EFFICIENCY =    0.967737
DEFECT DEPTH =    1.35864 EFFICIENCY =    0.857197
DEFECT DEPTH =   0.679319 EFFICIENCY =    0.503425
DEFECT DEPTH =   0.339659 EFFICIENCY =    0.18175.
DEFECT DEPTH =   0.169830 EFFICIENCY =    5.16609E-02
DEFECT DEPTH =   0.679319 EFFICIENCY =    0.503425
DEFECT DEPTH =    1.01898 EFFICIENCY =    0.735523


*** INSPECTION EFFICIENCY CURVE FOR LACK OF ROOT FUSION        ***
.......................................................................

DEFECT DEPTH =    206.513 EFFICIENCY =    0.985736
DEFECT DEPTH =    10.8691 EFFICIENCY =    0.980497
DEFECT DEPTH =    5.43455 EFFICIENCY =    0.953672
DEFECT DEPTH =    2.71727 EFFICIENCY =    0.836171
DEFECT DEPTH =    1.35864 EFFICIENCY =    0.510946
DEFECT DEPTH =   0.679319 EFFICIENCY =    0.189613
DEFECT DEPTH =   0.339659 EFFICIENCY =    5.36680E-02
DEFECT DEPTH =    1.18881 EFFICIENCY =    0.436639
DEFECT DEPTH =    1.69830 EFFICIENCY =    0.634000
DEFECT DEPTH =    2.20779 EFFICIENCY =    0.760316
DEFECT DEPTH =    206.513 EFFICIENCY =    0.985736
DEFECT DEPTH =    10.8691 EFFICIENCY =    0.980497
DEFECT DEPTH =    5.43455 EFFICIENCY =    0.953672
DEFECT DEPTH =    2.71727 EFFICIENCY =    0.836171
DEFECT DEPTH =    1.35864 EFFICIENCY =    0.510946
DEFECT DEPTH =   0.679319 EFFICIENCY =    0.189613
DEFECT DEPTH =   0.339659 EFFICIENCY =    5.36680E-02
DEFECT DEPTH =    1.18881 EFFICIENCY =    0.436639
DEFECT DEPTH =    1.69830 EFFICIENCY =    0.634000
DEFECT DEPTH =    2.20779 EFFICIENCY =    0.760316


*** INSPECTION EFFICIENCY CURVE FOR LACK OF SIDEWALL FUSION        ***
.......................................................................

DEFECT DEPTH =    206.513 EFFICIENCY =    0.964035
DEFECT DEPTH =    10.8691 EFFICIENCY =    0.963817
DEFECT DEPTH =    5.43455 EFFICIENCY =    0.960433
DEFECT DEPTH =    2.71727 EFFICIENCY =    0.919176
DEFECT DEPTH =    1.35864 EFFICIENCY =    0.746410
DEFECT DEPTH =   0.679319 EFFICIENCY =    0.392366
DEFECT DEPTH =   0.339659 EFFICIENCY =    0.133251
DEFECT DEPTH =   0.169830 EFFICIENCY =    3.69647E-02
DEFECT DEPTH =   0.679319 EFFICIENCY =    0.392366
DEFECT DEPTH =    1.01898 EFFICIENCY =    0.609615
DEFECT DEPTH =    206.513 EFFICIENCY =    0.964035
DEFECT DEPTH =    10.8691 EFFICIENCY =    0.963817
DEFECT DEPTH =    5.43455 EFFICIENCY =    0.960433
DEFECT DEPTH =    2.71727 EFFICIENCY =    0.919176
DEFECT DEPTH =    1.35864 EFFICIENCY =    0.746410
DEFECT DEPTH =   0.679319 EFFICIENCY =    0.392366
DEFECT DEPTH =   0.339659 EFFICIENCY =    0.133251
DEFECT DEPTH =   0.169830 EFFICIENCY =    3.69647E-02
DEFECT DEPTH =   0.679319 EFFICIENCY =    0.392366
DEFECT DEPTH =    1.01898 EFFICIENCY =    0.609615
```

```
*** INSPECTION EFFICIENCY CURVE FOR LACK OF INTERRUN FUSION      ***
----------------------------------------------------------------------------

DEFECT DEPTH =    206.513 EFFICIENCY =   0.122848
DEFECT DEPTH =    10.8691 EFFICIENCY =   0.122848
DEFECT DEPTH =    5.43455 EFFICIENCY =   0.122848
DEFECT DEPTH =    2.71727 EFFICIENCY =   0.122848
DEFECT DEPTH =    1.35864 EFFICIENCY =   0.122848
DEFECT DEPTH =   0.679319 EFFICIENCY =   0.122848
DEFECT DEPTH =   0.339659 EFFICIENCY =    9.44419E-02
DEFECT DEPTH =   0.169830 EFFICIENCY =    4.03631E-02
DEFECT DEPTH =  8.49148E-02 EFFICIENCY =   1.38890E-02
DEFECT DEPTH =  4.24574E-02 EFFICIENCY =   4.13489E-03
DEFECT DEPTH =    206.513 EFFICIENCY =   0.122848
DEFECT DEPTH =    10.8691 EFFICIENCY =   0.122848
DEFECT DEPTH =    5.43455 EFFICIENCY =   0.122848
DEFECT DEPTH =    2.71727 EFFICIENCY =   0.122848
DEFECT DEPTH =    1.35864 EFFICIENCY =   0.122848
DEFECT DEPTH =   0.679319 EFFICIENCY =   0.122848
DEFECT DEPTH =   0.339659 EFFICIENCY =    9.44419E-02
DEFECT DEPTH =   0.169830 EFFICIENCY =    4.03631E-02
DEFECT DEPTH =  8.49148E-02 EFFICIENCY =   1.38890E-02
DEFECT DEPTH =  4.24574E-02 EFFICIENCY =   4.13489E-03


*** INSPECTION EFFICIENCY CURVE FOR HEAT AFFECTED ZONE      ***
----------------------------------------------------------------------------

DEFECT DEPTH =    206.513 EFFICIENCY =   0.884283
DEFECT DEPTH =    10.8691 EFFICIENCY =   0.882347
DEFECT DEPTH =    5.43455 EFFICIENCY =   0.866898
DEFECT DEPTH =    2.71727 EFFICIENCY =   0.771915
DEFECT DEPTH =    1.35864 EFFICIENCY =   0.540142
DEFECT DEPTH =   0.679319 EFFICIENCY =   0.246855
DEFECT DEPTH =   0.339659 EFFICIENCY =    7.89472E-02
DEFECT DEPTH =    1.18881 EFFICIENCY =   0.481597
DEFECT DEPTH =    1.69830 EFFICIENCY =   0.630267
DEFECT DEPTH =    2.20779 EFFICIENCY =   0.717843
DEFECT DEPTH =    206.513 EFFICIENCY =   0.884283
DEFECT DEPTH =    10.8691 EFFICIENCY =   0.882347
DEFECT DEPTH =    5.43455 EFFICIENCY =   0.866898
DEFECT DEPTH =    2.71727 EFFICIENCY =   0.771915
DEFECT DEPTH =    1.35864 EFFICIENCY =   0.540142
DEFECT DEPTH =   0.679319 EFFICIENCY =   0.246855
DEFECT DEPTH =   0.339659 EFFICIENCY =    7.89472E-02
DEFECT DEPTH =    1.18881 EFFICIENCY =   0.481597
DEFECT DEPTH =    1.69830 EFFICIENCY =   0.630267
DEFECT DEPTH =    2.20779 EFFICIENCY =   0.717843


*** INSPECTION EFFICIENCY CURVE FOR LACK OF SIDEWALL FUSION SLAG      ***
----------------------------------------------------------------------------

DEFECT DEPTH =    206.513 EFFICIENCY =   0.990000
DEFECT DEPTH =    10.8691 EFFICIENCY =   0.990000
DEFECT DEPTH =    5.43455 EFFICIENCY =   0.990000
DEFECT DEPTH =    2.71727 EFFICIENCY =   0.990000
DEFECT DEPTH =    1.35864 EFFICIENCY =   0.989637
DEFECT DEPTH =   0.679319 EFFICIENCY =   0.846235
DEFECT DEPTH =   0.339659 EFFICIENCY =   0.375183
DEFECT DEPTH =   0.169830 EFFICIENCY =   0.110502
DEFECT DEPTH =  8.49148E-02 EFFICIENCY =   2.87740E-02
DEFECT DEPTH =   0.424574 EFFICIENCY =   0.520801
DEFECT DEPTH =    206.513 EFFICIENCY =   0.990000
DEFECT DEPTH =    10.8691 EFFICIENCY =   0.990000
DEFECT DEPTH =    5.43455 EFFICIENCY =   0.990000
DEFECT DEPTH =    2.71727 EFFICIENCY =   0.990000
DEFECT DEPTH =    1.35864 EFFICIENCY =   0.989637
DEFECT DEPTH =   0.679319 EFFICIENCY =   0.846235
DEFECT DEPTH =   0.339659 EFFICIENCY =   0.375183
DEFECT DEPTH =   0.169830 EFFICIENCY =   0.110502
DEFECT DEPTH =  8.49148E-02 EFFICIENCY =   2.87740E-02
DEFECT DEPTH =   0.424574 EFFICIENCY =   0.520801
```

```
*** INSPECTION EFFICIENCY CURVE FOR LACK OF INTERRUN FUSION SLAG    ***
---------------------------------------------------------------------------

DEFECT DEPTH =    206.513 EFFICIENCY =   0.979681
DEFECT DEPTH =    10.8691 EFFICIENCY =   0.979681
DEFECT DEPTH =    5.43455 EFFICIENCY =   0.979681
DEFECT DEPTH =    2.71727 EFFICIENCY =   0.979681
DEFECT DEPTH =    1.25864 EFFICIENCY =   0.979681
DEFECT DEPTH =   0.679319 EFFICIENCY =   0.979658
DEFECT DEPTH =   0.339659 EFFICIENCY =   0.949513
DEFECT DEPTH =   0.169830 EFFICIENCY =   0.766685
DEFECT DEPTH = 8.49148E-02 EFFICIENCY =   0.407208
DEFECT DEPTH = 4.24574E-02 EFFICIENCY =   0.143946
DEFECT DEPTH =    206.513 EFFICIENCY =   0.979681
DEFECT DEPTH =    10.8691 EFFICIENCY =   0.979681
DEFECT DEPTH =    5.43455 EFFICIENCY =   0.979681
DEFECT DEPTH =    2.71727 EFFICIENCY =   0.979681
DEFECT DEPTH =    1.35864 EFFICIENCY =   0.979681
DEFECT DEPTH =   0.679319 EFFICIENCY =   0.979658
DEFECT DEPTH =   0.339659 EFFICIENCY =   0.949513
DEFECT DEPTH =   0.169830 EFFICIENCY =   0.766685
DEFECT DEPTH = 8.49148E-02 EFFICIENCY =   0.407208
DEFECT DEPTH = 4.24574E-02 EFFICIENCY =   0.143946


*** INSPECTION EFFICIENCY CURVE FOR POST WELD HEAT TREATMENT    ***
---------------------------------------------------------------------------

DEFECT DEPTH =    206.513 EFFICIENCY =   0.884283
DEFECT DEPTH =    10.8691 EFFICIENCY =   0.882347
DEFECT DEPTH =    5.43455 EFFICIENCY =   0.866898
DEFECT DEPTH =    2.71727 EFFICIENCY =   0.771915
DEFECT DEPTH =    1.35864 EFFICIENCY =   0.540142
DEFECT DEPTH =   0.679319 EFFICIENCY =   0.245855
DEFECT DEPTH =   0.339659 EFFICIENCY = 7.89472E-02
DEFECT DEPTH =    1.18881 EFFICIENCY =   0.481597
DEFECT DEPTH =    1.69830 EFFICIENCY =   0.630267
DEFECT DEPTH =    2.20779 EFFICIENCY =   0.717843
DEFECT DEPTH =    206.513 EFFICIENCY =   0.884283
DEFECT DEPTH =    10.8691 EFFICIENCY =   0.882347
DEFECT DEPTH =    5.43455 EFFICIENCY =   0.866898
DEFECT DEPTH =    2.71727 EFFICIENCY =   0.771915
DEFECT DEPTH =    1.35864 EFFICIENCY =   0.540142
DEFECT DEPTH =   0.679319 EFFICIENCY =   0.246855
DEFECT DEPTH =   0.339659 EFFICIENCY = 7.89472E-02
DEFECT DEPTH =    1.18881 EFFICIENCY =   0.481597
DEFECT DEPTH =    1.69830 EFFICIENCY =   0.630267
DEFECT DEPTH =    2.20779 EFFICIENCY =   0.717843
```

```
*** INSPECTION CATEGORY BURIED                          ***

*** INSPECTION EFFICIENCY CURVE FOR CENTRE CRACK            ***
........................................................................

DEFECT DEPTH =     206.513 EFFICIENCY =   0.973799
DEFECT DEPTH =     10.8691 EFFICIENCY =   .973798
DEFECT DEPTH =     5.43455 EFFICIENCY =   0.972561
DEFECT DEPTH =     2.71727 EFFICIENCY =   0.932779
DEFECT DEPTH =     1.35864 EFFICIENCY =   0.711591
DEFECT DEPTH =    0.679319 EFFICIENCY =   0.328895
DEFECT DEPTH =    0.339659 EFFICIENCY =    1.03919E-01
DEFECT DEPTH =    0.169830 EFFICIENCY =    2.81617E-02
DEFECT DEPTH =    0.679319 EFFICIENCY =   0.328895
DEFECT DEPTH =     1.01890 EFFICIENCY =   0.550501
DEFECT DEPTH =     206.513 EFFICIENCY =   0.973799
DEFECT DEPTH =     10.8691 EFFICIENCY =   0.973798
DEFECT DEPTH =     5.43455 EFFICIENCY =   0.972561
DEFECT DEPTH =     2.71727 EFFICIENCY =   0.932779
DEFECT DEPTH =     1.35864 EFFICIENCY =   0.711591
DEFECT DEPTH =    0.679319 EFFICIENCY =   0.328895
DEFECT DEPTH =    0.339659 EFFICIENCY =    1.03919E-01
DEFECT DEPTH =    0.169830 EFFICIENCY =    2.81617E-02
DEFECT DEPTH =    0.679319 EFFICIENCY =   0.328895
DEFECT DEPTH =     1.01890 EFFICIENCY =   0.550501


*** INSPECTION EFFICIENCY CURVE FOR LACK OF ROOT FUSION        ***
........................................................................

DEFECT DEPTH =     206.513 EFFICIENCY =   0.986631
DEFECT DEPTH =     10.8691 EFFICIENCY =   0.968659
DEFECT DEPTH =     5.43455 EFFICIENCY =   0.904755
DEFECT DEPTH =     2.71727 EFFICIENCY =   0.680898
DEFECT DEPTH =     1.35864 EFFICIENCY =   0.314963
DEFECT DEPTH =    0.679319 EFFICIENCY =    9.80179E-02
DEFECT DEPTH =    0.990282 EFFICIENCY =   0.190991
DEFECT DEPTH =     4.03316 EFFICIENCY =   0.836229
DEFECT DEPTH =     2.00457 EFFICIENCY =   0.518070
DEFECT DEPTH =     3.01887 EFFICIENCY =   0.729520
DEFECT DEPTH =     206.513 EFFICIENCY =   0.986631
DEFECT DEPTH =     10.8691 EFFICIENCY =   0.968659
DEFECT DEPTH =     5.43455 EFFICIENCY =   0.904755
DEFECT DEPTH =     2.71727 EFFICIENCY =   0.680898
DEFECT DEPTH =     1.35864 EFFICIENCY =   0.314963
DEFECT DEPTH =    0.679319 EFFICIENCY =    9.80179E-02
DEFECT DEPTH =    0.990282 EFFICIENCY =   0.190991
DEFECT DEPTH =     4.03316 EFFICIENCY =   0.836229
DEFECT DEPTH =     2.00457 EFFICIENCY =   0.518070
DEFECT DEPTH =     3.01887 EFFICIENCY =   0.729520


*** INSPECTION EFFICIENCY CURVE FOR LACK OF SIDEWALL FUSION     ***
........................................................................

DEFECT DEPTH =     206.513 EFFICIENCY =   0.960381
DEFECT DEPTH =     10.8691 EFFICIENCY =   0.959395
DEFECT DEPTH =     5.43455 EFFICIENCY =   0.943875
DEFECT DEPTH =     2.71727 EFFICIENCY =   0.849786
DEFECT DEPTH =     1.35864 EFFICIENCY =   0.578334
DEFECT DEPTH =    0.679319 EFFICIENCY =   0.242459
DEFECT DEPTH =    0.339659 EFFICIENCY =    7.33652E-02
DEFECT DEPTH =     1.18881 EFFICIENCY =   0.507742
DEFECT DEPTH =     1.69830 EFFICIENCY =   0.687991
DEFECT DEPTH =     2.20779 EFFICIENCY =   0.791054
DEFECT DEPTH =     206.513 EFFICIENCY =   0.960381
DEFECT DEPTH =     10.8691 EFFICIENCY =   0.959395
DEFECT DEPTH =     5.43455 EFFICIENCY =   0.943875
DEFECT DEPTH =     2.71727 EFFICIENCY =   0.849786
DEFECT DEPTH =     1.35864 EFFICIENCY =   0.578334
DEFECT DEPTH =    0.679319 EFFICIENCY =   0.242459
DEFECT DEPTH =    0.339659 EFFICIENCY =    7.33652E-02
DEFECT DEPTH =     1.18881 EFFICIENCY =   0.507742
DEFECT DEPTH =     1.69830 EFFICIENCY =   0.687991
DEFECT DEPTH =     2.20779 EFFICIENCY =   0.791054
```

```
***  INSPECTION EFFICIENCY CURVE FOR LACK OF INTERRUN FUSION        ***
-------------------------------------------------------------------------

DEFECT DEPTH =     206.513 EFFICIENCY =    0.111129
DEFECT DEPTH =     10.8691 EFFICIENCY =    0.111129
DEFECT DEPTH =     5.43455 EFFICIENCY =    0.111129
DEFECT DEPTH =     2.71727 EFFICIENCY =    0.111129
DEFECT DEPTH =     1.35864 EFFICIENCY =    0.111129
DEFECT DEPTH =    0.679319 EFFICIENCY =    0.111012
DEFECT DEPTH =    0.339659 EFFICIENCY =    5.59191E-02
DEFECT DEPTH =    0.169830 EFFICIENCY =    2.10694E-02
DEFECT DEPTH =   8.49148E-02 EFFICIENCY =   6.64975E-03
DEFECT DEPTH =    0.543015 EFFICIENCY =    9.46754E-02
DEFECT DEPTH =     206.513 EFFICIENCY =    0.111129
DEFECT DEPTH =     10.8691 EFFICIENCY =    0.111129
DEFECT DEPTH =     5.43455 EFFICIENCY =    0.111129
DEFECT DEPTH =     2.71727 EFFICIENCY =    0.111129
DEFECT DEPTH =     1.35864 EFFICIENCY =    0.111129
DEFECT DEPTH =    0.679319 EFFICIENCY =    0.111012
DEFECT DEPTH =    0.339659 EFFICIENCY =    5.59191E-02
DEFECT DEPTH =    0.169830 EFFICIENCY =    2.10694E-02
DEFECT DEPTH =   8.49148E-02 EFFICIENCY =   6.64975E-03
DEFECT DEPTH =    0.543015 EFFICIENCY =    9.46754E-02


***  INSPECTION EFFICIENCY CURVE FOR HEAT AFFECTED ZONE             ***
-------------------------------------------------------------------------

DEFECT DEPTH =     206.513 EFFICIENCY =    0.875174
DEFECT DEPTH =     10.8691 EFFICIENCY =    0.868535
DEFECT DEPTH =     5.43455 EFFICIENCY =    0.822137
DEFECT DEPTH =     2.71727 EFFICIENCY =    0.657996
DEFECT DEPTH =     1.35864 EFFICIENCY =    0.379298
DEFECT DEPTH =    0.679319 EFFICIENCY =    0.142639
DEFECT DEPTH =    0.339659 EFFICIENCY =    4.14836E-02
DEFECT DEPTH =     1.18881 EFFICIENCY =    0.323839
DEFECT DEPTH =     1.69830 EFFICIENCY =    0.475360
DEFECT DEPTH =     2.20779 EFFICIENCY =    0.582700
DEFECT DEPTH =     206.513 EFFICIENCY =    0.875174
DEFECT DEPTH =     10.8691 EFFICIENCY =    0.868535
DEFECT DEPTH =     5.43455 EFFICIENCY =    0.822137
DEFECT DEPTH =     2.71727 EFFICIENCY =    0.657996
DEFECT DEPTH =     1.35864 EFFICIENCY =    0.379298
DEFECT DEPTH =    0.679319 EFFICIENCY =    0.142639
DEFECT DEPTH =    0.339659 EFFICIENCY =    4.14836E-02
DEFECT DEPTH =     1.18881 EFFICIENCY =    0.323839
DEFECT DEPTH =     1.69830 EFFICIENCY =    0.475360
DEFECT DEPTH =     2.20779 EFFICIENCY =    0.582700


***  INSPECTION EFFICIENCY CURVE FOR LACK OF SIDEWALL FUSION SLAG   ***
-------------------------------------------------------------------------

DEFECT DEPTH =     206.513 EFFICIENCY =    0.990000
DEFECT DEPTH =     10.8691 EFFICIENCY =    0.990000
DEFECT DEPTH =     5.43455 EFFICIENCY =    0.990000
DEFECT DEPTH =     2.71727 EFFICIENCY =    0.990000
DEFECT DEPTH =     1.35864 EFFICIENCY =    0.989139
DEFECT DEPTH =    0.679319 EFFICIENCY =    0.813489
DEFECT DEPTH =    0.339659 EFFICIENCY =    0.343356
DEFECT DEPTH =    0.169830 EFFICIENCY =    9.94085E-02
DEFECT DEPTH =   8.49148E-02 EFFICIENCY =   2.57671E-02
DEFECT DEPTH =    0.424574 EFFICIENCY =    0.482169
DEFECT DEPTH =     206.513 EFFICIENCY =    0.990000
DEFECT DEPTH =     10.8691 EFFICIENCY =    0.990000
DEFECT DEPTH =     5.43455 EFFICIENCY =    0.990000
DEFECT DEPTH =     2.71727 EFFICIENCY =    0.990000
DEFECT DEPTH =     1.35864 EFFICIENCY =    0.989139
DEFECT DEPTH =    0.679319 EFFICIENCY =    0.813489
DEFECT DEPTH =    0.339659 EFFICIENCY =    0.343356
DEFECT DEPTH =    0.169830 EFFICIENCY =    9.94085E-02
DEFECT DEPTH =   8.49148E-02 EFFICIENCY =   2.57671E-02
DEFECT DEPTH =    0.424574 EFFICIENCY =    0.482169
```

```
*** INSPECTION EFFICIENCY CURVE FOR LACK OF INTERRUN FUSION SLAG      ***
........................................................................

DEFECT DEPTH =     206.513 EFFICIENCY =    0.975945
DEFECT DEPTH =     10.8691 EFFICIENCY =    0.975945
DEFECT DEPTH =     5.43455 EFFICIENCY =    0.975945
DEFECT DEPTH =     2.71727 EFFICIENCY =    0.975945
DEFECT DEPTH =     1.35864 EFFICIENCY =    0.975945
DEFECT DEPTH =    0.679319 EFFICIENCY =    0.972182
DEFECT DEPTH =    0.339659 EFFICIENCY =    0.881057
DEFECT DEPTH =    0.169830 EFFICIENCY =    0.593617
DEFECT DEPTH =   8.49148E-02 EFFICIENCY =    0.254109
DEFECT DEPTH =   4.24574E-02 EFFICIENCY =   7.91767E-02
DEFECT DEPTH =     206.513 EFFICIENCY =    0.975945
DEFECT DEPTH =     10.8691 EFFICIENCY =    0.975945
DEFECT DEPTH =     5.43455 EFFICIENCY =    0.975945
DEFECT DEPTH =     2.71727 EFFICIENCY =    0.975945
DEFECT DEPTH =     1.35864 EFFICIENCY =    0.975945
DEFECT DEPTH =    0.679319 EFFICIENCY =    0.972182
DEFECT DEPTH =    0.339659 EFFICIENCY =    0.881057
DEFECT DEPTH =    0.169830 EFFICIENCY =    0.593617
DEFECT DEPTH =   8.49148E-02 EFFICIENCY =    0.254109
DEFECT DEPTH =   4.24574E-02 EFFICIENCY =   7.91767E-02


*** INSPECTION EFFICIENCY CURVE FOR POST WELD HEAT TREATMENT          ***
........................................................................

DEFECT DEPTH =     206.513 EFFICIENCY =    0.875174
DEFECT DEPTH =     10.8691 EFFICIENCY =    0.868535
DEFECT DEPTH =     5.43455 EFFICIENCY =    0.822137
DEFECT DEPTH =     2.71727 EFFICIENCY =    0.657996
DEFECT DEPTH =     1.35864 EFFICIENCY =    0.379298
DEFECT DEPTH =    0.679319 EFFICIENCY =    0.142639
DEFECT DEPTH =    0.339659 EFFICIENCY =   4.14636E-02
DEFECT DEPTH =     1.18881 EFFICIENCY =    0.323839
DEFECT DEPTH =     1.69830 EFFICIENCY =    0.475360
DEFECT DEPTH =     2.20779 EFFICIENCY =    0.582700
DEFECT DEPTH =     206.513 EFFICIENCY =    0.875174
DEFECT DEPTH =     10.8691 EFFICIENCY =    0.868535
DEFECT DEPTH =     5.43455 EFFICIENCY =    0.822137
DEFECT DEPTH =     2.71727 EFFICIENCY =    0.657996
DEFECT DEPTH =     1.35864 EFFICIENCY =    0.379298
DEFECT DEPTH =    0.679319 EFFICIENCY =    0.142639
DEFECT DEPTH =    0.339659 EFFICIENCY =   4.14636E-02
DEFECT DEPTH =     1.18881 EFFICIENCY =    0.323839
DEFECT DEPTH =     1.69830 EFFICIENCY =    0.475360
DEFECT DEPTH =     2.20779 EFFICIENCY =    0.582700
```

```
*** INSPECTION CATEGORY UPPER SURFACE BREAKING          ***

*** INSPECTION EFFICIENCY CURVE FOR CENTRE CRACK                    ***
.........................................................................

DEFECT DEPTH =    206.513 EFFICIENCY =    0.970103
DEFECT DEPTH =    10.8691 EFFICIENCY =    0.970059
DEFECT DEPTH =    5.43455 EFFICIENCY =    0.963092
DEFECT DEPTH =    2.71727 EFFICIENCY =    0.871677
DEFECT DEPTH =    1.35864 EFFICIENCY =    0.559232
DEFECT DEPTH =   0.679319 EFFICIENCY =    0.217620
DEFECT DEPTH =   0.339659 EFFICIENCY =    6.37174E-02
DEFECT DEPTH =    1.18881 EFFICIENCY =    0.482864
DEFECT DEPTH =    1.69830 EFFICIENCY =    0.683057
DEFECT DEPTH =    2.20779 EFFICIENCY =    0.803788
DEFECT DEPTH =    206.513 EFFICIENCY =    0.970103
DEFECT DEPTH =    10.8691 EFFICIENCY =    0.970059
DEFECT DEPTH =    5.43455 EFFICIENCY =    0.963092
DEFECT DEPTH =    2.71727 EFFICIENCY =    0.871677
DEFECT DEPTH =    1.35864 EFFICIENCY =    0.559232
DEFECT DEPTH =   0.679319 EFFICIENCY =    0.217620
DEFECT DEPTH =   0.339659 EFFICIENCY =    6.37174E-02
DEFECT DEPTH =    1.18881 EFFICIENCY =    0.482864
DEFECT DEPTH =    1.69830 EFFICIENCY =    0.683057
DEFECT DEPTH =    2.20779 EFFICIENCY =    0.803788


*** INSPECTION EFFICIENCY CURVE FOR LACK OF ROOT FUSION            ***
.........................................................................

DEFECT DEPTH =    206.513 EFFICIENCY =    0.985737
DEFECT DEPTH =    10.8691 EFFICIENCY =    0.948546
DEFECT DEPTH =    5.43455 EFFICIENCY =    0.832310
DEFECT DEPTH =    2.71727 EFFICIENCY =    0.522058
DEFECT DEPTH =    1.35864 EFFICIENCY =    0.197416
DEFECT DEPTH =   0.679319 EFFICIENCY =    5.60558E-02
DEFECT DEPTH =    2.17382 EFFICIENCY =    0.400661
DEFECT DEPTH =    2.98900 EFFICIENCY =    0.574048
DEFECT DEPTH =    3.80418 EFFICIENCY =    0.696821
DEFECT DEPTH =    4.61937 EFFICIENCY =    0.779358
DEFECT DEPTH =    206.513 EFFICIENCY =    0.985737
DEFECT DEPTH =    10.8691 EFFICIENCY =    0.948546
DEFECT DEPTH =    5.43455 EFFICIENCY =    0.832310
DEFECT DEPTH =    2.71727 EFFICIENCY =    0.522058
DEFECT DEPTH =    1.35864 EFFICIENCY =    0.197416
DEFECT DEPTH =   0.679319 EFFICIENCY =    5.60558E-02
DEFECT DEPTH =    2.17382 EFFICIENCY =    0.400661
DEFECT DEPTH =    2.98900 EFFICIENCY =    0.574048
DEFECT DEPTH =    3.80418 EFFICIENCY =    0.696821
DEFECT DEPTH =    4.61937 EFFICIENCY =    0.779358


*** INSPECTION EFFICIENCY CURVE FOR LACK OF SIDEWALL FUSION         ***
.........................................................................

DEFECT DEPTH =    206.513 EFFICIENCY =    0.956044
DEFECT DEPTH =    10.8691 EFFICIENCY =    0.952534
DEFECT DEPTH =    5.43455 EFFICIENCY =    0.913521
DEFECT DEPTH =    2.71727 EFFICIENCY =    0.758795
DEFECT DEPTH =    1.35864 EFFICIENCY =    0.430838
DEFECT DEPTH =   0.679319 EFFICIENCY =    0.154790
DEFECT DEPTH =   0.339659 EFFICIENCY =    4.38332E-02
DEFECT DEPTH =    1.18881 EFFICIENCY =    0.364501
DEFECT DEPTH =    1.69830 EFFICIENCY =    0.546755
DEFECT DEPTH =    2.20779 EFFICIENCY =    0.674906
DEFECT DEPTH =    206.513 EFFICIENCY =    0.956044
DEFECT DEPTH =    10.8691 EFFICIENCY =    0.952534
DEFECT DEPTH =    5.43455 EFFICIENCY =    0.913521
DEFECT DEPTH =    2.71727 EFFICIENCY =    0.758795
DEFECT DEPTH =    1.35864 EFFICIENCY =    0.430838
DEFECT DEPTH =   0.679319 EFFICIENCY =    0.154790
DEFECT DEPTH =   0.339659 EFFICIENCY =    4.38332E-02
DEFECT DEPTH =    1.18881 EFFICIENCY =    0.364501
DEFECT DEPTH =    1.69830 EFFICIENCY =    0.546755
DEFECT DEPTH =    2.20779 EFFICIENCY =    0.674906
```

```
*** INSPECTION EFFICIENCY CURVE FOR LACK OF INTERRUN FUSION          ***
.........................................................................

DEFECT DEPTH =    206.513 EFFICIENCY =    9.98117E-02
DEFECT DEPTH =    10.8691 EFFICIENCY =    9.98117E-02
DEFECT DEPTH =    5.43455 EFFICIENCY =    9.98117E-02
DEFECT DEPTH =    2.71727 EFFICIENCY =    9.98117E-02
DEFECT DEPTH =    1.35864 EFFICIENCY =    9.98117E-02
DEFECT DEPTH =    0.679319 EFFICIENCY =   8.12250E-02
DEFECT DEPTH =    0.339659 EFFICIENCY =   3.51176E-02
DEFECT DEPTH =    0.169830 EFFICIENCY =   1.22215E-02
DEFECT DEPTH =    8.49148E-02 EFFICIENCY =   3.66885E-03
DEFECT DEPTH =    0.424574 EFFICIENCY =   4.72389E-02
DEFECT DEPTH =    206.513 EFFICIENCY =    9.06117E-02
DEFECT DEPTH =    10.8691 EFFICIENCY =    9.98117E-02
DEFECT DEPTH =    5.43455 EFFICIENCY =    9.98117E-02
DEFECT DEPTH =    2.71727 EFFICIENCY =    9.98117E-02
DEFECT DEPTH =    1.35864 EFFICIENCY =    9.98117E-02
DEFECT DEPTH =    0.679319 EFFICIENCY =   8.12250E-02
DEFECT DEPTH =    0.339659 EFFICIENCY =   3.51176E-02
DEFECT DEPTH =    0.169830 EFFICIENCY =   1.22215E-02
DEFECT DEPTH =    8.49148E-02 EFFICIENCY =   3.66885E-03
DEFECT DEPTH =    0.424574 EFFICIENCY =   4.72389E-02


*** INSPECTION EFFICIENCY CURVE FOR HEAT AFFECTED ZONE               ***
.........................................................................

DEFECT DEPTH =    206.513 EFFICIENCY =    0.865775
DEFECT DEPTH =    10.8691 EFFICIENCY =    0.848297
DEFECT DEPTH =    5.43455 EFFICIENCY =    0.758696
DEFECT DEPTH =    2.71727 EFFICIENCY =    0.543697
DEFECT DEPTH =    1.35864 EFFICIENCY =    0.263680
DEFECT DEPTH =    0.679319 EFFICIENCY =   6.74740E-02
DEFECT DEPTH =    0.339659 EFFICIENCY =   2.41760E-02
DEFECT DEPTH =    1.86813 EFFICIENCY =    0.388927
DEFECT DEPTH =    3.05693 EFFICIENCY =    0.588585
DEFECT DEPTH =    4.24574 EFFICIENCY =    0.696199
DEFECT DEPTH =    206.513 EFFICIENCY =    0.865775
DEFECT DEPTH =    10.8691 EFFICIENCY =    0.848297
DEFECT DEPTH =    5.43455 EFFICIENCY =    0.758696
DEFECT DEPTH =    2.71727 EFFICIENCY =    0.543697
DEFECT DEPTH =    1.35864 EFFICIENCY =    0.263680
DEFECT DEPTH =    0.679319 EFFICIENCY =   6.74740E-02
DEFECT DEPTH =    0.339659 EFFICIENCY =   2.41760E-02
DEFECT DEPTH =    1.86813 EFFICIENCY =    0.388927
DEFECT DEPTH =    3.05693 EFFICIENCY =    0.588585
DEFECT DEPTH =    4.24574 EFFICIENCY =    0.696199


*** INSPECTION EFFICIENCY CURVE FOR LACK OF SIDEWALL FUSION SLAG     ***
.........................................................................

DEFECT DEPTH =    206.513 EFFICIENCY =    0.990000
DEFECT DEPTH =    10.8691 EFFICIENCY =    0.990000
DEFECT DEPTH =    5.43455 EFFICIENCY =    0.990000
DEFECT DEPTH =    2.71727 EFFICIENCY =    0.990000
DEFECT DEPTH =    1.35864 EFFICIENCY =    0.987782
DEFECT DEPTH =    0.679319 EFFICIENCY =   0.772719
DEFECT DEPTH =    0.339659 EFFICIENCY =   0.310058
DEFECT DEPTH =    0.169830 EFFICIENCY =   8.83079E-02
DEFECT DEPTH =    0.253839 EFFICIENCY =   0.186948
DEFECT DEPTH =    0.466579 EFFICIENCY =   0.503993
DEFECT DEPTH =    206.513 EFFICIENCY =    0.990000
DEFECT DEPTH =    10.8691 EFFICIENCY =    0.990000
DEFECT DEPTH =    5.43455 EFFICIENCY =    0.990000
DEFECT DEPTH =    2.71727 EFFICIENCY =    0.990000
DEFECT DEPTH =    1.35864 EFFICIENCY =    0.987782
DEFECT DEPTH =    0.679319 EFFICIENCY =   0.772719
DEFECT DEPTH =    0.339659 EFFICIENCY =   0.310058
DEFECT DEPTH =    0.169830 EFFICIENCY =   8.83079E-02
DEFECT DEPTH =    0.253839 EFFICIENCY =   0.186948
DEFECT DEPTH =    0.466579 EFFICIENCY =   0.503993
```

```
*** INSPECTION EFFICIENCY CURVE FOR LACK OF INTERRUN FUSION SLAG     ***
---------------------------------------------------------------------------

DEFECT DEPTH =    206.513 EFFICIENCY =   0.970883
DEFECT DEPTH =    10.8691 EFFICIENCY =   0.970883
DEFECT DEPTH =    5.43455 EFFICIENCY =   0.970883
DEFECT DEPTH =    2.71727 EFFICIENCY =   0.970883
DEFECT DEPTH =    1.35864 EFFICIENCY =   0.970883
DEFECT DEPTH =   0.679319 EFFICIENCY =   0.946369
DEFECT DEPTH =   0.339659 EFFICIENCY =   0.782214
DEFECT DEPTH =   0.169830 EFFICIENCY =   0.441517
DEFECT DEPTH =  8.49148E-02 EFFICIENCY =   0.162917
DEFECT DEPTH =  4.24574E-02 EFFICIENCY =    4.73287E-02
DEFECT DEPTH =    206.513 EFFICIENCY =   0.970883
DEFECT DEPTH =    10.8691 EFFICIENCY =   0.970883
DEFECT DEPTH =    5.43455 EFFICIENCY =   0.970883
DEFECT DEPTH =    2.71727 EFFICIENCY =   0.970883
DEFECT DEPTH =    1.35864 EFFICIENCY =   0.970883
DEFECT DEPTH =   0.679319 EFFICIENCY =   0.946369
DEFECT DEPTH =   0.339659 EFFICIENCY =   0.782214
DEFECT DEPTH =   0.169830 EFFICIENCY =   0.441517
DEFECT DEPTH =  8.49148E-02 EFFICIENCY =   0.162917
DEFECT DEPTH =  4.24574E-02 EFFICIENCY =    4.73287E-02


*** INSPECTION EFFICIENCY CURVE FOR POST WELD HEAT TREATMENT     ***
---------------------------------------------------------------------------

DEFECT DEPTH =    206.513 EFFICIENCY =   0.865775
DEFECT DEPTH =    10.8691 EFFICIENCY =   0.848297
DEFECT DEPTH =    5.43455 EFFICIENCY =   0.758696
DEFECT DEPTH =    2.71727 EFFICIENCY =   0.543697
DEFECT DEPTH =    1.35864 EFFICIENCY =   0.263680
DEFECT DEPTH =   0.679319 EFFICIENCY =   8.74740E-02
DEFECT DEPTH =   0.339659 EFFICIENCY =   2.41760E-02
DEFECT DEPTH =    1.86813 EFFICIENCY =   0.388927
DEFECT DEPTH =    3.05693 EFFICIENCY =   0.588585
DEFECT DEPTH =    4.24574 EFFICIENCY =   0.696199
DEFECT DEPTH =    206.513 EFFICIENCY =   0.865775
DEFECT DEPTH =    10.8691 EFFICIENCY =   0.848297
DEFECT DEPTH =    5.43455 EFFICIENCY =   0.758696
DEFECT DEPTH =    2.71727 EFFICIENCY =   0.543697
DEFECT DEPTH =    1.35864 EFFICIENCY =   0.263680
DEFECT DEPTH =   0.679319 EFFICIENCY =   8.74740E-02
DEFECT DEPTH =   0.339659 EFFICIENCY =   2.41760E-02
DEFECT DEPTH =    1.86813 EFFICIENCY =   0.388927
DEFECT DEPTH =    3.05693 EFFICIENCY =   0.588585
DEFECT DEPTH =    4.24576 EFFICIENCY =   0.696199


************ END OF WELD DEFECT ANALYSIS RUN ************
```

JULY 14, 1998
C:\RRA\CLAD.4
UNIFORM THICKNESS WELD - WITH X-RAY
RERUN WITH JUNE VERSION OF RR-PRODIGAL
INPUT FILE = 5.1   OUTPUT FILE = CLAD.4 = DANCER.WELD.00004
TITLE = UWELD1

STRUCTURE DESCRIPTION
****

                    STRUCTURE NAME = LONG
                    ....

                    STRUCTURE TYPE : CLAD
                    ....

                    DATABASE TITLE : PNNLvessel
                    ....

                    ZONES TITLE : DEFAULT
                    ....

                    STRUCTURE DEPTH :   11.000
                    ....

                    STRUCTURE LENGTH :   1000.00
                    ....

                    UPPER STRUCTURE WIDTH :   48.840
                    ....

                    LOWER STRUCTURE WIDTH :   48.840
                    ....

                    STRUCTURE WALL ANGLE :   0.000
                    ....

BUILD DESCRIPTION :
....

                    NUMBER OF STRUCTURE LAYERS :   2
                    ....

                        NUMBER OF RUNS IN LAYER(1) : 66

                        NUMBER OF RUNS IN LAYER(2) : 66

                    NUMBER OF START-STOPS :   0
                    ....

                    BUILD CIRCUMSTANCES :
                    ....
                                    FILL :
                                    ......
                                        PROCESS = SUB
                                        MATERIAL = ASC
                                        LOCATION = VENDOR
                                        POSITION = 1G
                                        ACCESS = GOOD
                                        JOINT GEOMETRY = STAN
                                        RESTRAINT = LOW

ACTIVITY DEFINITIONS :
****

      NUMBER OF ACTIVITIES =   2

        ACTIVITY(1) = LAYER

        THICKNESS   =   5.50   INNER/OUTER LAYER = INNER

        ACTIVITY(2) = LAYER

        THICKNESS   =   5.50   INNER/OUTER LAYER = INNER

     AMOUNT OF INSPECTION REQUIRED : 1.0000

     RANDOM NUMBER GENERATOR SEED :   0

************ END OF WELD DEFECT ANALYSIS RUN ************

```
JULY 16, 1998
C:\RRA\WALTZER.4
UNIFORM THICKNESS WELD - WITH X-RAY
RERUN WITH JUNE VERSION OF RR-PRODIGAL
INPUT FILE = 5.1   OUTPUT FILE = WALYER.4 = DANCER.WALTZER.00004
TITLE = UWELD1
```

STRUCTURE DESCRIPTION
****

                STRUCTURE NAME : LONG
                ....

                STRUCTURE TYPE : WELD+CLAD
                ....

                DATABASE TITLE : PNNLvessel
                ....

                ZONES TITLE : Customised
                ....

                WELD DEPTH : 217.382
                ....

                CLAD DEPTH : 11.000
                ....

                WELD LENGTH : 1000.000
                ....

                CLAD LENGTH : 1000.000
                ....

                UPPER CLAD WIDTH : 48.840
                ....

RUN PARAMETERS
****

                RUN NUMBER :   4
                ....

                TOTAL NUMBER OF SIMULATIONS :   50000
                ....

                NUMBER OF DATA BLOCKS :   50
                ....

                TIME DELAY FOR DATA LOCKS :   10
                ....

                DEPTH OF PULL THROUGH ZONE :   0.000
                ....

                PARENT THICKNESS: 217.382
                ....

                IN-LINE CLAD ORIENTATION
                ....

DEFECT-DATA STORE CONTENTS
****

COMPONENT IDENTIFIER : None
....

INITIAL-TYPE : SURF_I

% DEPTH	FREQ.	ASPECT:	<2	2-3	3-4	4-5	5-6	6-7	7-8	8-9	9-10	10-11	11-12	12-13	13-14	14->
1	0.670000E-02		6.8	3.4	8.9	7.2	16.1	12.8	8.9	9.8	6.0	5.1	6.0	3.8	1.7	3.4
2	0.348997E-01		2.4	3.3	6.2	16.7	11.2	14.4	12.8	10.8	10.0	6.4	4.5	3.6	1.6	2.9
3	0.660000E-03		9.4	28.1	15.8	9.4	6.2	6.2	6.2	3.1	3.1	3.1	0.0	0.0	0.0	6.2
4	0.140000E-03		57.1	42.9	0.0	0.0	0.0	0.0	0.0	0.0	0.0	0.0	0.0	0.0	0.0	0.0
5	0.000000E+00		0.0	0.0	0.0	0.0	0.0	0.0	0.0	0.0	0.0	0.0	0.0	0.0	0.0	0.0

(rows 6 through 100 all 0.000000E+00 with all aspect values 0.0)

CRACK OCCURRENCE PER WELD = 4.0380E-02

```
INITIAL-TYPE : CL
--------------
```

% DEPTH	FREQ.	ASPECTS: <2	2-3	3-4	4-5	5-6	6-7	7-8	8-9	9-10	10-11	11-12	12-13	13-14	14->
1	0.310795E-01	57.4	0.1	0.2	0.2	0.4	1.3	1.5	1.4	1.2	2.9	2.8	1.9	4.0	23.3
2	0.247737E+00	59.3	0.0	0.1	0.2	0.5	1.1	1.7	2.2	2.2	3.0	2.7	2.4	3.1	21.3
3	0.522000E-02	77.5	1.1	1.1	1.5	2.4	1.9	4.3	0.4	1.5	1.1	0.0	0.8	0.4	4.6
4	0.820000E-03	0.0	2.4	14.6	12.2	7.3	9.8	12.2	12.2	9.8	4.9	7.3	2.4	2.4	2.4
5	0.400000E-04	0.0	0.0	0.0	50.0	0.0	0.0	50.0	0.0	0.0	0.0	0.0	0.0	0.0	0.0
6	0.000000E+00	0.0	0.0	0.0	0.0	0.0	0.0	0.0	0.0	0.0	0.0	0.0	0.0	0.0	0.0
7	0.000000E+00	0.0	0.0	0.0	0.0	0.0	0.0	0.0	0.0	0.0	0.0	0.0	0.0	0.0	0.0
8	0.000000E+00	0.0	0.0	0.0	0.0	0.0	0.0	0.0	0.0	0.0	0.0	0.0	0.0	0.0	0.0
9	0.000000E+00	0.0	0.0	0.0	0.0	0.0	0.0	0.0	0.0	0.0	0.0	0.0	0.0	0.0	0.0
10	0.000000E+00	0.0	0.0	0.0	0.0	0.0	0.0	0.0	0.0	0.0	0.0	0.0	0.0	0.0	0.0
11	0.000000E+00	0.0	0.0	0.0	0.0	0.0	0.0	0.0	0.0	0.0	0.0	0.0	0.0	0.0	0.0
12	0.000000E+00	0.0	0.0	0.0	0.0	0.0	0.0	0.0	0.0	0.0	0.0	0.0	0.0	0.0	0.0
13	0.000000E+00	0.0	0.0	0.0	0.0	0.0	0.0	0.0	0.0	0.0	0.0	0.0	0.0	0.0	0.0
14	0.000000E+00	0.0	0.0	0.0	0.0	0.0	0.0	0.0	0.0	0.0	0.0	0.0	0.0	0.0	0.0
15	0.000000E+00	0.0	0.0	0.0	0.0	0.0	0.0	0.0	0.0	0.0	0.0	0.0	0.0	0.0	0.0
16	0.000000E+00	0.0	0.0	0.0	0.0	0.0	0.0	0.0	0.0	0.0	0.0	0.0	0.0	0.0	0.0
17	0.000000E+00	0.0	0.0	0.0	0.0	0.0	0.0	0.0	0.0	0.0	0.0	0.0	0.0	0.0	0.0
18	0.000000E+00	0.0	0.0	0.0	0.0	0.0	0.0	0.0	0.0	0.0	0.0	0.0	0.0	0.0	0.0
19	0.000000E+00	0.0	0.0	0.0	0.0	0.0	0.0	0.0	0.0	0.0	0.0	0.0	0.0	0.0	0.0
20	0.000000E+00	0.0	0.0	0.0	0.0	0.0	0.0	0.0	0.0	0.0	0.0	0.0	0.0	0.0	0.0
21	0.020000E+00	0.0	3.0	0.0	3.0	0.0	0.0	0.0	0.0	0.0	0.0	0.0	0.0	0.0	0.0
22	0.000000E+00	0.0	0.0	0.0	0.0	0.0	0.0	0.0	0.0	0.0	0.0	0.0	0.0	0.0	0.0
23	0.000000E+00	0.0	0.0	0.0	0.0	0.0	0.0	0.0	0.0	0.0	0.0	0.0	0.0	0.0	0.0
24	0.000000E+00	0.0	0.0	0.0	0.0	0.0	0.0	0.0	0.0	0.0	0.0	0.0	0.0	0.0	0.0
25	0.000000E+00	0.0	0.0	0.0	0.0	0.0	0.0	0.0	0.0	0.0	0.0	0.0	0.0	0.0	0.0
26	0.000000E+00	0.0	0.0	0.0	0.0	0.0	0.0	0.0	0.0	0.0	0.0	0.0	0.0	0.0	0.0
27	0.000000E+00	0.0	0.0	0.0	0.0	0.0	0.0	0.0	0.0	0.0	0.0	0.0	0.0	0.0	0.0
28	0.000000E+00	0.0	0.0	0.0	0.0	0.0	0.0	0.0	0.0	0.0	0.0	0.0	0.0	0.0	0.0
29	0.000000E+00	0.0	0.0	0.0	0.0	0.0	0.0	0.0	0.0	0.0	0.0	0.0	0.0	0.0	0.0
30	0.000000E+00	0.0	0.0	0.0	0.0	0.0	0.0	0.0	0.0	0.0	0.0	0.0	0.0	0.0	0.0
31	0.000000E+00	0.0	0.0	0.0	0.0	0.0	0.0	0.0	0.0	0.0	0.0	0.0	0.0	0.0	0.0
32	0.000000E+00	0.0	0.0	0.0	0.0	0.0	0.0	0.0	0.0	0.0	0.0	0.0	0.0	0.0	0.0
33	0.000000E+00	0.0	0.0	0.0	0.0	0.0	0.0	0.0	0.0	0.0	0.0	0.0	0.0	0.0	0.0
34	0.000000E+00	0.0	0.0	0.0	0.0	0.0	0.0	0.0	0.0	0.0	0.0	0.0	0.0	0.0	0.0
35	0.000000E+00	0.0	0.0	0.0	0.0	0.0	0.0	0.0	0.0	0.0	0.0	0.0	0.0	0.0	0.0
36	0.000000E+00	0.0	0.0	0.0	0.0	0.0	0.0	0.0	0.0	0.0	0.0	0.0	0.0	0.0	0.0
37	0.000000E+00	0.0	0.0	0.0	0.0	0.0	0.0	0.0	0.0	0.0	0.0	0.0	0.0	0.0	0.0
38	0.000000E+00	0.0	0.0	0.0	0.0	0.0	0.0	0.0	0.0	0.0	0.0	0.0	0.0	0.0	0.0
39	0.000000E+00	0.0	0.0	0.0	0.0	0.0	0.0	0.0	0.0	0.0	0.0	0.0	0.0	0.0	0.0
40	0.000000E+00	0.0	0.0	0.0	0.0	0.0	0.0	0.0	0.0	0.0	0.0	0.0	0.0	0.0	0.0
41	0.000000E+00	0.0	0.0	0.0	0.0	0.0	0.0	0.0	0.0	0.0	0.0	0.0	0.0	0.0	0.0
42	0.000000E+00	0.0	0.0	0.0	0.0	0.0	0.0	0.0	0.0	0.0	0.0	0.0	0.0	0.0	0.0
43	0.000000E+00	0.0	0.0	0.0	0.0	0.0	0.0	0.0	0.0	0.0	0.0	0.0	0.0	0.0	0.0
44	0.000000E+00	0.0	0.0	0.0	0.0	0.0	0.0	0.0	0.0	0.0	0.0	0.0	0.0	0.0	0.0
45	0.000000E+00	0.0	0.0	0.0	0.0	0.0	0.0	0.0	0.0	0.0	0.0	0.0	0.0	0.0	0.0
46	0.000000E+00	0.0	0.0	0.0	0.0	0.0	0.0	0.0	0.0	0.0	0.0	0.0	0.0	0.0	0.0
47	0.000000E+00	0.0	0.0	0.0	0.0	0.0	0.0	0.0	0.0	0.0	0.0	0.0	0.0	0.0	0.0
48	0.000000E+00	0.0	0.0	0.0	0.0	0.0	0.0	0.0	0.0	0.0	0.0	0.0	0.0	0.0	0.0
49	0.000000E+00	0.0	0.0	0.0	0.0	0.0	0.0	0.0	0.0	0.0	0.0	0.0	0.0	0.0	0.0
50	0.000000E+00	0.0	0.0	0.0	0.0	0.0	0.0	0.0	0.0	0.0	0.0	0.0	0.0	0.0	0.0
51	0.000000E+00	0.0	0.0	0.0	0.0	0.0	0.0	0.0	0.0	0.0	0.0	0.0	0.0	0.0	0.0
52	0.000000E+00	0.0	0.0	0.0	0.0	0.0	0.0	0.0	0.0	0.0	0.0	0.0	0.0	0.0	0.0
53	0.000000E+00	0.0	0.0	0.0	0.0	0.0	0.0	0.0	0.0	0.0	0.0	0.0	0.0	0.0	0.0
54	0.000000E+00	0.0	0.0	0.0	0.0	0.0	0.0	0.0	0.0	0.0	0.0	0.0	0.0	0.0	0.0
55	0.000000E+00	0.0	0.0	0.0	0.0	0.0	0.0	0.0	0.0	0.0	0.0	0.0	0.0	0.0	0.0
56	0.000000E+00	0.0	0.0	0.0	0.0	0.0	0.0	0.0	0.0	0.0	0.0	0.0	0.0	0.0	0.0
57	0.000000E+00	0.0	0.0	0.0	0.0	0.0	0.0	0.0	0.0	0.0	0.0	0.0	0.0	0.0	0.0
58	0.000000E+00	0.0	0.0	0.0	0.0	0.0	0.0	0.0	0.0	0.0	0.0	0.0	0.0	0.0	0.0
59	0.000000E+00	0.0	0.0	0.0	0.0	0.0	0.0	0.0	0.0	0.0	0.0	0.0	0.0	0.0	0.0
60	0.000000E+00	0.0	0.0	0.0	0.0	0.0	0.0	0.0	0.0	0.0	0.0	0.0	0.0	0.0	0.0
61	0.000000E+00	0.0	0.0	0.0	0.0	0.0	0.0	0.0	0.0	0.0	0.0	0.0	0.0	0.0	0.0
62	0.000000E+00	0.0	0.0	0.0	0.0	0.0	0.0	0.0	0.0	0.0	0.0	0.0	0.0	0.0	0.0
63	0.000000E+00	0.0	0.0	0.0	0.0	0.0	0.0	0.0	0.0	0.0	0.0	0.0	0.0	0.0	0.0
64	0.000000E+00	0.0	0.0	0.0	0.0	0.0	0.0	0.0	0.0	0.0	0.0	0.0	0.0	0.0	0.0
65	0.000000E+00	0.0	0.0	0.0	0.0	0.0	0.0	0.0	0.0	0.0	0.0	0.0	0.0	0.0	0.0
66	0.000000E+00	0.0	0.0	0.0	0.0	0.0	0.0	0.0	0.0	0.0	0.0	0.0	0.0	0.0	0.0
67	0.000000E+00	0.0	0.0	0.0	0.0	0.0	0.0	0.0	0.0	0.0	0.0	0.0	0.0	0.0	0.0
68	0.000000E+00	0.0	0.0	0.0	0.0	0.0	0.0	0.0	0.0	0.0	0.0	0.0	0.0	0.0	0.0
69	0.000000E+00	0.0	0.0	0.0	0.0	0.0	0.0	0.0	0.0	0.0	0.0	0.0	0.0	0.0	0.0
70	0.000000E+00	0.0	0.0	0.0	0.0	0.0	0.0	0.0	0.0	0.0	0.0	0.0	0.0	0.0	0.0
71	0.000000E+00	0.0	0.0	0.0	0.0	0.0	0.0	0.0	0.0	0.0	0.0	0.0	0.0	0.0	0.0
72	0.000000E+00	0.0	0.0	0.0	0.0	0.0	0.0	0.0	0.0	0.0	0.0	0.0	0.0	0.0	0.0
73	0.000000E+00	0.0	0.0	0.0	0.0	0.0	0.0	0.0	0.0	0.0	0.0	0.0	0.0	0.0	0.0
74	0.000000E+00	0.0	0.0	0.0	0.0	0.0	0.0	0.0	0.0	0.0	0.0	0.0	0.0	0.0	0.0
75	0.000000E+00	0.0	0.0	0.0	0.0	0.0	0.0	0.0	0.0	0.0	0.0	0.0	0.0	0.0	0.0
76	0.000000E+00	0.0	0.0	0.0	0.0	0.0	0.0	0.0	0.0	0.0	0.0	0.0	0.0	0.0	0.0
77	0.000000E+00	0.0	0.0	0.0	0.0	0.0	0.0	0.0	0.0	0.0	0.0	0.0	0.0	0.0	0.0
78	0.000000E+00	0.0	0.0	0.0	0.0	0.0	0.0	0.0	0.0	0.0	0.0	0.0	0.0	0.0	0.0
79	0.000000E+00	0.0	0.0	0.0	0.0	0.0	0.0	0.0	0.0	0.0	0.0	0.0	0.0	0.0	0.0
80	0.000000E+00	0.0	0.0	0.0	0.0	0.0	0.0	0.0	0.0	0.0	0.0	0.0	0.0	0.0	0.0
81	0.000000E+00	0.0	0.0	0.0	0.0	0.0	0.0	0.0	0.0	0.0	0.0	0.0	0.0	0.0	0.0
82	0.000000E+00	0.0	0.0	0.0	0.0	0.0	0.0	0.0	0.0	0.0	0.0	0.0	0.0	0.0	0.0
83	0.000000E+00	0.0	0.0	0.0	0.0	0.0	0.0	0.0	0.0	0.0	0.0	0.0	0.0	0.0	0.0
84	0.000000E+00	0.0	0.0	0.0	0.0	0.0	0.0	0.0	0.0	0.0	0.0	0.0	0.0	0.0	0.0
85	0.000000E+00	0.0	0.0	0.0	0.0	0.0	0.0	0.0	0.0	0.0	0.0	0.0	0.0	0.0	0.0
86	0.000000E+00	0.0	0.0	0.0	0.0	0.0	0.0	0.0	0.0	0.0	0.0	0.0	0.0	0.0	0.0
87	0.000000E+00	0.0	0.0	0.0	0.0	0.0	0.0	0.0	0.0	0.0	0.0	0.0	0.0	0.0	0.0
88	0.000000E+00	0.0	0.0	0.0	0.0	0.0	0.0	0.0	0.0	0.0	0.0	0.0	0.0	0.0	0.0
89	0.000000E+00	0.0	0.0	0.0	0.0	0.0	0.0	0.0	0.0	0.0	0.0	0.0	0.0	0.0	0.0
90	0.000000E+00	0.0	0.0	0.0	0.0	0.0	0.0	0.0	0.0	0.0	0.0	0.0	0.0	0.0	0.0
91	0.000000E+00	0.0	0.0	0.0	0.0	0.0	0.0	0.0	0.0	0.0	0.0	0.0	0.0	0.0	0.0
92	0.000000E+00	0.0	0.0	0.0	0.0	0.0	0.0	0.0	0.0	0.0	0.0	0.0	0.0	0.0	0.0
93	0.000000E+00	0.0	0.0	0.0	0.0	0.0	0.0	0.0	0.0	0.0	0.0	0.0	0.0	0.0	0.0
94	0.000000E+00	0.0	0.0	0.0	0.0	0.0	0.0	0.0	0.0	0.0	0.0	0.0	0.0	0.0	0.0
95	0.000000E+00	0.0	0.0	0.0	0.0	0.0	0.0	0.0	0.0	0.0	0.0	0.0	0.0	0.0	0.0
96	0.000000E+00	0.0	0.0	0.0	0.0	0.0	0.0	0.0	0.0	0.0	0.0	0.0	0.0	0.0	0.0
97	0.000000E+00	0.0	0.0	0.0	0.0	0.0	0.0	0.0	0.0	0.0	0.0	0.0	0.0	0.0	0.0
98	0.000000E+00	0.0	0.0	0.0	0.0	0.0	0.0	0.0	0.0	0.0	0.0	0.0	0.0	0.0	0.0
99	0.000000E+00	0.0	0.0	0.0	0.0	0.0	0.0	0.0	0.0	0.0	0.0	0.0	0.0	0.0	0.0
100	0.000000E+00	0.0	0.0	0.0	0.0	0.0	0.0	0.0	0.0	0.0	0.0	0.0	0.0	0.0	0.0

```
CRACK OCCURRENCE PER WELD = 2.8490E-01
------ --------------------
```

INITIAL-TYPE : 4-8

# DEPTH	FREQ.	ASPECTS:	<2	2-3	3-4	4-5	5-6	6-7	7-8	8-9	9-10	10-11	11-12	12-13	13-14	14->
1	0.93729E-02		25.6	1.1	1.7	1.8	2.3	2.5	3.4	3.6	3.3	3.7	3.3	4.6	3.2	39.8
2	0.50554E-02		14.1	2.4	3.9	4.5	6.5	6.7	7.2	5.8	7.6	5.2	5.5	5.5	4.4	20.4
3	0.47063E-03		3.0	5.6	14.8	16.7	14.8	13.7	7.6	7.4	5.9	3.7	3.0	1.9	0.7	1.1
4	0.13508E-03		14.8	18.9	20.5	17.2	14.1	7.0	4.7	1.6	1.3	0.0	0.0	0.0	0.0	0.0
5	0.54045E-04		22.2	23.8	23.8	15.9	3.2	3.2	3.2	4.8	0.0	0.0	0.0	0.0	0.0	0.0
6	0.54613E-05		25.0	50.0	20.0	5.0	0.0	0.0	0.0	0.0	0.0	0.0	0.0	0.0	0.0	0.0
7	0.49268E-05		58.3	33.3	8.3	0.0	0.0	0.0	0.0	0.0	0.0	0.0	0.0	0.0	0.0	0.0
8	0.94280E-06		100.0	0.0	0.0	0.0	0.0	0.0	0.0	0.0	0.0	0.0	0.0	0.0	0.0	0.0
9	0.45545E-06		0.0	100.0	0.0	0.0	0.0	0.0	0.0	0.0	0.0	0.0	0.0	0.0	0.0	0.0
10	0.44654E-06		0.0	0.0	0.0	100.0	0.0	0.0	0.0	0.0	0.0	0.0	0.0	0.0	0.0	0.0
11	0.00000E+00		0.0	0.0	0.0	0.0	0.0	0.0	0.0	0.0	0.0	0.0	0.0	0.0	0.0	0.0
12	0.00000E+00		0.0	0.0	0.0	0.0	0.0	0.0	0.0	0.0	0.0	0.0	0.0	0.0	0.0	0.0
13	0.42394E-06		100.0	0.0	0.0	0.0	0.0	0.0	0.0	0.0	0.0	0.0	0.0	0.0	0.0	0.0
14	0.83901E-06		100.0	0.0	0.0	0.0	0.0	0.0	0.0	0.0	0.0	0.0	0.0	0.0	0.0	0.0

(rows 15–102 contain 0.00000E+00 frequency with all-zero aspect ratios, except row 22: 0.40530E-06 with 100.0 in the <2 column)

CRACK OCCURRENCE PER WELD = 1.60090E-02

INITIAL-TYPE : 0-11

% DEPTH	FREQ.	ASPECTS: <2	2-3	3-4	4-5	5-6	6-7	7-8	8-9	9-10	10-11	11-12	12-13	13-14	14->
1	0.437331E-02	30.5	1.9	2.4	2.9	3.1	3.7	4.3	3.8	4.0	4.8	4.0	4.4	4.1	28.9
2	0.559860E-03	16.7	2.5	3.2	4.5	5.3	6.1	7.9	6.9	6.5	6.4	6.3	4.9	17.9	
3	0.359966E-03	2.8	7.0	7.7	9.9	21.1	14.8	9.2	7.7	7.7	2.1	3.5	0.7	1.4	4.2
4	0.446748E-04	8.6	22.9	28.6	14.3	5.7	2.9	0.6	5.9	0.0	2.9	0.0	0.0	2.9	0.0
5	0.167033E-05	0.0	0.0	0.5	0.0	100.0	0.0	0.0	0.0	0.0	0.0	0.0	0.0	0.0	0.0
6	0.212116E-05	25.0	25.0	25.0	0.0	25.0	0.0	0.0	0.0	0.0	0.0	0.0	0.0	0.0	0.0
7	0.229540E-05	0.0	33.3	33.3	0.0	0.0	33.3	0.0	0.0	0.0	0.0	0.0	0.0	0.0	0.0
8	0.123798E-05	0.0	100.0	0.0	0.0	0.0	0.0	0.0	0.0	0.0	0.0	0.0	0.0	0.0	0.0
9	0.457606E-06	0.0	100.0	0.0	0.0	0.0	0.0	0.0	0.0	0.0	0.0	0.0	0.0	0.0	0.0
10	0.443482E-06	0.0	0.0	0.0	100.0	0.0	0.0	0.0	0.0	0.0	0.0	0.0	0.0	0.0	0.0
11	0.500000E+00	0.0	0.0	0.0	0.0	0.0	0.0	0.0	0.0	0.0	0.0	0.0	0.0	0.0	0.0
12	0.000000E+00	0.0	0.0	0.0	0.0	0.0	0.0	0.0	0.0	0.0	0.0	0.0	0.0	0.0	0.0
13	0.000000E+00	0.0	0.0	0.0	0.0	0.0	0.0	0.0	0.0	0.0	0.0	0.0	0.0	0.0	0.0
14	0.422167E-06	100.0	0.0	0.0	0.0	0.0	0.0	0.0	0.0	0.0	0.0	0.0	0.0	0.0	0.0

(Rows 15 through 100 all show FREQ. = 0.000000E+00 with all aspect ratio values = 0.0)

CRACK OCCURRENCE PER WELD = 1.4387E-02

INITIAL-TYPE : 11-35

% DEPTH	FREQ.	ASPECTS:	<2	2-3	3-4	4-5	5-6	6-7	7-8	8-9	9-10	10-11	11-12	12-13	13-14	14->
1	0.279283E-02		26.0	5.8	6.0	5.0	5.2	6.0	3.4	4.2	5.2	2.6	5.4	2.4	2.9	21.0
2	0.235581E-01		30.5	2.0	2.4	2.9	3.4	4.4	3.7	4.5	4.4	3.9	4.8	3.8	4.6	24.4
3	0.497519E-02		8.4	2.9	3.2	5.2	6.5	4.8	8.8	8.1	4.8	6.8	7.3	6.5	4.8	15.9
4	0.107421E-02		0.9	4.9	7.7	10.4	10.1	8.7	11.1	7.8	7.3	7.0	3.7	5.6	4.3	10.5
5	0.437812E-03		1.9	10.9	16.9	20.3	13.9	10.5	5.0	6.4	2.6	5.3	0.6	0.0	0.0	5.4
6	0.136038E-03		9.2	16.9	26.1	20.4	9.9	11.3	2.6	1.4	1.4	0.6	0.7	0.0	0.0	0.0
7	0.841612E-04		19.2	26.0	28.8	7.7	8.7	5.6	2.9	1.0	0.0	0.0	0.0	0.0	0.0	0.0
8	0.405680E-04		25.0	22.9	35.4	6.2	6.2	4.2	0.0	0.0	0.0	0.0	0.0	0.0	0.0	0.0
9	0.190145E-04		51.6	29.0	9.7	6.5	0.0	3.2	0.0	0.0	0.0	0.0	0.0	0.0	0.0	0.0
10	0.184841E-04		35.1	44.6	10.6	5.4	0.0	0.0	0.0	0.0	0.0	0.0	0.0	0.0	0.0	0.0
11	0.999228E-05		58.3	23.5	17.6	0.0	0.0	0.0	0.0	0.0	0.0	0.0	0.0	0.0	0.0	0.0
12	0.814046E-05		68.8	18.8	12.5	0.0	0.0	0.0	0.0	0.0	0.0	0.0	0.0	0.0	0.0	0.0
13	0.467275E-05		90.9	9.1	0.0	0.0	0.0	0.0	0.0	0.0	0.0	0.0	0.0	0.0	0.0	0.0
14	0.607333E-05		61.5	38.5	0.0	0.0	0.0	0.0	0.0	0.0	0.0	0.0	0.0	0.0	0.0	0.0
15	0.520162E-05		75.0	25.0	0.0	0.0	0.0	0.0	0.0	0.0	0.0	0.0	0.0	0.0	0.0	0.0
16	0.829777E-06		50.0	50.0	0.0	0.0	0.0	0.0	0.0	0.0	0.0	0.0	0.0	0.0	0.0	0.0
17	0.347042E-05		83.3	16.7	0.0	0.0	0.0	0.0	0.0	0.0	0.0	0.0	0.0	0.0	0.0	0.0
18	0.821034E-06		100.0	0.0	0.0	0.0	0.0	0.0	0.0	0.0	0.0	0.0	0.0	0.0	0.0	0.0
19	0.122539E-05		100.0	0.0	0.0	0.0	0.0	0.0	0.0	0.0	0.0	0.0	0.0	0.0	0.0	0.0
20	0.814617E-06		100.0	0.0	0.0	0.0	0.0	0.0	0.0	0.0	0.0	0.0	0.0	0.0	0.0	0.0
21	0.406672E-06		100.0	0.0	0.0	0.0	0.0	0.0	0.0	0.0	0.0	0.0	0.0	0.0	0.0	0.0
22	0.000000E+00		0.0	0.0	0.0	0.0	0.0	0.0	0.0	0.0	0.0	0.0	0.0	0.0	0.0	0.0
23	0.404507E-06		100.0	0.0	0.0	0.0	0.0	0.0	0.0	0.0	0.0	0.0	0.0	0.0	0.0	0.0
24	0.403567E-06		100.0	0.0	0.0	0.0	0.0	0.0	0.0	0.0	0.0	0.0	0.0	0.0	0.0	0.0
25	0.403417E-06		100.0	0.0	0.0	0.0	0.0	0.0	0.0	0.0	0.0	0.0	0.0	0.0	0.0	0.0
26	0.402713E-06		100.0	0.0	0.0	0.0	0.0	0.0	0.0	0.0	0.0	0.0	0.0	0.0	0.0	0.0
27	0.000000E+00		0.0	0.0	0.0	0.0	0.0	0.0	0.0	0.0	0.0	0.0	0.0	0.0	0.0	0.0
28	0.000000E+00		0.0	0.0	0.0	0.0	0.0	0.0	0.0	0.0	0.0	0.0	0.0	0.0	0.0	0.0
29	0.000000E+00		0.0	0.0	0.0	0.0	0.0	0.0	0.0	0.0	0.0	0.0	0.0	0.0	0.0	0.0
30	0.000000E+00		0.0	0.0	0.0	0.0	0.0	0.0	0.0	0.0	0.0	0.0	0.0	0.0	0.0	0.0
31	0.000000E+00		0.0	0.0	0.0	0.0	0.0	0.0	0.0	0.0	0.0	0.0	0.0	0.0	0.0	0.0
32	0.000000E+00		0.0	0.0	0.0	0.0	0.0	0.0	0.0	0.0	0.0	0.0	0.0	0.0	0.0	0.0
33	0.000000E+00		0.0	0.0	0.0	0.0	0.0	0.0	0.0	0.0	0.0	0.0	0.0	0.0	0.0	0.0
34	0.000000E+00		0.0	0.0	0.0	0.0	0.0	0.0	0.0	0.0	0.0	0.0	0.0	0.0	0.0	0.0
35	0.000000E+00		0.0	0.0	0.0	0.0	0.0	0.0	0.0	0.0	0.0	0.0	0.0	0.0	0.0	0.0
36	0.000000E+00		0.0	0.0	0.0	0.0	0.0	0.0	0.0	0.0	0.0	0.0	0.0	0.0	0.0	0.0
37	0.000000E+00		0.0	0.0	0.0	0.0	0.0	0.0	0.0	0.0	0.0	0.0	0.0	0.0	0.0	0.0
38	0.000000E+00		0.0	0.0	0.0	0.0	0.0	0.0	0.0	0.0	0.0	0.0	0.0	0.0	0.0	0.0
39	0.000000E+00		0.0	0.0	0.0	0.0	0.0	0.0	0.0	0.0	0.0	0.0	0.0	0.0	0.0	0.0
40	0.000000E+00		0.0	0.0	0.0	0.0	0.0	0.0	0.0	0.0	0.0	0.0	0.0	0.0	0.0	0.0
41	0.000000E+00		0.0	0.0	0.0	0.0	0.0	0.0	0.0	0.0	0.0	0.0	0.0	0.0	0.0	0.0
42	0.000000E+00		0.0	0.0	0.0	0.0	0.0	0.0	0.0	0.0	0.0	0.0	0.0	0.0	0.0	0.0
43	0.000000E+00		0.0	0.0	0.0	0.0	0.0	0.0	0.0	0.0	0.0	0.0	0.0	0.0	0.0	0.0
44	0.000000E+00		0.0	0.0	0.0	0.0	0.0	0.0	0.0	0.0	0.0	0.0	0.0	0.0	0.0	0.0
45	0.000000E+00		0.0	0.0	0.0	0.0	0.0	0.0	0.0	0.0	0.0	0.0	0.0	0.0	0.0	0.0
46	0.000000E+00		0.0	0.0	0.0	0.0	0.0	0.0	0.0	0.0	0.0	0.0	0.0	0.0	0.0	0.0
47	0.000000E+00		0.0	0.0	0.0	0.0	0.0	0.0	0.0	0.0	0.0	0.0	0.0	0.0	0.0	0.0
48	0.000000E+00		0.0	0.0	0.0	0.0	0.0	0.0	0.0	0.0	0.0	0.0	0.0	0.0	0.0	0.0
49	0.000000E+00		0.0	0.0	0.0	0.0	0.0	0.0	0.0	0.0	0.0	0.0	0.0	0.0	0.0	0.0
50	0.000000E+00		0.0	0.0	0.0	0.0	0.0	0.0	0.0	0.0	0.0	0.0	0.0	0.0	0.0	0.0
51	0.000000E+00		0.0	0.0	0.0	0.0	0.0	0.0	0.0	0.0	0.0	0.0	0.0	0.0	0.0	0.0
52	0.000000E+00		0.0	0.0	0.0	0.0	0.0	0.0	0.0	0.0	0.0	0.0	0.0	0.0	0.0	0.0
53	0.000000E+00		0.0	0.0	0.0	0.0	0.0	0.0	0.0	0.0	0.0	0.0	0.0	0.0	0.0	0.0
54	0.000000E+00		0.0	0.0	0.0	0.0	0.0	0.0	0.0	0.0	0.0	0.0	0.0	0.0	0.0	0.0
55	0.000000E+00		0.0	0.0	0.0	0.0	0.0	0.0	0.0	0.0	0.0	0.0	0.0	0.0	0.0	0.0
56	0.000000E+00		0.0	0.0	0.0	0.0	0.0	0.0	0.0	0.0	0.0	0.0	0.0	0.0	0.0	0.0
57	0.000000E+00		0.0	0.0	0.0	0.0	0.0	0.0	0.0	0.0	0.0	0.0	0.0	0.0	0.0	0.0
58	0.000000E+00		0.0	0.0	0.0	0.0	0.0	0.0	0.0	0.0	0.0	0.0	0.0	0.0	0.0	0.0
59	0.000000E+00		0.0	0.0	0.0	0.0	0.0	0.0	0.0	0.0	0.0	0.0	0.0	0.0	0.0	0.0
60	0.000000E+00		0.0	0.0	0.0	0.0	0.0	0.0	0.0	0.0	0.0	0.0	0.0	0.0	0.0	0.0
61	0.000000E+00		0.0	0.0	0.0	0.0	0.0	0.0	0.0	0.0	0.0	0.0	0.0	0.0	0.0	0.0
62	0.000000E+00		0.0	0.0	0.0	0.0	0.0	0.0	0.0	0.0	0.0	0.0	0.0	0.0	0.0	0.0
63	0.000000E+00		0.0	0.0	0.0	0.0	0.0	0.0	0.0	0.0	0.0	0.0	0.0	0.0	0.0	0.0
64	0.000000E+00		0.0	0.0	0.0	0.0	0.0	0.0	0.0	0.0	0.0	0.0	0.0	0.0	0.0	0.0
65	0.000000E+00		0.0	0.0	0.0	0.0	0.0	0.0	0.0	0.0	0.0	0.0	0.0	0.0	0.0	0.0
66	0.000000E+00		0.0	0.0	0.0	0.0	0.0	0.0	0.0	0.0	0.0	0.0	0.0	0.0	0.0	0.0
67	0.000000E+00		0.0	0.0	0.0	0.0	0.0	0.0	0.0	0.0	0.0	0.0	0.0	0.0	0.0	0.0
68	0.000000E+00		0.0	0.0	0.0	0.0	0.0	0.0	0.0	0.0	0.0	0.0	0.0	0.0	0.0	0.0
69	0.000000E+00		0.0	0.0	0.0	0.0	0.0	0.0	0.0	0.0	0.0	0.0	0.0	0.0	0.0	0.0
70	0.000000E+00		0.0	0.0	0.0	0.0	0.0	0.0	0.0	0.0	0.0	0.0	0.0	0.0	0.0	0.0
71	0.000000E+00		0.0	0.0	0.0	0.0	0.0	0.0	0.0	0.0	0.0	0.0	0.0	0.0	0.0	0.0
72	0.000000E+00		0.0	0.0	0.0	0.0	0.0	0.0	0.0	0.0	0.0	0.0	0.0	0.0	0.0	0.0
73	0.000000E+00		0.0	0.0	0.0	0.0	0.0	0.0	0.0	0.0	0.0	0.0	0.0	0.0	0.0	0.0
74	0.000000E+00		0.0	0.0	0.0	0.0	0.0	0.0	0.0	0.0	0.0	0.0	0.0	0.0	0.0	0.0
75	0.000000E+00		0.0	0.0	0.0	0.0	0.0	0.0	0.0	0.0	0.0	0.0	0.0	0.0	0.0	0.0
76	0.000000E+00		0.0	0.0	0.0	0.0	0.0	0.0	0.0	0.0	0.0	0.0	0.0	0.0	0.0	0.0
77	0.000000E+00		0.0	0.0	0.0	0.0	0.0	0.0	0.0	0.0	0.0	0.0	0.0	0.0	0.0	0.0
78	0.000000E+00		0.0	0.0	0.0	0.0	0.0	0.0	0.0	0.0	0.0	0.0	0.0	0.0	0.0	0.0
79	0.000000E+00		0.0	0.0	0.0	0.0	0.0	0.0	0.0	0.0	0.0	0.0	0.0	0.0	0.0	0.0
80	0.000000E+00		0.0	0.0	0.0	0.0	0.0	0.0	0.0	0.0	0.0	0.0	0.0	0.0	0.0	0.0
81	0.000000E+00		0.0	0.0	0.0	0.0	0.0	0.0	0.0	0.0	0.0	0.0	0.0	0.0	0.0	0.0
82	0.000000E+00		0.0	0.0	0.0	0.0	0.0	0.0	0.0	0.0	0.0	0.0	0.0	0.0	0.0	0.0
83	0.000000E+00		0.0	0.0	0.0	0.0	0.0	0.0	0.0	0.0	0.0	0.0	0.0	0.0	0.0	0.0
84	0.000000E+00		0.0	0.0	0.0	0.0	0.0	0.0	0.0	0.0	0.0	0.0	0.0	0.0	0.0	0.0
85	0.000000E+00		0.0	0.0	0.0	0.0	0.0	0.0	0.0	0.0	0.0	0.0	0.0	0.0	0.0	0.0
86	0.000000E+00		0.0	0.0	0.0	0.0	0.0	0.0	0.0	0.0	0.0	0.0	0.0	0.0	0.0	0.0
87	0.000000E+00		0.0	0.0	0.0	0.0	0.0	0.0	0.0	0.0	0.0	0.0	0.0	0.0	0.0	0.0
88	0.000000E+00		0.0	0.0	0.0	0.0	0.0	0.0	0.0	0.0	0.0	0.0	0.0	0.0	0.0	0.0
89	0.000000E+00		0.0	0.0	0.0	0.0	0.0	0.0	0.0	0.0	0.0	0.0	0.0	0.0	0.0	0.0
90	0.000000E+00		0.0	0.0	0.0	0.0	0.0	0.0	0.0	0.0	0.0	0.0	0.0	0.0	0.0	0.0
91	0.000000E+00		0.0	0.0	0.0	0.0	0.0	0.0	0.0	0.0	0.0	0.0	0.0	0.0	0.0	0.0
92	0.000000E+00		0.0	0.0	0.0	0.0	0.0	0.0	0.0	0.0	0.0	0.0	0.0	0.0	0.0	0.0
93	0.000000E+00		0.0	0.0	0.0	0.0	0.0	0.0	0.0	0.0	0.0	0.0	0.0	0.0	0.0	0.0
94	0.000000E+00		0.0	0.0	0.0	0.0	0.0	0.0	0.0	0.0	0.0	0.0	0.0	0.0	0.0	0.0
95	0.000000E+00		0.0	0.0	0.0	0.0	0.0	0.0	0.0	0.0	0.0	0.0	0.0	0.0	0.0	0.0
96	0.000000E+00		0.0	0.0	0.0	0.0	0.0	0.0	0.0	0.0	0.0	0.0	0.0	0.0	0.0	0.0
97	0.000000E+00		0.0	0.0	0.0	0.0	0.0	0.0	0.0	0.0	0.0	0.0	0.0	0.0	0.0	0.0
98	0.000000E+00		0.0	0.0	0.0	0.0	0.0	0.0	0.0	0.0	0.0	0.0	0.0	0.0	0.0	0.0
99	0.000000E+00		0.0	0.0	0.0	0.0	0.0	0.0	0.0	0.0	0.0	0.0	0.0	0.0	0.0	0.0
100	0.000000E+00		0.0	0.0	0.0	0.0	0.0	0.0	0.0	0.0	0.0	0.0	0.0	0.0	0.0	0.0

CRACK OCCURRENCE PER WELD = 3.3173E-02

```
INITIAL-TYPE : 25-50
-------------

# DEPTH  FREQ.    ASPECTS:  <2    2-3    3-4    4-5    5-6    6-7    7-8    8-9   9-10  10-11  11-12  12-13  13-14  14->
--------------------------------------------------------------------------------------------------------------------------
  1   0.563462E-02   26.7    4.0    5.5    4.4    5.3    5.8    4.9    3.9    4.0    5.0    3.2    4.3    3.4   19.8
  2   0.443345E-01   30.1    2.0    2.5    3.0    3.4    3.4    4.0    4.3    4.8    4.5    4.4    4.6    3.9   25.0
  3   0.911447E-02    9.8    2.5    3.6    5.5    4.3    7.9    8.3    7.9    8.6    4.7    5.8    5.9    5.0   16.3
  4   0.186873E-02    1.5    4.0    8.0   10.4   10.6   10.7    8.9    8.4    8.0    5.9    5.6    4.1    3.3   10.5
  5   0.665030E-03    3.1   10.3   15.8   17.2   14.1   13.8    8.7    4.7    5.4    2.9    2.7    0.7    0.0    0.4
  6   0.324598E-03    9.5   16.1   14.8   18.3   13.3   10.3    6.0    4.3    1.1    1.4    1.4    0.4    0.4    0.0
  7   0.142971E-03   17.8   25.9   22.3   17.8    8.6    3.0    3.0    0.5    0.5    0.0    0.5    0.0    0.0    0.0
  8   0.106310E-03   22.6   26.1   23.5   17.4    6.1    2.6    0.9    0.9    0.0    0.0    0.0    0.0    0.0    0.0
  9   0.533066E-04   32.6   31.5   19.1    7.9    4.5    0.0    4.5    0.0    0.0    0.0    0.0    0.0    0.0    0.0
 10   0.320558E-04   43.2   36.1   15.7    4.8    0.0    1.2    0.0    0.0    0.0    0.0    0.0    0.0    0.0    0.0
 11   0.332520E-04   42.0   24.0   30.0    4.0    0.0    0.0    0.0    0.0    0.0    0.0    0.0    0.0    0.0    0.0
 12   0.156620E-04   47.6   23.5    8.8    0.0    0.0    0.0    0.0    0.0    0.0    0.0    0.0    0.0    0.0    0.0
 13   0.993026E-05   52.6   43.1    5.3    0.0    0.0    0.0    0.0    0.0    0.0    0.0    0.0    0.0    0.0    0.0
 14   0.608054E-05   61.5   30.8    7.7    0.0    0.0    0.0    0.0    0.0    0.0    0.0    0.0    0.0    0.0    0.0
 15   0.102790E-04   80.0    6.7    6.7    6.7    0.0    0.0    0.0    0.0    0.0    0.0    0.0    0.0    0.0    0.0
 16   0.432920E-05   88.9    0.0   11.1    0.0    0.0    0.0    0.0    0.0    0.0    0.0    0.0    0.0    0.0    0.0
 17   0.370806E-05   77.8   22.2    0.0    0.0    0.0    0.0    0.0    0.0    0.0    0.0    0.0    0.0    0.0    0.0
 18   0.410289E-05   90.0   10.0    0.0    0.0    0.0    0.0    0.0    0.0    0.0    0.0    0.0    0.0    0.0    0.0
 19   0.816491E-06  100.0    0.0    0.0    0.0    0.0    0.0    0.0    0.0    0.0    0.0    0.0    0.0    0.0    0.0
 20   0.815193E-06  100.0    0.0    0.0    0.0    0.0    0.0    0.0    0.0    0.0    0.0    0.0    0.0    0.0    0.0
 21   0.121943E-05  100.0    0.0    0.0    0.0    0.0    0.0    0.0    0.0    0.0    0.0    0.0    0.0    0.0    0.0
 22   0.809996E-06  100.0    0.0    0.0    0.0    0.0    0.0    0.0    0.0    0.0    0.0    0.0    0.0    0.0    0.0
 23   0.808798E-06  100.0    0.0    0.0    0.0    0.0    0.0    0.0    0.0    0.0    0.0    0.0    0.0    0.0    0.0
 24   0.161499E-05  100.0    0.0    0.0    0.0    0.0    0.0    0.0    0.0    0.0    0.0    0.0    0.0    0.0    0.0
 25   0.403143E-06  100.0    0.0    0.0    0.0    0.0    0.0    0.0    0.0    0.0    0.0    0.0    0.0    0.0    0.0
 26   0.402836E-06  100.0    0.0    0.0    0.0    0.0    0.0    0.0    0.0    0.0    0.0    0.0    0.0    0.0    0.0
 27   0.402156E-06  100.0    0.0    0.0    0.0    0.0    0.0    0.0    0.0    0.0    0.0    0.0    0.0    0.0    0.0
 28   0.401645E-06  100.0    0.0    0.0    0.0    0.0    0.0    0.0    0.0    0.0    0.0    0.0    0.0    0.0    0.0
 29   0.802540E-06  100.0    0.0    0.0    0.0    0.0    0.0    0.0    0.0    0.0    0.0    0.0    0.0    0.0    0.0
 30   0.000000E+00    0.0    0.0    0.0    0.0    0.0    0.0    0.0    0.0    0.0    0.0    0.0    0.0    0.0    0.0
 31   0.400715E-06  100.0    0.0    0.0    0.0    0.0    0.0    0.0    0.0    0.0    0.0    0.0    0.0    0.0    0.0
 32   0.000000E+00    0.0    0.0    0.0    0.0    0.0    0.0    0.0    0.0    0.0    0.0    0.0    0.0    0.0    0.0
 33   0.267286E-05  100.0    0.0    0.0    0.0    0.0    0.0    0.0    0.0    0.0    0.0    0.0    0.0    0.0    0.0
 34   0.000000E+00    0.0    0.0    0.0    0.0    0.0    0.0    0.0    0.0    0.0    0.0    0.0    0.0    0.0    0.0
 35   0.000000E+00    0.0    0.0    0.0    0.0    0.0    0.0    0.0    0.0    0.0    0.0    0.0    0.0    0.0    0.0
 36   0.000000E+00    0.0    0.0    0.0    0.0    0.0    0.0    0.0    0.0    0.0    0.0    0.0    0.0    0.0    0.0
 37   0.000000E+00    0.0    0.0    0.0    0.0    0.0    0.0    0.0    0.0    0.0    0.0    0.0    0.0    0.0    0.0
 38   0.399539E-06  100.0    0.0    0.0    0.0    0.0    0.0    0.0    0.0    0.0    0.0    0.0    0.0    0.0    0.0
 39   0.000000E+00    0.0    0.0    0.0    0.0    0.0    0.0    0.0    0.0    0.0    0.0    0.0    0.0    0.0    0.0
 40   0.000000E+00    0.0    0.0    0.0    0.0    0.0    0.0    0.0    0.0    0.0    0.0    0.0    0.0    0.0    0.0
 41   0.000000E+00    0.0    0.0    0.0    0.0    0.0    0.0    0.0    0.0    0.0    0.0    0.0    0.0    0.0    0.0
 42   0.000000E+00    0.0    0.0    0.0    0.0    0.0    0.0    0.0    0.0    0.0    0.0    0.0    0.0    0.0    0.0
 43   0.000000E+00    0.0    0.0    0.0    0.0    0.0    0.0    0.0    0.0    0.0    0.0    0.0    0.0    0.0    0.0
 44   0.000000E+00    0.0    0.0    0.0    0.0    0.0    0.0    0.0    0.0    0.0    0.0    0.0    0.0    0.0    0.0
 45   0.000000E+00    0.0    0.0    0.0    0.0    0.0    0.0    0.0    0.0    0.0    0.0    0.0    0.0    0.0    0.0
 46   0.000000E+00    0.0    0.0    0.0    0.0    0.0    0.0    0.0    0.0    0.0    0.0    0.0    0.0    0.0    0.0
 47   0.000000E+00    0.0    0.0    0.0    0.0    0.0    0.0    0.0    0.0    0.0    0.0    0.0    0.0    0.0    0.0
 48   0.000000E+00    0.0    0.0    0.0    0.0    0.0    0.0    0.0    0.0    0.0    0.0    0.0    0.0    0.0    0.0
 49   0.000000E+00    0.0    0.0    0.0    0.0    0.0    0.0    0.0    0.0    0.0    0.0    0.0    0.0    0.0    0.0
 50   0.000000E+00    0.0    0.0    0.0    0.0    0.0    0.0    0.0    0.0    0.0    0.0    0.0    0.0    0.0    0.0
 51   0.000000E+00    0.0    0.0    0.0    0.0    0.0    0.0    0.0    0.0    0.0    0.0    0.0    0.0    0.0    0.0
 52   0.000000E+00    0.0    0.0    0.0    0.0    0.0    0.0    0.0    0.0    0.0    0.0    0.0    0.0    0.0    0.0
 53   0.000000E+00    0.0    0.0    0.0    0.0    0.0    0.0    0.0    0.0    0.0    0.0    0.0    0.0    0.0    0.0
 54   0.000000E+00    0.0    0.0    0.0    0.0    0.0    0.0    0.0    0.0    0.0    0.0    0.0    0.0    0.0    0.0
 55   0.000000E+00    0.0    0.0    0.0    0.0    0.0    0.0    0.0    0.0    0.0    0.0    0.0    0.0    0.0    0.0
 56   0.000000E+00    0.0    0.0    0.0    0.0    0.0    0.0    0.0    0.0    0.0    0.0    0.0    0.0    0.0    0.0
 57   0.000000E+00    0.0    0.0    0.0    0.0    0.0    0.0    0.0    0.0    0.0    0.0    0.0    0.0    0.0    0.0
 58   0.000000E+00    0.0    0.0    0.0    0.0    0.0    0.0    0.0    0.0    0.0    0.0    0.0    0.0    0.0    0.0
 59   0.000000E+00    0.0    0.0    0.0    0.0    0.0    0.0    0.0    0.0    0.0    0.0    0.0    0.0    0.0    0.0
 60   0.000000E+00    0.0    0.0    0.0    0.0    0.0    0.0    0.0    0.0    0.0    0.0    0.0    0.0    0.0    0.0
 61   0.000000E+00    0.0    0.0    0.0    0.0    0.0    0.0    0.0    0.0    0.0    0.0    0.0    0.0    0.0    0.0
 62   0.000000E+00    0.0    0.0    0.0    0.0    0.0    0.0    0.0    0.0    0.0    0.0    0.0    0.0    0.0    0.0
 63   0.000000E+00    0.0    0.0    0.0    0.0    0.0    0.0    0.0    0.0    0.0    0.0    0.0    0.0    0.0    0.0
 64   0.000000E+00    0.0    0.0    0.0    0.0    0.0    0.0    0.0    0.0    0.0    0.0    0.0    0.0    0.0    0.0
 65   0.000000E+00    0.0    0.0    0.0    0.0    0.0    0.0    0.0    0.0    0.0    0.0    0.0    0.0    0.0    0.0
 66   0.000000E+00    0.0    0.0    0.0    0.0    0.0    0.0    0.0    0.0    0.0    0.0    0.0    0.0    0.0    0.0
 67   0.000000E+00    0.0    0.0    0.0    0.0    0.0    0.0    0.0    0.0    0.0    0.0    0.0    0.0    0.0    0.0
 68   0.000000E+00    0.0    0.0    0.0    0.0    0.0    0.0    0.0    0.0    0.0    0.0    0.0    0.0    0.0    0.0
 69   0.000000E+00    0.0    0.0    0.0    0.0    0.0    0.0    0.0    0.0    0.0    0.0    0.0    0.0    0.0    0.0
 70   0.000000E+00    0.0    0.0    0.0    0.0    0.0    0.0    0.0    0.0    0.0    0.0    0.0    0.0    0.0    0.0
 71   0.000000E+00    0.0    0.0    0.0    0.0    0.0    0.0    0.0    0.0    0.0    0.0    0.0    0.0    0.0    0.0
 72   0.000000E+00    0.0    0.0    0.0    0.0    0.0    0.0    0.0    0.0    0.0    0.0    0.0    0.0    0.0    0.0
 73   0.000000E+00    0.0    0.0    0.0    0.0    0.0    0.0    0.0    0.0    0.0    0.0    0.0    0.0    0.0    0.0
 74   0.000000E+00    0.0    0.0    0.0    0.0    0.0    0.0    0.0    0.0    0.0    0.0    0.0    0.0    0.0    0.0
 75   0.000000E+00    0.0    0.0    0.0    0.0    0.0    0.0    0.0    0.0    0.0    0.0    0.0    0.0    0.0    0.0
 76   0.000000E+00    0.0    0.0    0.0    0.0    0.0    0.0    0.0    0.0    0.0    0.0    0.0    0.0    0.0    0.0
 77   0.000000E+00    0.0    0.0    0.0    0.0    0.0    0.0    0.0    0.0    0.0    0.0    0.0    0.0    0.0    0.0
 78   0.000000E+00    0.0    0.0    0.0    0.0    0.0    0.0    0.0    0.0    0.0    0.0    0.0    0.0    0.0    0.0
 79   0.000000E+00    0.0    0.0    0.0    0.0    0.0    0.0    0.0    0.0    0.0    0.0    0.0    0.0    0.0    0.0
 80   0.000000E+00    0.0    0.0    0.0    0.0    0.0    0.0    0.0    0.0    0.0    0.0    0.0    0.0    0.0    0.0
 81   0.000000E+00    0.0    0.0    0.0    0.0    0.0    0.0    0.0    0.0    0.0    0.0    0.0    0.0    0.0    0.0
 82   0.000000E+00    0.0    0.0    0.0    0.0    0.0    0.0    0.0    0.0    0.0    0.0    0.0    0.0    0.0    0.0
 83   0.000000E+00    0.0    0.0    0.0    0.0    0.0    0.0    0.0    0.0    0.0    0.0    0.0    0.0    0.0    0.0
 84   0.000000E+00    0.0    0.0    0.0    0.0    0.0    0.0    0.0    0.0    0.0    0.0    0.0    0.0    0.0    0.0
 85   0.000000E+00    0.0    0.0    0.0    0.0    0.0    0.0    0.0    0.0    0.0    0.0    0.0    0.0    0.0    0.0
 86   0.000000E+00    0.0    0.0    0.0    0.0    0.0    0.0    0.0    0.0    0.0    0.0    0.0    0.0    0.0    0.0
 87   0.000000E+00    0.0    0.0    0.0    0.0    0.0    0.0    0.0    0.0    0.0    0.0    0.0    0.0    0.0    0.0
 88   0.000000E+00    0.0    0.0    0.0    0.0    0.0    0.0    0.0    0.0    0.0    0.0    0.0    0.0    0.0    0.0
 89   0.000000E+00    0.0    0.0    0.0    0.0    0.0    0.0    0.0    0.0    0.0    0.0    0.0    0.0    0.0    0.0
 90   0.000000E+00    0.0    0.0    0.0    0.0    0.0    0.0    0.0    0.0    0.0    0.0    0.0    0.0    0.0    0.0
 91   0.000000E+00    0.0    0.0    0.0    0.0    0.0    0.0    0.0    0.0    0.0    0.0    0.0    0.0    0.0    0.0
 92   0.000000E+00    0.0    0.0    0.0    0.0    0.0    0.0    0.0    0.0    0.0    0.0    0.0    0.0    0.0    0.0
 93   0.000000E+00    0.0    0.0    0.0    0.0    0.0    0.0    0.0    0.0    0.0    0.0    0.0    0.0    0.0    0.0
 94   0.000000E+00    0.0    0.0    0.0    0.0    0.0    0.0    0.0    0.0    0.0    0.0    0.0    0.0    0.0    0.0
 95   0.000000E+00    0.0    0.0    0.0    0.0    0.0    0.0    0.0    0.0    0.0    0.0    0.0    0.0    0.0    0.0
 96   0.000000E+00    0.0    0.0    0.0    0.0    0.0    0.0    0.0    0.0    0.0    0.0    0.0    0.0    0.0    0.0
 97   0.000000E+00    0.0    0.0    0.0    0.0    0.0    0.0    0.0    0.0    0.0    0.0    0.0    0.0    0.0    0.0
 98   0.000000E+00    0.0    0.0    0.0    0.0    0.0    0.0    0.0    0.0    0.0    0.0    0.0    0.0    0.0    0.0
 99   0.000000E+00    0.0    0.0    0.0    0.0    0.0    0.0    0.0    0.0    0.0    0.0    0.0    0.0    0.0    0.0
100   0.000000E+00    0.0    0.0    0.0    0.0    0.0    0.0    0.0    0.0    0.0    0.0    0.0    0.0    0.0    0.0

CRACK OCCURRENCE PER WELD = 4.2418E-02
```

INITIAL-TYPE : 50-75

# DEPTH	FREQ	ASPECTS:	<2	2-3	3-4	4-5	5-6	6-7	7-8	8-9	9-10	10-11	11-12	12-13	13-14	14->
1	0.362053E-02		23.4	5.4	5.1	7.1	4.2	4.0	4.2	5.6	3.6	4.5	4.5	5.4	4.0	16.7
2	0.434433E-01		26.5	2.4	2.2	2.9	3.1	4.0	4.0	4.4	4.4	4.7	4.2	4.9	4.6	27.5
3	0.253303E-01		28.0	2.5	2.6	3.6	4.3	4.1	4.7	4.7	4.9	4.8	4.8	4.9	3.0	22.3
4	0.419480E-02		1.8	1.6	5.2	6.7	6.7	8.1	7.9	10.2	8.3	8.8	6.4	7.0	5.5	15.2
5	0.280164E-03		2.7	5.2	7.5	11.3	11.1	11.5	11.9	6.9	7.6	5.7	5.4	4.4	3.6	5.0
6	0.586372E-03		4.4	5.7	15.2	18.9	14.5	12.2	9.8	7.8	4.1	1.7	1.0	0.7	0.0	0.0
7	0.258459E-03		11.3	15.1	18.9	17.5	12.7	6.6	6.6	3.8	2.8	2.4	1.9	0.5	0.0	0.0
8	0.113834E-03		15.8	22.2	20.5	15.1	9.6	7.5	4.8	2.7	1.4	0.0	0.0	0.0	0.0	0.0
9	0.865431E-04		16.8	25.4	21.6	20.8	10.6	1.6	2.4	0.8	0.0	0.3	0.0	0.0	0.0	0.0
10	0.545048E-04		31.6	32.9	19.7	6.6	6.6	2.6	0.0	0.0	0.3	0.0	0.0	0.0	0.0	0.0
11	0.369586E-04		31.6	29.8	22.8	14.0	0.0	1.8	0.0	0.0	0.0	0.0	0.0	0.0	0.0	0.0
12	0.273699E-04		54.2	41.7	4.2	0.0	0.0	0.0	0.0	0.0	0.0	0.0	0.0	0.0	0.0	0.0
13	0.200156E-04		40.0	40.0	16.7	0.0	3.3	0.0	0.0	0.0	0.0	0.0	0.0	0.0	0.0	0.0
14	0.879490E-05		55.6	27.8	11.1	0.0	5.6	0.0	0.0	0.0	0.0	0.0	0.0	0.0	0.0	0.0
15	0.709178E-05		82.4	0.0	11.8	5.9	0.0	0.0	0.0	0.0	0.0	0.0	0.0	0.0	0.0	0.0
16	0.869683E-05		64.3	28.6	0.0	7.1	0.0	0.0	0.0	0.0	0.0	0.0	0.0	0.0	0.0	0.0
17	0.471802E-05		80.0	20.0	0.0	0.0	0.0	0.0	0.0	0.0	0.0	0.0	0.0	0.0	0.0	0.0
18	0.369128E-05		88.9	11.1	0.0	0.0	0.0	0.0	0.0	0.0	0.0	0.0	0.0	0.0	0.0	0.0
19	0.367699E-05		88.9	11.1	0.0	0.0	0.0	0.0	0.0	0.0	0.0	0.0	0.0	0.0	0.0	0.0
20	0.122111E-06		100.0	0.0	0.0	0.0	0.0	0.0	0.0	0.0	0.0	0.0	0.0	0.0	0.0	0.0
21	0.203113E-05		100.0	0.0	0.0	0.0	0.0	0.0	0.0	0.0	0.0	0.0	0.0	0.0	0.0	0.0
22	0.203529E-05		100.0	0.0	0.0	0.0	0.0	0.0	0.0	0.0	0.0	0.0	0.0	0.0	0.0	0.0
23	0.161642E-05		100.0	0.0	0.0	0.0	0.0	0.0	0.0	0.0	0.0	0.0	0.0	0.0	0.0	0.0
24	0.403569E-06		100.0	0.0	0.0	0.0	0.0	0.0	0.0	0.0	0.0	0.0	0.0	0.0	0.0	0.0
25	0.161241E-05		75.0	25.0	0.0	0.0	0.0	0.0	0.0	0.0	0.0	0.0	0.0	0.0	0.0	0.0
26	0.161037E-05		75.0	25.0	0.0	0.0	0.0	0.0	0.0	0.0	0.0	0.0	0.0	0.0	0.0	0.0
27	0.403304E-06		100.0	0.0	0.0	0.0	0.0	0.0	0.0	0.0	0.0	0.0	0.0	0.0	0.0	0.0
28	0.403895E-06		100.0	0.0	0.0	0.0	0.0	0.0	0.0	0.0	0.0	0.0	0.0	0.0	0.0	0.0
29	0.403929E-06		100.0	0.0	0.0	0.0	0.0	0.0	0.0	0.0	0.0	0.0	0.0	0.0	0.0	0.0
30	0.401119E-06		100.0	0.0	0.0	0.0	0.0	0.0	0.0	0.0	0.0	0.0	0.0	0.0	0.0	0.0
31	0.000000E+00		0.0	0.0	0.0	0.0	0.0	0.0	0.0	0.0	0.0	0.0	0.0	0.0	0.0	0.0
32	0.000000E+00		0.0	0.0	0.0	0.0	0.0	0.0	0.0	0.0	0.0	0.0	0.0	0.0	0.0	0.0
33	0.400262E-06		100.0	0.0	0.0	0.0	0.0	0.0	0.0	0.0	0.0	0.0	0.0	0.0	0.0	0.0
34	0.000000E+00		0.0	0.0	0.0	0.0	0.0	0.0	0.0	0.0	0.0	0.0	0.0	0.0	0.0	0.0
35	0.399945E-06		100.0	0.0	0.0	0.0	0.0	0.0	0.0	0.0	0.0	0.0	0.0	0.0	0.0	0.0
36	0.000000E+00		0.0	0.0	0.0	0.0	0.0	0.0	0.0	0.0	0.0	0.0	0.0	0.0	0.0	0.0
37	0.000000E+00		0.0	0.0	0.0	0.0	0.0	0.0	0.0	0.0	0.0	0.0	0.0	0.0	0.0	0.0
38	0.000000E+00		0.0	0.0	0.0	0.0	0.0	0.0	0.0	0.0	0.0	0.0	0.0	0.0	0.0	0.0
39	0.398400E-06		100.0	0.0	0.0	0.0	0.0	0.0	0.0	0.0	0.0	0.0	0.0	0.0	0.0	0.0
40	0.000000E+00		0.0	0.0	0.0	0.0	0.0	0.0	0.0	0.0	0.0	0.0	0.0	0.0	0.0	0.0
41	0.000000E+00		0.0	0.0	0.0	0.0	0.0	0.0	0.0	0.0	0.0	0.0	0.0	0.0	0.0	0.0
42	0.399465E-06		100.0	0.0	0.0	0.0	0.0	0.0	0.0	0.0	0.0	0.0	0.0	0.0	0.0	0.0
43	0.000000E+00		0.0	0.0	0.0	0.0	0.0	0.0	0.0	0.0	0.0	0.0	0.0	0.0	0.0	0.0
44	0.000000E+00		0.0	0.0	0.0	0.0	0.0	0.0	0.0	0.0	0.0	0.0	0.0	0.0	0.0	0.0
45	0.000000E+00		0.0	0.0	0.0	0.0	0.0	0.2	0.0	0.0	0.0	0.0	0.0	0.0	0.0	0.0
46	0.000000E+00		0.0	0.0	0.0	0.0	0.0	0.0	0.0	0.0	0.0	0.0	0.0	0.0	0.0	0.0
47	0.000000E+00		0.0	0.0	0.0	0.0	0.0	0.0	0.0	0.0	0.0	0.0	0.0	0.0	0.0	0.0
48	0.000000E+00		0.0	0.0	0.0	0.0	0.0	0.0	0.0	0.0	0.0	0.0	0.0	0.0	0.0	0.0
49	0.000000E+00		0.0	0.0	0.0	0.0	0.0	0.0	0.0	0.0	0.0	0.0	0.0	0.0	0.0	0.0
50	0.000000E+00		0.0	0.0	0.0	0.0	0.0	0.0	0.0	0.0	0.0	0.0	0.0	0.0	0.0	0.0
51	0.000000E+00		0.0	0.0	0.0	0.0	0.0	0.0	0.0	0.0	0.0	0.0	0.0	0.0	0.0	0.0
52	0.000000E+00		0.0	0.0	0.0	0.0	0.0	0.0	0.0	0.0	0.0	0.0	0.0	0.0	0.0	0.0
53	0.000000E+00		0.0	0.0	0.0	0.0	0.0	0.0	0.0	0.0	0.0	0.0	0.0	0.0	0.0	0.0
54	0.000000E+00		0.0	0.0	0.0	0.0	0.0	0.0	0.0	0.0	0.0	0.0	0.0	0.0	0.0	0.0
55	0.000000E+00		0.0	0.0	0.0	0.0	0.0	0.0	0.0	0.0	0.0	0.0	0.0	0.0	0.0	0.0
56	0.000000E+00		0.0	0.0	0.0	0.0	0.0	0.0	0.0	0.0	0.0	0.0	0.0	0.0	0.0	0.0
57	0.000000E+00		0.0	0.0	0.0	0.0	0.0	0.0	0.0	0.0	0.0	0.0	0.0	0.0	0.0	0.0
58	0.000000E+00		0.0	0.0	0.0	0.0	0.0	0.0	0.0	0.0	0.0	0.0	0.0	0.0	0.0	0.0
59	0.000000E+00		0.0	0.0	0.0	0.0	0.0	0.0	0.0	0.0	0.0	0.0	0.0	0.0	0.0	0.0
60	0.000000E+00		0.0	0.0	0.0	0.0	0.0	0.0	0.0	0.0	0.0	0.0	0.0	0.0	0.0	0.0
61	0.000000E+00		0.0	0.0	0.0	0.0	0.0	0.0	0.0	0.0	0.0	0.0	0.0	0.0	0.0	0.0
62	0.000000E+00		0.0	0.0	0.0	0.0	0.0	0.0	0.0	0.0	0.0	0.0	0.0	0.0	0.0	0.0
63	0.000000E+00		0.0	0.0	0.0	0.0	0.0	0.0	0.0	0.0	0.0	0.0	0.0	0.0	0.0	0.0
64	0.000000E+00		0.0	0.0	0.0	0.0	0.0	0.0	0.0	0.0	0.0	0.0	0.0	0.0	0.0	0.0
65	0.000000E+00		0.0	0.0	0.0	0.0	0.0	0.0	0.0	0.0	0.0	0.0	0.0	0.0	0.0	0.0
66	0.000000E+00		0.0	0.0	0.0	0.0	0.0	0.0	0.0	0.0	0.0	0.0	0.0	0.0	0.0	0.0
67	0.000000E+00		0.0	0.0	0.0	0.0	0.0	0.0	0.0	0.0	0.0	0.0	0.0	0.0	0.0	0.0
68	0.000000E+00		0.0	0.0	0.0	0.0	0.0	0.0	0.0	0.0	0.0	0.0	0.0	0.0	0.0	0.0
69	0.000000E+00		0.0	0.0	0.0	0.0	0.0	0.0	0.0	0.0	0.0	0.0	0.0	0.0	0.0	0.0
70	0.000000E+00		0.0	0.0	0.0	0.0	0.0	0.0	0.0	0.0	0.0	0.0	0.0	0.0	0.0	0.0
71	0.000000E+00		0.0	0.0	0.0	0.0	0.0	0.0	0.0	0.0	0.0	0.0	0.0	0.0	0.0	0.0
72	0.000000E+00		0.0	0.0	0.0	0.0	0.0	0.0	0.0	0.0	0.0	0.0	0.0	0.0	0.0	0.0
73	0.000000E+00		0.0	0.0	0.0	0.0	0.0	0.0	0.0	0.0	0.0	0.0	0.0	0.0	0.0	0.0
74	0.000000E+00		0.0	0.0	0.0	0.0	0.0	0.0	0.0	0.0	0.0	0.0	0.0	0.0	0.0	0.0
75	0.000000E+00		0.0	0.0	0.0	0.0	0.0	0.0	0.0	0.0	0.0	0.0	0.0	0.0	0.0	0.0
76	0.000000E+00		0.0	0.0	0.0	0.0	0.0	0.0	0.0	0.0	0.0	0.0	0.0	0.0	0.0	0.0
77	0.000000E+00		0.0	0.0	0.0	0.0	0.0	0.0	0.0	0.0	0.0	0.0	0.0	0.0	0.0	0.0
78	0.000000E+00		0.0	0.0	0.0	0.0	0.0	0.0	0.0	0.0	0.0	0.0	0.0	0.0	0.0	0.0
79	0.000000E+00		0.0	0.0	0.0	0.0	0.0	0.0	0.0	0.0	0.0	0.0	0.0	0.0	0.0	0.0
80	0.000000E+00		0.0	0.0	0.0	0.0	0.0	0.0	0.0	0.0	0.0	0.0	0.0	0.0	0.0	0.0
81	0.000000E+00		0.0	0.0	0.0	0.0	0.0	0.0	0.0	0.0	0.0	0.0	0.0	0.0	0.0	0.0
82	0.000000E+00		0.0	0.0	0.0	0.0	0.0	0.0	0.0	0.0	0.0	0.0	0.0	0.0	0.0	0.0
83	0.000000E+00		0.0	0.0	0.0	0.0	0.0	0.0	0.0	0.0	0.0	0.0	0.0	0.0	0.0	0.0
84	0.000000E+00		0.0	0.0	0.0	0.0	0.0	0.0	0.0	0.0	0.0	0.0	0.0	0.0	0.0	0.0
85	0.000000E+00		0.0	0.0	0.0	0.0	0.0	0.0	0.0	0.0	0.0	0.0	0.0	0.0	0.0	0.0
86	0.000000E+00		0.0	0.0	0.0	0.0	0.0	0.0	0.0	0.0	0.0	0.0	0.0	0.0	0.0	0.0
87	0.000000E+00		0.0	0.0	0.0	0.0	0.0	0.0	0.0	0.0	0.0	0.0	0.0	0.0	0.0	0.0
88	0.000000E+00		0.0	0.0	0.0	0.0	0.0	0.0	0.0	0.0	0.0	0.0	0.0	0.0	0.0	0.0
89	0.000000E+00		0.0	0.0	0.0	0.0	0.0	0.0	0.0	0.0	0.0	0.0	0.0	0.0	0.0	0.0
90	0.000000E+00		0.0	0.0	0.0	0.0	0.0	0.0	0.0	0.0	0.0	0.0	0.0	0.0	0.0	0.0
91	0.000000E+00		0.0	0.0	0.0	0.0	0.0	0.0	0.0	0.0	0.0	0.0	0.0	0.0	0.0	0.0
92	0.000000E+00		0.0	0.0	0.0	0.0	0.0	0.0	0.0	0.0	0.0	0.0	0.0	0.0	0.0	0.0
93	0.000000E+00		0.0	0.0	0.0	0.0	0.0	0.0	0.0	0.0	0.0	0.0	0.0	0.0	0.0	0.0
94	0.000000E+00		0.0	0.0	0.0	0.0	0.0	0.0	0.0	0.0	0.0	0.0	0.0	0.0	0.0	0.0
95	0.000000E+00		0.0	0.0	0.0	0.0	0.0	0.0	0.0	0.0	0.0	0.0	0.0	0.0	0.0	0.0
96	0.000000E+00		0.0	0.0	0.0	0.0	0.0	0.0	0.0	0.0	0.0	0.0	0.0	0.0	0.0	0.0
97	0.000000E+00		0.0	0.0	0.0	0.0	0.0	0.0	0.0	0.0	0.0	0.0	0.0	0.0	0.0	0.0
98	0.000000E+00		0.0	0.0	0.0	0.0	0.0	0.0	0.0	0.0	0.0	0.0	0.0	0.0	0.0	0.0
99	0.000000E+00		0.0	0.0	0.0	0.0	0.0	0.0	0.0	0.0	0.0	0.0	0.0	0.0	0.0	0.0
100	0.000000E+00		0.0	0.0	0.0	0.0	0.0	0.0	0.0	0.0	0.0	0.0	0.0	0.0	0.0	0.0

CRACK OCCURRENCE PER WELD = 7.6638E-02

```
INITIAL-TYPE : 75-100
-------------
```

% DEPTH	FREQ.	ASPECTS: <2	2-3	3-4	4-5	5-6	6-7	7-8	8-9	9-10	10-11	11-12	12-13	13-14	14->
1	0.297742E-03	19.2	3.5	5.2	4.6	4.1	3.3	2.9	4.5	2.7	2.5	3.4	3.7	3.3	36.2
2	0.429104E-03	26.7	1.8	2.1	2.3	3.0	3.5	3.5	4.3	4.5	4.4	4.3	4.2	4.1	31.3
3	0.243123E-03	26.1	2.3	2.9	3.8	4.0	4.8	4.5	4.9	4.7	5.0	4.6	4.8	3.8	21.8
4	0.301442E-03	3.2	1.4	3.9	7.1	7.9	8.0	5.2	8.4	8.7	8.0	6.1	5.2	6.4	18.6
5	0.914751E-03	2.0	7.8	10.4	13.1	11.4	14.1	9.4	5.7	6.3	4.9	3.5	4.3	1.8	5.5
6	0.395447E-03	2.7	9.8	17.3	17.3	13.2	11.4	9.4	7.1	5.9	2.4	2.0	1.6	0.8	0.4
7	0.180597E-03	10.3	15.5	18.4	14.4	12.1	12.1	6.3	6.0	1.7	0.0	0.6	0.0	0.0	0.4
8	0.901714E-04	23.3	24.0	14.0	17.4	13.4	0.8	3.3	3.3	1.7	0.0	0.0	0.0	0.0	0.0
9	0.653022E-04	27.6	18.4	27.4	14.5	7.9	2.6	1.3	0.0	0.0	0.0	0.0	0.0	0.0	0.0
10	0.359519E-04	26.9	36.5	11.5	5.8	9.6	5.8	1.9	1.9	0.0	0.0	0.0	0.0	0.0	0.0
11	0.231316E-04	26.2	31.0	23.4	9.5	7.1	2.4	0.0	0.0	0.0	0.0	0.0	0.0	0.0	0.0
12	0.141597E-04	48.4	35.5	12.9	0.0	3.2	0.0	0.0	0.0	0.0	0.0	0.0	0.0	0.0	0.0
13	0.717101E-05	60.0	20.0	20.0	0.0	0.0	0.0	0.0	0.0	0.0	0.0	0.0	0.0	0.0	0.0
14	0.631712E-05	64.3	21.4	7.1	7.1	0.0	0.0	0.0	0.0	0.0	0.0	0.0	0.0	0.0	0.0
15	0.777561E-05	63.6	27.3	4.5	4.5	0.0	0.0	0.0	0.0	0.0	0.0	0.0	0.0	0.0	0.0
16	0.270887E-05	66.7	16.7	16.7	0.0	0.0	0.0	0.0	0.0	0.0	0.0	0.0	0.0	0.0	0.0
17	0.144630E-05	75.0	25.0	0.0	0.0	0.0	0.0	0.0	0.0	0.0	0.0	0.0	0.0	0.0	0.0
18	0.205293E-05	60.0	40.0	0.0	0.0	0.0	0.0	0.0	0.0	0.0	0.0	0.0	0.0	0.0	0.0
19	0.483380E-06	100.0	0.0	0.0	0.0	0.0	0.0	0.0	0.0	0.0	0.0	0.0	0.0	0.0	0.0
20	0.000000E+00	0.0	0.0	0.0	0.0	0.0	0.0	0.0	0.0	0.0	0.0	0.0	0.0	0.0	0.0
21	0.404374E-06	0.0	100.0	0.0	0.0	0.0	0.0	0.0	0.0	0.0	0.0	0.0	0.0	0.0	0.0
22	0.000000E+00	0.0	0.0	0.0	0.0	0.0	0.0	0.0	0.0	0.0	0.0	0.0	0.0	0.0	0.0
23	0.000000E+00	0.0	0.0	0.0	0.0	0.0	0.0	0.0	0.0	0.0	0.0	0.0	0.0	0.0	0.0
24	0.000000E+00	0.0	0.0	0.0	0.0	0.0	0.0	0.0	0.0	0.0	0.0	0.0	0.0	0.0	0.0
25	0.000000E+00	0.0	0.0	0.0	0.0	0.0	0.0	0.0	0.0	0.0	0.0	0.0	0.0	0.0	0.0
26	0.000000E+00	0.0	0.0	0.0	0.0	0.0	0.0	0.0	0.0	0.0	0.0	0.0	0.0	0.0	0.0
27	0.000000E+00	0.0	0.0	0.0	0.0	0.0	0.0	0.0	0.0	0.0	0.0	0.0	0.0	0.0	0.0
28	0.000000E+00	0.0	0.0	0.0	0.0	0.0	0.0	0.0	0.0	0.0	0.0	0.0	0.0	0.0	0.0
29	0.000000E+00	0.0	0.0	0.0	0.0	0.0	0.0	0.0	0.0	0.0	0.0	0.0	0.0	0.0	0.0
30	0.000000E+00	0.0	0.0	0.0	0.0	0.0	0.0	0.0	0.0	0.0	0.0	0.0	0.0	0.0	0.0
31	0.000000E+00	0.0	0.0	0.0	0.0	0.0	0.0	0.0	0.0	0.0	0.0	0.0	0.0	0.0	0.0
32	0.000000E+00	0.0	0.0	0.0	0.0	0.0	0.0	0.0	0.0	0.0	0.0	0.0	0.0	0.0	0.0
33	0.000000E+00	0.0	0.0	0.0	0.0	0.0	0.0	0.0	0.0	0.0	0.0	0.0	0.0	0.0	0.0
34	0.000000E+00	0.0	0.0	0.0	0.0	0.0	0.0	0.0	0.0	0.0	0.0	0.0	0.0	0.0	0.0
35	0.000000E+00	0.0	0.0	0.0	0.0	0.0	0.0	0.0	0.0	0.0	0.0	0.0	0.0	0.0	0.0
36	0.000000E+00	0.0	0.0	0.0	0.0	0.0	0.0	0.0	0.0	0.0	0.0	0.0	0.0	0.0	0.0
37	0.000000E+00	0.0	0.0	0.0	0.0	0.0	0.0	0.0	0.0	0.0	0.0	0.0	0.0	0.0	0.0
38	0.000000E+00	0.0	0.0	0.0	0.0	0.0	0.0	0.0	0.0	0.0	0.0	0.0	0.0	0.0	0.0
39	0.000000E+00	0.0	0.0	0.0	0.0	0.0	0.0	0.0	0.0	0.0	0.0	0.0	0.0	0.0	0.0
40	0.000000E+00	0.0	0.0	0.0	0.0	0.0	0.0	0.0	0.0	0.0	0.0	0.0	0.0	0.0	0.0
41	0.000000E+00	0.0	0.0	0.0	0.0	0.0	0.0	0.0	0.0	0.0	0.0	0.0	0.0	0.0	0.0
42	0.000000E+00	0.0	0.0	0.0	0.0	0.0	0.0	0.0	0.0	0.0	0.0	0.0	0.0	0.0	0.0
43	0.000000E+00	0.0	0.0	0.0	0.0	0.0	0.0	0.0	0.0	0.0	0.0	0.0	0.0	0.0	0.0
44	0.000000E+00	0.0	0.0	0.0	0.0	0.0	0.0	0.0	0.0	0.0	0.0	0.0	0.0	0.0	0.0
45	0.000000E+00	0.0	0.0	0.0	0.0	0.0	0.0	0.0	0.0	0.0	0.0	0.0	0.0	0.0	0.0
46	0.000000E+00	0.0	0.0	0.0	0.0	0.0	0.0	0.0	0.0	0.0	0.0	0.0	0.0	0.0	0.0
47	0.000000E+00	0.0	0.0	0.0	0.0	0.0	0.0	0.0	0.0	0.0	0.0	0.0	0.0	0.0	0.0
48	0.000000E+00	0.0	0.0	0.0	0.0	0.0	0.0	0.0	0.0	0.0	0.0	0.0	0.0	0.0	0.0
49	0.000000E+00	0.0	0.0	0.0	0.0	0.0	0.0	0.0	0.0	0.0	0.0	0.0	0.0	0.0	0.0
50	0.000000E+00	0.0	0.0	0.0	0.0	0.0	0.0	0.0	0.0	0.0	0.0	0.0	0.0	0.0	0.0
51	0.000000E+00	0.0	0.0	0.0	0.0	0.0	0.0	0.0	0.0	0.0	0.0	0.0	0.0	0.0	0.0
52	0.000000E+00	0.0	0.0	0.0	0.0	0.0	0.0	0.0	0.0	0.0	0.0	0.0	0.0	0.0	0.0
53	0.000000E+00	0.0	0.0	0.0	0.0	0.0	0.0	0.0	0.0	0.0	0.0	0.0	0.0	0.0	0.0
54	0.000000E+00	0.0	0.0	0.0	0.0	0.0	0.0	0.0	0.0	0.0	0.0	0.0	0.0	0.0	0.0
55	0.000000E+00	0.0	0.0	0.0	0.0	0.0	0.0	0.0	0.0	0.0	0.0	0.0	0.0	0.0	0.0
56	0.000000E+00	0.0	0.0	0.0	0.0	0.0	0.0	0.0	0.0	0.0	0.0	0.0	0.0	0.0	0.0
57	0.000000E+00	0.0	0.0	0.0	0.0	0.0	0.0	0.0	0.0	0.0	0.0	0.0	0.0	0.0	0.0
58	0.000000E+00	0.0	0.0	0.0	0.0	0.0	0.0	0.0	0.0	0.0	0.0	0.0	0.0	0.0	0.0
59	0.000000E+00	0.0	0.0	0.0	0.0	0.0	0.0	0.0	0.0	0.0	0.0	0.0	0.0	0.0	0.0
60	0.000000E+00	0.0	0.0	0.0	0.0	0.0	0.0	0.0	0.0	0.0	0.0	0.0	0.0	0.0	0.0
61	0.000000E+00	0.0	0.0	0.0	0.0	0.0	0.0	0.0	0.0	0.0	0.0	0.0	0.0	0.0	0.0
62	0.000000E+00	0.0	0.0	0.0	0.0	0.0	0.0	0.0	0.0	0.0	0.0	0.0	0.0	0.0	0.0
63	0.000000E+00	0.0	0.0	0.0	0.0	0.0	0.0	0.0	0.0	0.0	0.0	0.0	0.0	0.0	0.0
64	0.000000E+00	0.0	0.0	0.0	0.0	0.0	0.0	0.0	0.0	0.0	0.0	0.0	0.0	0.0	0.0
65	0.000000E+00	0.0	0.0	0.0	0.0	0.0	0.0	0.0	0.0	0.0	0.0	0.0	0.0	0.0	0.0
66	0.000000E+00	0.0	0.0	0.0	0.0	0.0	0.0	0.0	0.0	0.0	0.0	0.0	0.0	0.0	0.0
67	0.000000E+00	0.0	0.0	0.0	0.0	0.0	0.0	0.0	0.0	0.0	0.0	0.0	0.0	0.0	0.0
68	0.000000E+00	0.0	0.0	0.0	0.0	0.0	0.0	0.0	0.0	0.0	0.0	0.0	0.0	0.0	0.0
69	0.000000E+00	0.0	0.0	0.0	0.0	0.0	0.0	0.0	0.0	0.0	0.0	0.0	0.0	0.0	0.0
70	0.000000E+00	0.0	0.0	0.0	0.0	0.0	0.0	0.0	0.0	0.0	0.0	0.0	0.0	0.0	0.0
71	0.000000E+00	0.0	0.0	0.0	0.0	0.0	0.0	0.0	0.0	0.0	0.0	0.0	0.0	0.0	0.0
72	0.000000E+00	0.0	0.0	0.0	0.0	0.0	0.0	0.0	0.0	0.0	0.0	0.0	0.0	0.0	0.0
73	0.000000E+00	0.0	0.0	0.0	0.0	0.0	0.0	0.0	0.0	0.0	0.0	0.0	0.0	0.0	0.0
74	0.000000E+00	0.0	0.0	0.0	0.0	0.0	0.0	0.0	0.0	0.0	0.0	0.0	0.0	0.0	0.0
75	0.000000E+00	0.0	0.0	0.0	0.0	0.0	0.0	0.0	0.0	0.0	0.0	0.0	0.0	0.0	0.0
76	0.000000E+00	0.0	0.0	0.0	0.0	0.0	0.0	0.0	0.0	0.0	0.0	0.0	0.0	0.0	0.0
77	0.000000E+00	0.0	0.0	0.0	0.0	0.0	0.0	0.0	0.0	0.0	0.0	0.0	0.0	0.0	0.0
78	0.000000E+00	0.0	0.0	0.0	0.0	0.0	0.0	0.0	0.0	0.0	0.0	0.0	0.0	0.0	0.0
79	0.000000E+00	0.0	0.0	0.0	0.0	0.0	0.0	0.0	0.0	0.0	0.0	0.0	0.0	0.0	0.0
80	0.000000E+00	0.0	0.0	0.0	0.0	0.0	0.0	0.0	0.0	0.0	0.0	0.0	0.0	0.0	0.0
81	0.000000E+00	0.0	0.0	0.0	0.0	0.0	0.0	0.0	0.0	0.0	0.0	0.0	0.0	0.0	0.0
82	0.000000E+00	0.0	0.0	0.0	0.0	0.0	0.0	0.0	0.0	0.0	0.0	0.0	0.0	0.0	0.0
83	0.000000E+00	0.0	0.0	0.0	0.0	0.0	0.0	0.0	0.0	0.0	0.0	0.0	0.0	0.0	0.0
84	0.000000E+00	0.0	0.0	0.0	0.0	0.0	0.0	0.0	0.0	0.0	0.0	0.0	0.0	0.0	0.0
85	0.000000E+00	0.0	0.0	0.0	0.0	0.0	0.0	0.0	0.0	0.0	0.0	0.0	0.0	0.0	0.0
86	0.000000E+00	0.0	0.0	0.0	0.0	0.0	0.0	0.0	0.0	0.0	0.0	0.0	0.0	0.0	0.0
87	0.000000E+00	0.0	0.0	0.0	0.0	0.0	0.0	0.0	0.0	0.0	0.0	0.0	0.0	0.0	0.0
88	0.000000E+00	0.0	0.0	0.0	0.0	0.0	0.0	0.0	0.0	0.0	0.0	0.0	0.0	0.0	0.0
89	0.000000E+00	0.0	0.0	0.0	0.0	0.0	0.0	0.0	0.0	0.0	0.0	0.0	0.0	0.0	0.0
90	0.000000E+00	0.0	0.0	0.0	0.0	0.0	0.0	0.0	0.0	0.0	0.0	0.0	0.0	0.0	0.0
91	0.000000E+00	0.0	0.0	0.0	0.0	0.0	0.0	0.0	0.0	0.0	0.0	0.0	0.0	0.0	0.0
92	0.000000E+00	0.0	0.0	0.0	0.0	0.0	0.0	0.0	0.0	0.0	0.0	0.0	0.0	0.0	0.0
93	0.000000E+00	0.0	0.0	0.0	0.0	0.0	0.0	0.0	0.0	0.0	0.0	0.0	0.0	0.0	0.0
94	0.000000E+00	0.0	0.0	0.0	0.0	0.0	0.0	0.0	0.0	0.0	0.0	0.0	0.0	0.0	0.0
95	0.000000E+00	0.0	0.0	0.0	0.0	0.0	0.0	0.0	0.0	0.0	0.0	0.0	0.0	0.0	0.0
96	0.000000E+00	0.0	0.0	0.0	0.0	0.0	0.0	0.0	0.0	0.0	0.0	0.0	0.0	0.0	0.0
97	0.000000E+00	0.0	0.0	0.0	0.0	0.0	0.0	0.0	0.0	0.0	0.0	0.0	0.0	0.0	0.0
98	0.000000E+00	0.0	0.0	0.0	0.0	0.0	0.0	0.0	0.0	0.0	0.0	0.0	0.0	0.0	0.0
99	0.000000E+00	0.0	0.0	0.0	0.0	0.0	0.0	0.0	0.0	0.0	0.0	0.0	0.0	0.0	0.0
100	0.000000E+00	0.0	0.0	0.0	0.0	0.0	0.0	0.0	0.0	0.0	0.0	0.0	0.0	0.0	0.0

```
CRACK OCCURRENCE PER WELD = 7.4843E-03
-----------------------------
```

INITIAL-TYPE : SURF_O

% DEPTH	FREQ.	ASPECTS:	<2	2-3	3-4	4-5	5-6	6-7	7-8	8-9	9-10	10-11	11-12	12-13	13-14	14->
1	0.128565E-03		16.0	0.0	2.7	1.0	2.7	3.7	8.8	4.5	5.1	6.1	2.7	4.4	6.1	34.0
2	0.913144E-04		31.0	3.0	4.4	5.1	4.4	6.7	4.4	6.9	4.4	5.7	4.8	3.2	3.0	13.6
3	0.123950E-04		12.8	3.0	7.1	13.5	12.8	12.1	10.6	8.5	5.7	7.1	0.7	1.4	0.7	2.1
4	0.255490E-05		5.4	5.4	13.5	10.8	18.9	13.5	16.2	2.7	2.7	5.4	2.7	2.7	0.0	0.0
5	0.386135E-06		58.8	17.6	5.9	17.6	0.0	0.0	0.0	0.0	0.0	0.0	0.0	0.0	0.0	0.0
6	0.760298E-06		18.8	18.8	25.0	25.0	12.5	0.0	0.0	0.0	0.0	0.0	0.0	0.0	0.0	0.0
7	0.852801E-06		44.4	22.2	0.0	11.1	11.1	11.1	0.0	0.0	0.0	0.0	0.0	0.0	0.0	0.0
8	0.931133E-07		80.0	20.0	0.0	0.0	0.0	0.0	0.0	0.0	0.0	0.0	0.0	0.0	0.0	0.0
9	0.182674E-07		50.0	50.0	0.0	0.0	0.0	0.0	0.0	0.0	0.0	0.0	0.0	0.0	0.0	0.0
10	0.366874E-07		0.0	100.0	0.0	0.0	0.0	0.0	0.0	0.0	0.0	0.0	0.0	0.0	0.0	0.0
11	0.174441E-07		100.0	0.0	0.0	0.0	0.0	0.0	0.0	0.0	0.0	0.0	0.0	0.0	0.0	0.0
12	0.343740E-07		100.0	0.0	0.0	0.0	0.0	0.0	0.0	0.0	0.0	0.0	0.0	0.0	0.0	0.0
13	0.692365E-07		100.0	0.0	0.0	0.0	0.0	0.0	0.0	0.0	0.0	0.0	0.0	0.0	0.0	0.0
14	0.000000E+00		0.0	0.0	0.0	0.0	0.0	0.0	0.0	0.0	0.0	0.0	0.0	0.0	0.0	0.0

CRACK OCCURRENCE PER WELD = 2.3711E-04

Appendix F

Guidance for Users of RR-PRODIGAL

Appendix F

Guidance for Users of RR-PRODIGAL

F.1 Introduction

This appendix provides a number of useful details about the Rolls-Royce and Associates (RRA) methodology which are not covered in the document from RRA. These insights came from trial applications of the RR-PRODIGAL code a. VNL, and through discussions with the technical staff at RRA.

F.2 Help Menus

The RR-PRODIGAL code uses menu-driven inputs, along with extensive interactive internal documentation which is available through "help pages." Many details about the code can be learned from study of these pages. In large measure, the code relies on such help menus as opposed to highly detailed paper documentation. For example, one of the help menus provides a detailed description of a typical RR-PRODIGAL session.

F.3 Generic versus Vessel-Specific Predictions

RR-PRODIGAL calculates expected distributions of flaws for a population of welds which have a common set of attributes, including material type, wall thickness, configuration of weld passes, welding processes, and inspection procedures. Flaws in specific welds will differ from the expected distribution due to random factors that are not quantified in the model. The material in a given vessel weld will be a statistical sample from the large population addressed by RR-PRODIGAL. In this regard, data from examinations of given vessel welds are expected to differ somewhat from the RR-PRODIGAL predictions.

Random variability from vessel-to-vessel and from weld-to-weld is not addressed by RR-PRODIGAL. However, the model permits better evaluations of vessel failure probabilities than are possible with the use of generic flaw distributions. A generic flaw distribution cannot address systematic differences between vessel welds due to differences in vessel designs, fabrication practices, and inspection methods. Nevertheless, the output from RR-PRODIGAL does not address other vessel-specific differences, which can be assessed only from detailed examinations of individual welds.

F.4 Welding Processes

The RR-PRODIGAL code permits only one welding process per weld. Therefore, it is not possible to simulate a submerged arc weld which has been repaired using shielded metal (manual) arc welding. However, the effects of repair welding can be estimated by performing the weld simulation twice, once for each of the two welding processes. One or more of the user-defined output zones can be defined to correspond to the repair welded region of the vessel wall.

F.5 Number of Start/Stops

The input to RR-PRODIGAL asks for the number of weld start/stops. This input specifies the number of stop/starts per meter of weld, rather than the number per weld bead. The submerged arc process would typically have zero start/stops due to the use of continuous lengths of welding wire filler metal. Each replacement of a welding rod in a manual process would represent a start/stop.

F.6 Types of Flaws Addressed

RR-PRODIGAL only addresses flaw types that have structural significance. For example, the simulation includes the potentially significant flaw type of "pores with tails," but excludes other porosity characterized as rounded indications. Discussions with welding experts indicated that much of the slag present in welds is not crack-like in nature. On this basis, the model excludes the flaw category of "fat slag." Since the data on observed flaws in welds may not differentiate between various types of pores and slag defects, the RR-PRODIGAL code can be expected to somewhat underestimate the number of smaller flaws in welds.

The approach of the RR-PRODIGAL methodology is to address specific flaw-producing mechanisms that can occur during the manufacture of a weld. It is implied that only mechanisms which produce structurally significant flaws are addressed. Mechanisms are ignored if they result only in flaws too small to be significant to structural integrity (e.g., depths much less than the weld bead dimensions). It is therefore expected that data on observed flaws could include large numbers of very small flaws which would be excluded by the RR-PRODIGAL methodology. The number of these small "ignored flaws" can be very large, and can dominate the total population. The flaw data for the PVRUF vessel as presented in Appendix D illustrates how large numbers of insignificant small flaws (with depths of less than 2 to 4 mm) can be present in welds.

F.7 Base Metal Flaws

The RR-PRODIGAL code does not address flaws in the base metal of vessels, but rather considers only welding flaws. Fracture mechanics calculations by Rolls Royce on UK vessels have neglected the contributions of base metal flaws to failure probabilities. Discussions with Rolls Royce technical staff suggest that the assumption by the Oak Ridge National Laboratory (ORNL) of a 10:1 ratio between the densities of weld flaws and base metal flaws is too conservative, and that a ratio of 100:1 or greater would be more appropriate. In general, base metal flaws are believed to have benign orientations and thereby have little impact on structural integrity. The PNNL examinations of the PVRUF vessel indicate that weld repair of base metal regions is the most likely mechanism for producing larger flaws with radial orientations in plate and forging components.

F.8 Predicted Flaw Attributes

The output from the current version of RR-PRODIGAL gives information on through-wall flaw sizes, flaw lengths, flaw aspect ratios, and the locations of the flaws relative to the vessel inner surface. Other information such as the mechanisms associated with the occurrence of flaws (e.g., centerline cracks, sidewall slag, etc.) is not provided, although such parameters are simulated in the calculations. The equations and parameters used by RR-PRODIGAL to generate all attributes associated with the simulated flaw distributions are described in Appendix A. This information offers the reader insight into the detailed characteristics of vessel flaws.

F.9 Forward Propagation Model

The RR-PRODIGAL weld simulation includes a model for predicting the "forward propagation" of flaws. This model is based on estimates of conditional probabilities that a flaw-generating mechanism will occur in a weld pass, given that it has already occurred in the prior weld pass. The alternative is for an initiated flaw to be confined to a single weld layer. Whenever forward propagation is predicted, the RR-PRODIGAL model assumes that the flaw propagation occurs in steps of exactly one weld layer.

F.10 Measures of Flaw Densities

Flaw densities for welds can be stated in terms of flaws per cubic meter of weld metal, or alternatively as flaws per meter of weld length. In probabilistic fracture mechanics calculations such as with the VISA-II code (Simonen et al. 1986), the flaw density measure is flaws per unit of weld length, whereas other studies have used the measure of flaws per unit volume. Calculations to convert from one measure to the other require information about the geometry of the weld joint.

RRA technical staff have expressed a preference for flaws per unit weld length rather than flaws per unit volume. Increasing the volume of weld metal will increase the expected number of flaws, given that all other factors remain unchanged. However, other scaling factors such as the area of the weld groove sidewall, number of weld root passes, and the size of the weld passes do not increase in proportion to the increase in the volume of weld metal.

Nevertheless, the selection of a specific flaw density measure should not be a significant issue for pressurized thermal shock calculations, given that the wall thicknesses for pressurized water reactor vessels are limited to a relatively small range. The selection of the density measure would be important for applications in which the range of wall thicknesses is much greater (e.g., involving extrapolation from a 10-in. wall for vessels to a 1.0-in. wall for a piping component). In such cases, the volume of weld metal could be a less important parameter for scaling purposes than, for example, the area of the weld groove sidewall. Calculations with the RR-PRODIGAL code can account for all of these geometric differences, along with other specific differences in welding and inspection factors.

F.11 Flaw Location

The location of a flaw within the vessel wall is defined as the distance between the innermost flaw tip and the inner surface of the vessel. Initiated flaws are assigned random locations within weld beads. Internal flaws are classified as buried flaws even if the simulation places the inner tip very close to the vessel surface. No surface proximity rules are applied to convert buried flaws to inner surface flaws.

F.12 Aspect Ratio

The flaw aspect ratio is defined for (both surface and buried flaws) as the ratio of the total flaw length to the flaw through-wall depth. Simulated aspect ratios from RR-PRODIGAL are typically 4:1 or less. It has been noted that pores with tails have aspect ratios of less than 1:1, which implies flaws with their long direction extending into the vessel wall.

F.13 Defect Width

Defect width is defined as the separation between opposite sides of a crack-like flaw. RR-PRODIGAL simulates the randomness in defect widths, using a different distribution function for each type of flaw (e.g., centerline cracks versus lack of fusion). The defect width is taken to be independent of the defect length and through-wall depth.

F.14 Weld Width

This input to RR-PRODIGAL specifies the physical dimension between the two sidewalls of the weld groove. This dimension is used in the simulation in combination with the independently specified parameter of weld runs per layer to determine if flaws in adjacent weld layers should be treated as a single flaw, in accordance with flaw proximity criteria.

F.15 Inspection Efficiency

Output from RR-PRODIGAL gives a series of tables for inspection efficiencies of the radiographic examination, as a function of the through-wall depth of the flaw. These tables should be interpreted as probability-of-detection curves. Inspection efficiency does not include any effects of flaw size errors, or of repair criteria as they may relate to the impact of inspections on vessel failure probabilities. The code output give specific inspection efficiencies for each type of flaw (e.g., interrun slag) for each of three regions of the vessel (inner surface breaking, buried, and outer surface breaking).

F.16 Ultrasonic Inspection

RR-PRODIGAL addresses the effects of radiographic inspection of vessel welds, but does not currently simulate the effects of ultrasonic inspections. This potentially useful feature could be implemented as future enhancement to the code. Effects of flaw detection through ultrasonic examinations must be addressed with auxiliary calculations which can modify the distributions provided by the code as output files.

F.17 Surface Examination

The RRA model simulates surface examinations by the dye penetrant (PT) method. It is also appropriate to use this model to simulate the effects of magnetic particle (MT) examinations, although such predictions will be somewhat conservative because the model neglects the ability of MT examinations to detect the presence of near-surface buried flaws. While details regarding the surface examination model have not been described in RRA reports, the model is said to take into account such factors as flaw length and width (i.e., separation between the faces of the cracks). Parameters of the simulation model are based on expert elicitation, with all values being hardwired into the code. Numerical results from RR-PRODIGAL simulations indicate that detection probabilities for surface examinations can be very high (e.g., greater than 99 percent).

F.18 Amount of Inspection

This input to RR-PRODIGAL is usually set equal to 1.0. Values less than 1.0 apply for those cases where the entire weld length is not inspected, such as when physical access prevents the inspection of portions of the weld. The factor can be estimated by consideration of the size and locations of the obstructions that prevent access to the welds.

F.19 Repairs of Detected Flaws

The RRA model assumes that repairs are performed for all flaws that are detected by radiography and surface examinations. In the actual practice of vessel fabrication, no repairs are made for smaller flaws whose sizes are acceptable in accordance with the governing flaw acceptance criteria. This simplifying assumption causes RR-PRODIGAL to somewhat underpredict the actual number of smaller flaws in welds.

F.20 Machining

The operation of machining is defined as any operation that removes material from the as-welded surfaces, which includes grinding. The vessels of interest to RRA in the UK usually have machined inner surfaces, whereas the clad inner surfaces of US vessels typically remain in the as-welded condition. It is appropriate for US vessels to specify a machining operation for vessel outer surfaces and for the inner surfaces of vessel welds prior to the application of cladding.

Machining can remove all or only part of the innermost weld layer, or could remove as much as 1-1/2 layers. Simulated machining operations will typically increase the number of surface defects, because the removal of material will expose defects that were previously confined within the weld beads. On the other hand, the effectiveness of surface inspection is greatly increased for the machined surface relative to that for the as-welded surface. As a result, the predicted overall effect of machining is to decrease the number of surface flaws.

F.21 Post Weld Heat Treatment

The RRA model simulates the extension of cracks during post-weld heat treatments (PWHT) which are performed as a standard practice in vessel fabrication. However, the code user must specify that such a heat treatment is performed. The calculated crack extension applies only to heat affected zone (HAZ) cracks. Evidently the flaw extensions due to PWHT are relatively small, being less than a weld bead in depth.

F.22 Best Estimate versus Bounding Calculations

The RR-PRODIGAL model predicts the expected or average number and sizes of defects for a population of welds as defined by some general attributes that describe the welding and inspection processes used to make the weld. In developing the model, it was acknowledged that individual welds will vary from the population average. It is expected that detailed flaw data from individual vessels and welds will exhibit a level of scatter about the flaw distribution predicted for the average weld. In this regard, RRA considered the inclusion of additional attributes such as "welder proficiency" or "quality factor" to allow the model to address weld-to-weld variations. This feature was not incorporated for various reasons, including the added requirement that a code user would have to define subjective inputs to the model.

Different assumptions made in the RR-PRODIGAL model can result in calculations that may overestimate or underestimate the number of flaws in a weld. The uncertainties in estimates are greatest for small flaws whose depths are much less than the weld bead dimension. In this regard, Rolls Royce staff have stated that the RRA methodology was developed with the primary objective of establishing the number of larger flaws whose depths extend beyond a single weld bead. Therefore, the uncertainty should be least for larger flaws which have depth dimensions on the order of one or two weld beads. The uncertainty increases for still larger flaws which extend over several weld beads. Such flaws have low probabilities of occurrence. They are seldom observed, and would result in weld repairs whenever they are observed. Therefore, the model is also used to estimate the numbers of flaws that go undetected during the vessel fabrication process.

F.23 Monte Carlo Simulation

The RR-PRODIGAL code is based on a detailed model of multipass welding and the mechanisms that generate defects in welds. This model is implemented numerically as a Monte Carlo simulation. Documentation of the code by RRA staff does not provide a detailed flow chart or logic for the Monte Carlo simulation. Typical applications of the RR-PRODIGAL code have involved the simulation of defects in some 50,000 welds of a one-meter unit length. This is equivalent to estimating the

number and sizes of flaws in 50,000 m of weld. Output from the code is provided in terms of flaws per meter of weld for each of the selected flaw size categories. Input to the code permits the user to increase or decrease the number of simulations from the standard value of 50,000.

F.24 Confidence Limits

The output from RR-PRODIGAL gives only the expected numbers of flaws, and does not provide statistical confidence limits for estimates of flaw occurrence rates which are associated with the finite number of Monte Carlo simulations.

F.25 Weibull Fitting of Histograms

At one time, the RR-PRODIGAL code had a provision to approximate the predicted histograms of flaw depths with Weibull distribution functions. One of the output files from RR-PRODIGAL corresponds to the Weibull parameters. This provision has fallen into disuse because it was found to be difficult to adequately fit a Weibull distribution over the full range of flaw sizes. The quality of the derived fits was particularly poor in the tail regions that describe larger flaws.

F.26 References

Simonen, F. A., K. I. Johnson, A. M. Liebetrau, D. W. Engel, E. P. Simonen. 1986. *VISA-II-A Computer Code for Predicting the Probability of Reactor Pressure Vessel Failure*, NUREG/CR-4486, PNL-5775.

Appendix G

Installation Guide for RR-PRODIGAL

Appendix G

Installation Guide for RR-PRODIGAL

This document serves as a guide to the installation of a PRODIGAL system. Follow the instructions below. If a problem arises and the software will not install correctly, please contact:

Product Support Desk
Rolls-Royce Control Systems (SEAS)
+44 01332 771700

G.1 System Requirements

PRODIGAL is compatible with SUN Solaris 1 (SUNOS 4.1.3 or higher) and SUN Solaris 2.x with the following minimum requirements:

OPENWINDOWS3
64MB RAM memory
100MB disk space
Colour or grayscale monitor

G.2 Installation

PRODIGAL is available on a number of media. Ensure that you have a suitable media device connected to your workstation before starting the installation.

(1) Log on to the workstation with the media device mounted.

(2) Change directory to the location below which PRODIGAL is to be installed, e.g.,

    cd/home

It is advisable to keep the installation path fairly short, ideally 30 characters or less.

(3) Make a directory to house PRODIGAL, e.g.,

    Mkdir prodigal_vx   (where x is the version)

(See Trouble-shooting, section 3(ii)).

(4) Insert the PRODIGAL medium (tape, etc.) into the media device.

(5) Enter the following command to extract the PRODIGAL installation script:

tar xvf <device name> rr-prodigal.install

(6) Run the installation script, i.e:

rr-prodigal.install

(7) Answer the questions asked by the script (such as location and device name). Answer "N" to the question regarding "is this an upgrade to Version 1."

(8) Include the required line in your .cshrc script as instructed by the end of the installation script.

(9) Execute PRODIGAL (making sure you have run your .cshrc) by typing:

rr-prodigal &

G.3 Trouble-Shooting

(1) If you cannot access the installation script from the media device:

Check that you are logged on the workstation directly attached to the device and that the device is mounted. The script (on sequential media such as tape) will be the first item.

(2) If the installation script fails:

Check you have sufficient disk space in the partition you are using. Check you have permission to create files.

(3) If PRODIGAL will not execute:

If the rr-prodigal command is not recognized, make sure you have sourced the prodigal definitions script either directly or through your .cshrc.

If PRODIGAL starts but fails during startup check that

    i.   Your installation path does not exceed 30-50 characters

    ii. On some early versions of PRODIGAL (up to v_2_2) the installation path must not contain a dot (.) character. Later versions have corrected this.

If problems persist contact Rolls-Royce at the number given above. Supply the exact error message/symptoms.

G.4 Installation Structure

The installation takes the form of a number of folders and files and will follow the layout on the next page.

```
                              <installation location>
          ┌──────────┬────────┬────────┬──────────┬────────┐
     definitions   help    input   output   repository   reuse
```
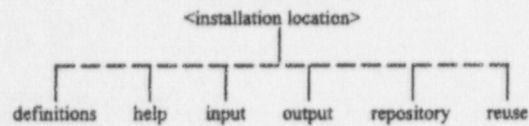
definitions: holds the PRODIGAL definitions script which defines the required environment variables.

help: holds the PRODIGAL-specific help texts for the on-line help utility

input: holds all PRODIGAL input decks

output: holds all PRODIGAL output results

repository: holds all system control files
            holds all executables
            holds all user preferences
            holds PRODIGAL input/output databases
            holds PRODIGAL expert system databases

reuse: leads to subdirectories holding help texts for standard Rolls-Royce libraries and tools used in the
            PRODIGAL suite.

This is the minimum set of folders/files required. There may be additional folders supplied on the medium in special
circumstances. These folders will typically be used to hold data for demonstration purposes.

U.S. NUCLEAR REGULATORY COMMISSION

BIBLIOGRAPHIC DATA SHEET

(See instructions on the reverse)

1. REPORT NUMBER (Assigned by NRC. Add Vol., Supp., Rev., and Addendum Numbers, if any.)
NUREG/CR-5505
PNNL-11898

2. TITLE AND SUBTITLE

RR-PRODIGAL - A Model for Estimating the Probabilities
of Defects in Reactor Pressure Vessel Welds

3.	DATE REPORT PUBLISHED
MONTH	YEAR
October	1998

4. FIN OR GRANT NUMBER
L2606

5. AUTHOR(S)

O. J. V. Chapman/RRA
F. A. Simonen/PNNL

6. TYPE OF REPORT

Technical

7. PERIOD COVERED *(Inclusive Dates)*

8. PERFORMING ORGANIZATION – NAME AND ADDRESS *(If NRC, provide Division, Office or Region, U.S. Nuclear Regulatory Commission, and mailing address; if contractor, provide name and mailing address.)*

Pacific Northwest National Laboratory
Richland, WA 99352

Subcontractor:
Rolls-Royce and Associates
Derby, DE2 8BJ
United Kingdom

9. SPONSORING ORGANIZATION – NAME AND ADDRESS *(If NRC, type "Same as above"; if contractor, provide NRC Division, Office or Region, U.S. Nuclear Regulatory Commission, and mailing address.)*

Division of Engineering Technology
Office of Nuclear Regulatory Research
U.S. Nuclear Regulatory Commission
Washington, DC 20555-0001

10. SUPPLEMENTARY NOTES
S. N. Malik, NRC Project Manager

11. ABSTRACT *(200 words or less)*

The U.S. Nuclear Regulatory Commission (NRC) has supported research at Pacific Northwest
National Laboratory (PNNL) to establish bases for estimating the number and sizes of
flaws in reactor pressure vessel welds. This report describes a collaborative effort
between PNNL and Rolls Royce and Associates (RRA), which developed an approach to
predict flaw distributions based on knowledge of the vessel dimensions, welding
practices, and inspection procedures. The approach uses knowledge of welding experts
and mathematical modelling to simulate the weld manufacture and the errors that lead to
different types of defects. The model addresses main vessel welds and cladding welds.
Two meetings were held to enable RRA and PNNL to engage in discussions with experts in
the areas of vessel welding and inspection practices. The discussions confirmed the
basic soundness of the original RRA methodology, and provided insights which improved
the quality of the assumptions and inputs to the model. The final product of the
project was the RR-PRODIGAL computer code, which has been applied to predict the flaws
in the Pressure Vessel User Research Facility (PVRUF) vessel, with good agreement being
observed. This report describes the flaw simulation methodology, provides guidance in
use of the computer code, and describes example calculations.

12. KEY WORDS/DESCRIPTORS *(List words or phrases that will assist researchers in locating the report.)*

Welding
Flaw Distributions
Pressurized Water Reactor
Reactor Pressure Vessel

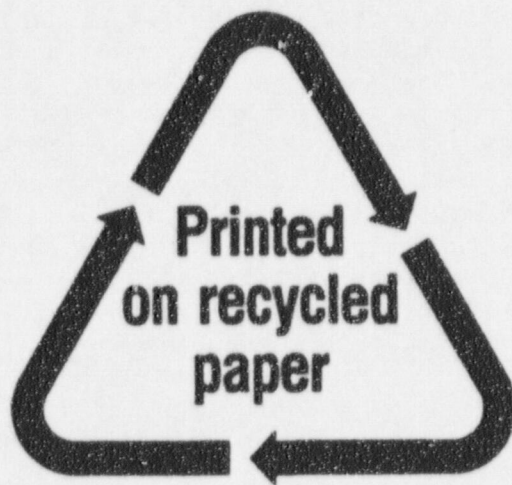| 13. AVAILABILITY STATEMENT |
|---|
| unlimited |

14. SECURITY CLASSIFICATION
(This Page)
unclassified
(This Report)
unclassified

15. NUMBER OF PAGES

16. PRICE

UNITED STATES
NUCLEAR REGULATORY COMMISSION
WASHINGTON, DC 20555-0001

———

OFFICIAL BUSINESS
PENALTY FOR PRIVATE USE, $300

SPECIAL STANDARD MAIL
POSTAGE AND FEES PAID
USNRC
PERMIT NO. G-67

```
1205551544 86      1  1AN1R5
US NRC-OCIO
DIV-INFORMATION MANAGEMENT
TPS-PDR-NUREG
2WFN-6E7                     DC  20555
WASHINGTON
```